INSTITUTO TECNOLÓGICO Y DE ESTUDIOS SUPERIORES DE MONTERREY

CAMPUS MONTERREY

PROGRAMA DE GRADUADOS EN MECATRÓNICA Y TECNOLOGÍAS DE INFORMACIÓN

MODELING OF DCT COEFFICIENTS IN THE H.264 VIDEO ENCODER

THESIS

PRESENTED IN PARTIAL FULFILLMENT OF THE REQUIREMENTS FOR THE DEGREE OF:

MASTER IN TELECOMMUNICATIONS MANAGEMENT

BY:

ROBERTO RIVERA JIMÉNEZ

MONTERREY, N.L. APRIL, 2008

INSTITUTO TECNOLÓGICO Y DE ESTUDIOS SUPERIORES DE MONTERREY

CAMPUS MONTERREY

PROGRAMA DE GRADUADOS EN MECATRÓNICA Y TECNOLOGÍAS DE INFORMACIÓN

The members of the Thesis Committee hereby recommend accepting the thesis presented by Roberto Rivera Jiménez in partial fulfillment of the requirements for the degree of Master in Telecommunications Management

THESIS COMMITTEE:

_____

Ramón Martín Rodríguez Dagnino, Ph.D.
Thesis Advisor

_____

José Ramón Rodríguez Cruz, Ph.D.
Synodal

_____

Roberto Rodríguez Said, Ph.D.
Synodal

_____

Graciano Dieck Assad, Ph.D.
Director of the Graduate Program in Mechatronics and Information Technologies
April 2008

MODELING OF DCT COEFFICIENTS IN THE H.264 VIDEO ENCODER

BY:

ROBERTO RIVERA JIMÉNEZ

THESIS

Presented to the Graduate Program in Mechatronics
and Information Technologies

This work is a partial requirement for the degree of
Master in Telecommunications Management

INSTITUTO TECNOLÓGICO Y DE ESTUDIOS
SUPERIORES DE MONTERREY

MONTERREY, N.L. APRIL, 2008

To my family

Acknowledgments

I would like to thank my parents, Roberto and Hilda, for their unconditional support and love; my brothers, Dante and Jesús, for all their help; and all my family for their motivation.

I would also like to thank my thesis advisor, Dr. Ramón Martín Rodríguez Dagnino, for his guidance and advice; and my thesis committee, Dr. José Ramón Rodríguez Cruz and Dr. Roberto Rodríguez Said, for their comments and observations that improved this work.

Thanks to the CONACYT for giving me the opportunity of realize my graduate studies.

Special thanks to all the teachers that I have had in my life, for all the things that I have learned from them.

Abstract

DCT stands for Discrete Cosine Transform (Ahmed, Natarajan, & Rao, 1974); it is an important tool used in video and image compression systems (Richardson, 2003). The understanding of the DCT coefficients' statistical distribution has many applications; one of them is the rate control for video coding, which requires knowledge of the rate-distortion relation as a function of the encoder parameters and the video source statistics (Kamaci & Altunbasak, 2005)

This thesis focuses in the rate and distortion relations as a function of the quantization parameter and the statistics of the DCT coefficients. The objective of this work is to compare three theoretical Probability Density Functions (Laplace, Cauchy and Generalized Gaussian) in terms of: how well they represent the empirical DCT coefficient data; and how well the models based on them can predict the actual distortion and the actual rate of the coded video.

Table of Contents

List of tables

List of figures

Chapter I

OVERVIEW

I.1 INTRODUCTION

The advances in video coding technology and standardization, together with the improvements in network infrastructures, storage capacity, and computing power are enabling an increasing number of video applications. Among these are: multimedia messaging, video conferencing, Internet video streaming, high-definition TV broadcasting, DVD, Blu-ray Disc, and HD DVD (Schwarz, Marpe, & Wiegand, 2007).

Video sources are by nature analog and they need to be digitally encoded before they can be stored in digital media or transmitted over digital telecommunications networks. The difficulty is the extensive amount of data required to represent them (Sharifi, 1995).

H.264/AVC (Advanced Video Coding) is a video codec standard of the International Telecommunication Union - Telecommunication Standardization Sector proposed in 2003 (ITU-T Rec. H.264, 2005). It is the result of the Joint Video Team (JVT) formed by the Moving Picture Experts Group (MPEG) and the ITU's Video Coding Experts Group (Wenger, 2003). It is also known as MPEG-4 part 10 AVC (Wiegand, Sullivan, Bjøtegaard, & Luthra, 2003).

"The primary goals of H.264/AVC are improved coding efficiency and improved network adaptation" (Stockhammer, Hannuksela, & Wiegand, 2003).

In H.264/AVC the only part standardized is the central decoder, this is achieved by restricting the encoded bitstream and syntax, and defining the decoding process of the syntax elements in such way that every standardized decoder will produce similar results when given an encoded bitstream that conforms to the constraints of the standard (Wiegand, Sullivan, Bjøtegaard, & Luthra, 2003). This allows maximal freedom to improve the implementations in a tailored way to specific applications (Wiegand et al., 2003).

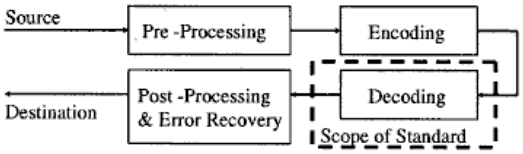

Fig. I-1: Scope of video coding standardization, obtained from Wiegand et al. (2003)

I.2 JUSTIFICATION

DCT stands for Discrete Cosine Transform (Ahmed, Natarajan, & Rao, 1974) and it is an important tool used in video and image compression systems (Richardson, 2003). The understanding of the statistical distribution of the DCT coefficients can be useful in quantizer design and noise mitigation for image enhancement (Lam & Goodman, 2000). Entropy coding benefits from modeling the amplitude distribution of the DCT coefficients, and then using a collection of entropic codebooks each fitting a modeled PDF of the true data (Aiazzi, Alparone, & Baronti, 1999).

Knowledge of the DCT coefficients' probability distribution is particularly important in rate control for video coding, "since the problems of bit allocation and quantization scale selection require knowledge of the rate-distortion relation as a function of the encoder parameters and the video source statistics" (Kamaci & Altunbasak, 2005).

The scope of this thesis is in the rate and distortion relations as a function of the encoder parameters and the DCT coefficients' statistics.

I.3 OBJECTIVE

The objective of this thesis is to compare three theoretical Probability Density Functions (the Laplace, Cauchy and Generalized Gaussian) in terms of: how well they represent the empirical DCT coefficient data; how well the models based on them can predict the actual rate of the coded video; and how well the models based on them can predict the actual distortion of the coded video.

I.4 ANTECEDENTS

This section briefly describes some of the prior works in the subject of DCT coefficient modeling.

Reiningek & Gibson (1983) used the Laplacian, Gaussian and Gamma modeling in images and compared them using the Kolmogorov-Smirnov (KS) test of goodness-of-fit. They concluded that, for a large class of images, the DC coefficient was best modeled by a Gaussian PDF, and the AC coefficients were best modeled by a Laplacian distribution.

Müller (1993) used the Laplacian and Generalized Gaussian DCT modeling in images and compared them using the χ^2 test of goodness-of-fit. His results showed that the shape parameter of the G.G. was generally far from the Laplacian case and the χ^2 values were considerable lower in the G.G. case (thus it had a better fit than the Laplacian).

Birney & Fischer (1995) used the Laplacian and Generalized Gaussian DCT modeling in images, and designed quantizers and codes based on them. Their results showed that the ones based on the Generalized Gaussian PDF were always superior in Mean-squared Error than the ones based on Laplacian PDF, but by a little margin that did not outweigh the computational cost. Joshi & Fischer (1995), without doing the quantizer and code design, found similar results.

Lam & Goodman (2000) presented a rigorous mathematical analysis using a doubly stochastic model of images and used it to explain why previous observations from the literature lead to the proposal of the Laplacian and Gaussian PDF as a way to model the DCT coefficients.

Chang et al. (2005) proposed results of distribution test that indicated that, for many natural images, the Generalized Gamma Function ($G\Gamma F$) was a better representation of the DCT coefficients than the Generalized Gaussian and the Laplacian. However, is important to note that the $G\Gamma F$ only exists for positive numbers, and the DCT coefficients in video (obtained from residuals, which are the

differences between the predicted and the actual values) can be positive or negative.

Altunbasak & Kamaci (2004) proposed the use of the Cauchy PDF as a way to model the DCT coefficients in H.264. Their results showed that it performed better than the widely used Laplacian PDF. They also proposed exact analytical models for the Entropy and Distortion based on it. Kamaci, Altunbasak, & Mersereau (2005) expanded their previous results and proposed a Frame bit allocation scheme using the Cauchy PDF.

Syu (2005) showed exact analytical models for the Entropy and Distortion of the H.264 encoded video based on the Laplace PDF. Those had a very low computational cost and were specifically used in a resource limited encoder.

Sun et al. (2005) used the Generalized Gaussian Distribution in order to model the DCT coefficients in MPEG-4 encoded videos. They also proposed approximate analytical models for the Entropy and Distortion based on the Generalized Gaussian PDF.

I.5 CONTRIBUTIONS

Some of the contributions of this thesis are the comparisions of the Cauchy and the Generalized Gaussian Probability Density Functions; in the antecedents sections there is literature that compares each to the Laplace PDF, but a direct comparission between the two could not be found.

The main contribution of this work is the derivation of exact anaytical models for the Entropy and Distortion, based on the Generalized Gaussian PDF.

I.6 STRUCTURE OF THE THESIS

The thesis is divided as follows: Chapter II presents the background and important terminology used in the field of digital video. Chapter III presents concepts used in video compression and shows the basic structure of a CODEC. Chapter IV gives a brief description of the encoding process in H.264. Chapter V presents the Probability Density Functions used in this thesis to represent the DCT coefficients. Chapter VI is the main part of the thesis; it presents experimental results of the comparison of those PDFs.

Chapter II

DIGITAL VIDEO

II.1 FUNDAMENTALS

A pixel, also called picture element or pel, is a digital sample of the intensity (of the color or the brightness) value of a picture at a single point (Symes, 2004).

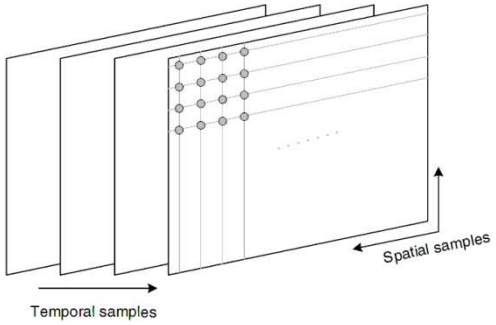

Fig. II-1: Spatial and temporal sampling of a video sequence, obtained from Richardson (2003).

A scene that has movement is represented by a group of still images; each of them is called a frame (González-López, 2006). A frame contains lines of spatial information of a video signal (Symes, 2004). “A field consists of odd- or even-numbered lines of spatial samples” (Richardson, 2003). If the two fields of a frame are captured at different time instants, the frame is referred to as an interlaced frame; if not it is referred to as a progressive frame (Sullivan & Wiegand, 2005).

"The human eye contains more than 100 million sensors with a brightness control system that allows clear vision over a brightness range of more than ten million to one. The two eyes together with the brain give the ability to recognize objects in three-dimensional space" (Luther, 1997).

"The sensitivity of the human eye varies from color to color and from person to person, for the same color. In addition, two different persons may perceive the same color with the same intensity differently. Furthermore, the human eye is more sensitive to yellow or yellow-green than red and violet" (Ramírez-Velarde, 2004).

II.1.1 Color formats

An analog video camera produces three distinct continuous signals, one for each color component Red, Green and Blue; these three colors, are called the additive primaries. RGB is the standard for video cameras (Ramírez-Velarde, 2004).

Video coding often uses a color representation that has three components: Y, C_b, and C_r. Component Y is called *luma* and represents brightness. The two *chroma* components C_b and C_r represent the deviation from gray to blue and red, respectively (Sullivan & Wiegand, 2005).

$$Y = k_r R + k_g G + k_b B$$
$$C_r = R - Y$$
$$C_g = G - Y$$
$$C_b = B - Y$$

Where the k's are weighting factors ($k_r + k_g + k_b = 1$). Neither k_g nor C_g are needed because, knowing the other components, they can be fully specified with the previous relations (Richardson, 2003).

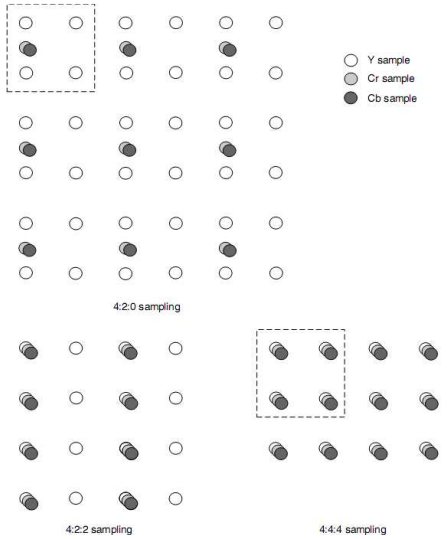

Fig. II-2: YC_bC_r sampling patterns, obtained from Richardson (2003).

YC_bC_r 4:4:4 sampling means that the three components have the same resolution. The numbers indicate the relative sampling rate of each component in the horizontal direction. In YC_bC_r 4:2:2 C_b and C_r have the same vertical resolution as Y but half the horizontal resolution. In YC_bC_r 4:2:0 C_b and C_r each have half the horizontal and vertical resolution of Y. The term 4:2:0 is misleading because the numbers do not have a logical interpretation (Richardson, 2003). Because the human visual system is more sensitive to luma than chroma, the YC_bC_r 4:2:0 sampling structure is the most widely used (Sullivan & Wiegand, 2005).

II.2 COMPRESSION

"Data compression can be viewed as a means for efficient representation of a digital source of data such as text, image, sound or any combination of all these types such as video. The goal of data compression is to represent a source in digital form with as few bits as possible while meeting the minimum requirement of reconstruction of the original" (Pu, 2006).

II.2.1 Lossless compression

"A compression approach is lossless only if it is possible to exactly reconstruct the original data from the compressed version. There is no loss of any information during the compression and decompression processes. Lossless compression is called reversible compression since the original data may be recovered perfectly by decompression" (Pu, 2006).

Lossless compression works by taking away redundant data: “information that, if removed, can be recreated from the remaining data” (Symes, 2004).

II.2.2 Lossy compression

A compression method is lossy if it is not possible to reconstruct the original exactly from the compressed version. Lossy compression is also called irreversible compression (Pu, 2006).

Ideally, lossy compression removes irrelevant information, that would mean that the recipient cannot perceive that it is missing. Information that is close to irrelevant, would mean that the quality loss is small compared to the reduction in the size of data (Symes, 2004).

“Approximate reconstruction may be desirable since it may lead to more effective compression. However, it often requires a good balance between the visual quality and the computation complexity” (Pu, 2006).

“Data such as multimedia images, video and audio are more easily compressed by lossy compression techniques because of the way that human visual and hearing systems work” (Pu, 2006). Lossy video compression systems are based on the principle of removing subjective redundancy, data that can be removed without radically affecting the viewer’s quality perception (Richardson, 2003).

II.2.3 Video Compression

Video compression is the process of compacting or condensing a digital video sequence into a smaller number of bits (Richardson, 2003).

Compression involves a complementary pair of systems, a compressor (encoder) and a decompressor (decoder). The encoder converts the source data into a compressed form prior to transmission or storage and the decoder converts the compressed form back into a representation of the original video data. “The encoder/decoder pair is often described as a CODEC (enCOder/ DECoder)” (Richardson, 2003).

According to Yuen & Wu (as cited in Winkler, 2005), a variety of artifacts can be distinguished in a compressed video sequence:

- The *blocking effect* or *blockiness* refers to a block pattern in the compressed sequence.

- *Blur* manifests itself as a loss of spatial detail and a reduction of edge sharpness.

- *Color bleeding* is the smearing of colors between areas of strongly differing chrominance.

- Slanted lines often exhibit the *staircase effect*

- *Ringing* is fundamentally is most evident along high-contrast edges in otherwise smooth areas.

- *False edges*.

- *Jagged motion*.

- *Mosquito noise,* a temporal artifact seen mainly in smoothly textured regions as luminance/chrominance fluctuations around high-contrast edges or moving objects.

- *Flickering* appears when a scene has high texture content.

- *Aliasing* can be noticed when the content of the scene is above the Nyquist rate, either spatially or temporally.

Fig. II-3: Typical compression artifacts, obtained from Winkler, 2005

II.2.4 Transmission Errors

Digitally compressed video is typically transferred over a packet-switched network. Two different types of impairments can occur when transporting media over noisy channels. Packets may be corrupted and thus discarded, or they may be delayed to the point where they are not received in time for decoding. To the

application, both have the same effect: part of the media stream is not available (Winkler, 2005).

Such losses can affect both the semantics and the syntax of the media stream. When the losses affect syntactic information, not only the data relevant to the lost block are corrupted, but also any other data that depend on this syntactic information. (Winkler, 2005).

II.3 QUALITY MEASUREMENT

II.3.1 Subjective Quality Measurement

Subjective evaluation that directly reflects human perception is considered to be the most accurate method of video quality measurement. It requires a large number of evaluators and a specially designed testing room (Choe & Lee, 2007).

Subjective testing for visual quality assessment has been formalized in ITU-R Rec. BT.500-11 (2002; as referenced in Winkler, 2005) and ITU-T Rec. P.910 (1999; as referenced in Winkler, 2005), which suggest “standard viewing conditions, criteria for the selection of observers and test material, assessment procedures, and data analysis methods” (Winkler, 2005).

“The perception of visual quality is influenced by spatial fidelity (how clearly parts of the scene can be seen) and temporal fidelity (whether motion appears natural and ‘smooth’). Other important influences on perceived quality include visual attention (an observer perceives a scene by fixating on a sequence of points in the image rather than by taking in everything simultaneously) and the so-called ‘recency effect’ (our opinion of a visual sequence is more heavily influenced by recently-viewed material than older video material). All of these factors make it very difficult to measure visual quality accurately and quantitatively” (Richardson, 2003).

Another disadvantage is that subjective quality measurement cannot be applied in real time, that is, during the encoding process (Choe & Lee, 2007).

II.3.2 Objective Quality Measurement

“Measuring visual quality using objective criteria gives accurate, repeatable results but as yet there are no objective measurement systems that completely reproduce the subjective experience of a human observer” (Richardson, 2003). Nevertheless, the complexity and cost of subjective quality measurement make it attractive to be able to measure quality automatically using an algorithm. (Richardson, 2003).

For a transform of size $N \times N$, the II.3.2.1 Mean Squared Error (MSE) is defined as:

$$MSE = \frac{1}{N^2} \sum_{i=0}^{N-1} \sum_{j=0}^{N-1} (C_{ij} - R_{ij})^2$$

Where C_{ij} is the actual value, and R_{ij} is the reference or reconstructed value as (Richardson, 2003).

For a transform of size $N \times N$, the II.3.2.1 Mean Absolute Error (MAE) is defined as:

$$MAE = \frac{1}{N^2} \sum_{i=0}^{N-1} \sum_{j=0}^{N-1} \left| C_{ij} - R_{ij} \right|$$

Where C_{ij} is the actual value, and R_{ij} is the reference or reconstructed value as (Richardson, 2003).

For a transform of size $N \times N$, the II.3.2.1 Sum of Absolute Errors (SAE) is defined as:

$$SAE = \sum_{i=0}^{N-1} \sum_{j=0}^{N-1} \left| C_{ij} - R_{ij} \right|$$

Where C_{ij} is the actual value, and R_{ij} is the reference or reconstructed value as (Richardson, 2003).

The Peak Signal to Noise Ratio (PSNR) depends on the MSE between an original and a reconstructed image or video frame, "relative to $(2^n - 1)^2$ (the square of the highest-possible signal value in the image, where n is the number of bits per image sample)". (Richardson, 2003).

$$PSNR_{db} = 10log \frac{(2^n - 1)^2}{MSE}$$

The PSNR is widely used as a video quality metric. However, it has been reported that the PSNR does not necessarily reflect human visual perception and may not directly be used as a perceptual quality measure since there are other coding artifacts such as ringing and blurring (Choe & Lee, 2007).

Chapter III

VIDEO CODEC

A video CODEC encodes a source image or video sequence into a compressed form and decodes it to produce a copy or approximation of the source sequence (Richardson, 2003).

"The basic communication problem may be posed as conveying source data with the highest fidelity possible within an available bit rate, or it may be posed as conveying the source data using the lowest bit rate possible while maintaining specified reproduction fidelity. In either case, a fundamental tradeoff is made between bit rate and fidelity. The ability of a source coding system to make this tradeoff well is called its coding efficiency or rate-distortion performance, and the coding system itself is referred to as a codec" (Sullivan & Wiegand, 2005).

According to Sullivan & Wiegand (2005), video codecs are primarily characterized in terms of:

- *Throughput of the channel*: a characteristic influenced by the transmission channel bit rate and the amount of protocol and error-correction coding overhead incurred by the transmission system.

- Distortion of the decoded video: distortion is primarily induced by the video codec and by channel errors in the path to the video decoder.

  In practical video transmission systems the following additional issues must be considered as well:

- Delay (startup latency and end-to-end delay): Delay characteristics are influenced by many parameters, including processing delay, buffering, structural delays of video and channel codecs, and the speed at which data are conveyed through the transmission channel.

- Complexity (in terms of computation, memory capacity, and memory access requirements). The complexity of the video codec, protocol stacks, and network. Hence, the practical source coding design problem is posed as follows: given a maximum allowed delay and a maximum allowed complexity, achieve an optimal tradeoff between bit rate and distortion for the range of network environments envisioned in the scope of the applications. The various application scenarios of video communication show very different optimum working points, and these working points have shifted over time as the constraints on complexity have been eased by Moore's law and as higher bit-rate channels have become available.

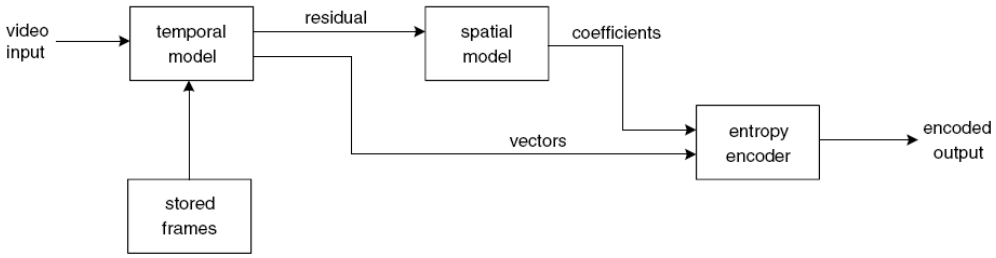

Fig. III-1: Video encoder block diagram, obtained from Richardson (2003).

A video encoder consists of three main functional units: a temporal model, a spatial model and an entropy coder (Richardson, 2003).

III.1 TEMPORAL MODEL

The goal of the temporal model is to reduce redundancy between transmitted frames by forming a predicted frame and subtracting this from the current frame. This process yields a residual (difference) frame and the more accurate the prediction process, the less energy is contained in the residual frame. "The residual frame is encoded and sent to the decoder which recreates the predicted frame, adds the decoded residual and reconstructs the current frame. The predicted frame is created from one or more past or future frames ('reference frames'). The accuracy of the prediction can usually be improved by compensating for motion between the reference frame(s) and the current frame" (Richardson, 2003).

The input to the temporal model is an uncompressed video sequence. “The output of the temporal model is a residual frame (created by subtracting the prediction from the actual current frame) and a set of model parameters, typically a set of motion vectors describing how the motion was compensated” (Richardson, 2003).

III.1.1 Prediction from the Previous Video Frame

The simplest method of temporal prediction is to use the previous frame as the predictor for the current frame. “The obvious problem with this simple prediction is that a lot of energy remains in the residual frame and this means that there is still a significant amount of information to compress after temporal prediction. Much of the residual energy is due to object movements between the two frames and a better prediction may be formed by compensating for motion between the two frames” (Richardson, 2003).

“Changes between video frames may be caused by object motion, camera motion, uncovered regions and lighting changes. With the exception of uncovered regions and lighting changes, these differences correspond to pixel movements between frames. It is possible to estimate the trajectory of each pixel between successive video frames, producing a field of pixel trajectories” (Richardson, 2003).

III.2 SPATIAL MODEL

The residual frame forms the input to the spatial model which makes use of similarities between neighboring samples in the residual frame to reduce spatial redundancy. Usually this is achieved by applying a transform to the residual samples and quantizing the results. The output of the spatial model is a set of quantized transform coefficients (Richardson, 2003).

III.2.1 Transformation

“A transform is a mathematical rule that may be used to convert one set of values to a different set” (Symes, 2004).

“Subband coding is a generalization of transform coding. In it, an information-carrying signal is first decomposed into a number of separate frequency components. This process of dividing the full frequency band into separate ideally flat subbands removes the redundancy in the input signal and provides a set of uncorrelated subbands. Due to the orthogonality of different subbands, each subband can be encoded independently” (Sharifi, 1995).

III.2.1.1 DCT

Ahmed, Natarajan & Rao (1974) defined the DCT of a data sequence *X(m)*, *m* = 0, 1, …, (*M* - 1) as:

$$G_X(0) = \frac{\sqrt{2}}{M} \sum_{m=0}^{M-1} X(m)$$

$$G_X(k) = \frac{2}{M} \sum_{m=0}^{M-1} X(m) \cos \frac{(2m+1)k \prod}{2M} \quad k=1, 2, \ldots, (M-1)$$

Where $G_x(k)$ is the *k*th DCT coefficient.

The inverse cosine discrete transform (IDCT) is defined as:

$$X(m) = \frac{1}{\sqrt{2}} G_x(0) + \sum_{k=1}^{M-1} G_x(k) \cos \frac{(2m+1)k \prod}{2M}, \quad m=0, 1, \ldots, (M-1)$$

If the inverse transform is written in matrix form and Λ is the *(M × M)* matrix that denotes the cosine transformation, then the orthogonal property can be expressed as:

$$\Lambda^T \Lambda = \frac{M}{2}[I]$$

where Λ^T is the transpose of Λ and [I] is the *(M × M)* identity matrix (Ahmed et al. 1974).

“The performance of the DCT, particularly important in transform coding, is associated with the Karhunen-Loève transform. KLT is an optimal transform for data compression in a statistical sense because it decorrelates a signal in the transform domain, packs the most information in a few coefficients, and minimizes mean-square error between the reconstructed and original signal compared to any other transform. However, KLT is constructed from the eigenvalues and the corresponding eigenvectors of a covariance matrix of the data to be transformed; it is signal-dependent, and there is no general algorithm for its fast computation” (Britanak, 2001).

Wang & Hunt (1985; as cited in Britanak 2001) mention different types of DCT transforms:

$$DCT-I: [C_{N+1}^{I}]_{nk} = \sqrt{\frac{2}{N}}\left[\epsilon_n \epsilon_k \cos\frac{\pi nk}{N}\right], n, k = 0,1, \dots, N$$

$$DCT-II: [C_{N}^{II}]_{nk} = \sqrt{\frac{2}{N}}\left[\epsilon_k \cos\frac{\pi(2n+1)k}{2N}\right], n, k = 0,1, \dots, N-1$$

$$DCT-III: [C_{N}^{III}]_{nk} = \sqrt{\frac{2}{N}}\left[\epsilon_n \cos\frac{\pi(2k+1)n}{2N}\right], n, k = 0,1, \dots, N-1$$

$$DCT-IV: [C_{N}^{IV}]_{nk} = \sqrt{\frac{2}{N}}\left[\cos\frac{\pi(2n+1)(2k+1)}{4N}\right], n, k = 0,1, \dots, N-1$$

$$\epsilon_p = \begin{cases} \frac{1}{\sqrt{2}} & p = 0 \; or \; p = N \\ 1 & otherwise \end{cases}$$

Where N is assumed to be an integer power of 2 (Wang & Hunt, 1985; as cited in Britanak 2001).

III.2.2 Quantization

The quantizer can be defined as consisting of a set of intervals or cells $S = \{S_i; i \in \mathfrak{I}\}$, where the index set $\mathfrak{I}$ is ordinarily a collection of consecutive integers beginning with 0 or 1, together with a set of reproduction values or points or levels $C = \{y_i; i \in \mathfrak{I}\}$, so that the overall quantizer q is defined by $q(x) = y_i$ for $x \in S_i$, which can be expressed concisely as (Gray & Neuhoff, 1998):

$$q(x) = \sum_i y_i 1_{S_i}(x)$$

Where the indicator function $1_S(x)$ is 1 if $x \in S_i$ and 0 otherwise. Assuming that S is a partition of the real line. That is, the cells are disjoint and exhaustive (Gray & Neuhoff, 1998).

"A quantizer is said to be uniform if, as in the round off case, the levels y_i are equispaced, say Δ apart, and the thresholds a_i are midway between adjacent levels. If an infinite number of levels are allowed, then all cells S_i will have width equal to Δ, the separation between levels. If only a finite number of levels are

allowed, then all but two cells will have width Δ and the outermost cells will be semi-infinite" (Gray & Neuhoff, 1998).

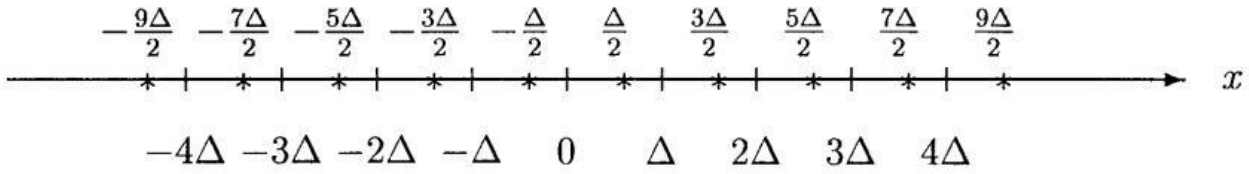

Fig. III-2: Uniform Quantizer, obtained from Gray & Neuhoff (1998).

The class of quantizer that has been used in all standard video codecs is based around the uniform threshold quantizer (UTQ). It has equal step sizes with reconstruction values nailed to the centroid of the steps. (Ghanbari, 2003)

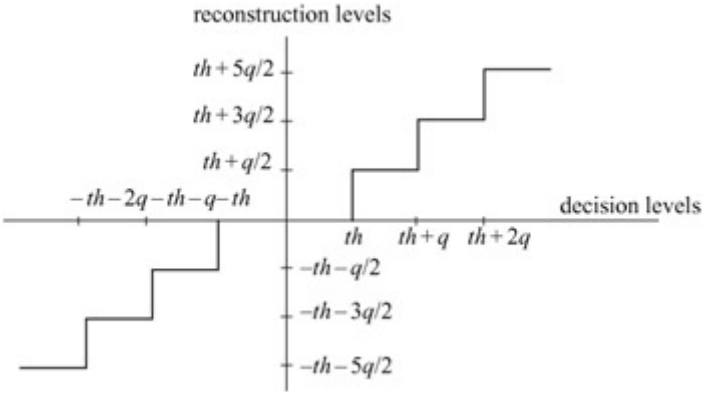

Fig. III-3: Quantization characteristics, obtained from Ghanbari (2003).

The two key parameters that define a UTQ are the threshold value, *th*, and the step size, *q*. "The centroid value is typically defined mid way between quantization intervals. Note that, although AC transform coefficients have non-uniform characteristics, and hence can be better quantized with non-uniform quantizer step sizes (the DC coefficient has a fairly uniform distribution), bit rate control would be easier if they were quantized linearly. Hence, a key property of UTQ is that the step sizes can be easily adapted to facilitate rate control". (Ghanbari, 2003).

In practice, rather than transmitting a quantized coefficient to the decoder, its ratio to the quantizer step size, called the quantization index, *I*.

$$I(u,v) = \left\lfloor \frac{F(u,v)}{q} \right\rfloor$$

At the decoder, the reconstructed coefficients, $F^q(u,v)$, after inverse quantization are given by:

$$F^q(u,v) = \left\{ I(u,v) \pm \frac{1}{2} \right\} \times q$$

One of the main problems of linear quantizers in DPCM is that for lower bit rates the number of quantization levels is limited and hence the quantizer step size is large. In coding of plain areas of the picture, if a quantizer with an even number of levels is used, then the reconstructed pixels oscillate between -q/2 and q/2. This type of noise at these areas, in particular at low luminance levels, is visible and is called granular noise. (Ghanbari, 2003).

Larger quantizer step sizes with an odd number of levels (dead zone) reduce the granular noise, but cause loss of pixel resolution at the plain areas. This type of noise when the quantizer step size is relatively large is annoying and is called contouring noise. (Ghanbari, 2003).

III.3 ENTROPY CODING

Entropy Coding is a process by which discrete-valued source symbols are represented in a manner that takes advantage of the relative probabilities of the various possible values of each source symbol (Sullivan & Wiegand, 2005).

The parameters of the temporal model and the spatial model are compressed by the entropy encoder. This removes statistical redundancy in the data and produces a compressed bit stream or file. “A compressed sequence consists of coded motion vector parameters, coded residual coefficients and header information” (Richardson, 2003).

The entropy of an information source is defined as (Shannon, 1948):

$$H = \sum_{j=1}^{n} p_j log \frac{1}{p_j} = -\sum_{j=1}^{n} p_j log p_j$$

for independent symbols. Where p_j is the probability of symbol j and n is the number of symbols.

If the logarithm of the base 2 is used, the entropy is represented in terms of bits, which is a contraction of *binary unit* (Abramson, 1963).

Without entropy coding, a quantizer with L levels would require $log_2[L]$ bits to represent each sample at the quantizer output. Entropy coding reduces this value to $H(Q) \leq log_2[L]$ (Sharifi, 1995).

“The Entropy $H(Q)$ of the output of a quantizer is the minimum amount of information which must be transmitted in order to be able to determine the quantizer output with an arbitrarily small error” (Gish & Pierce, 1968).

III.3.1 Huffman Coding

Huffman (1952) proposed a technique for the construction of minimum-redundancy codes. A “minimum-redundancy code” is defined as an ensemble code which, for a message ensemble consisting of a finite number of members, *N*, and for a given number of coding digits, *D*, yields the lowest possible average message length (Huffman, 1952).

$$L_{av} = \sum_{i}^{N} P(i)L(i)$$

Where N is the number of messages in the ensemble, $P(i)$ is the probability of the ith message and $L(i)$ is the number of coding digits assigned to it (Huffman, 1952).

The procedure involves two processes, source reduction followed by codeword construction. In the source reduction, the two least probable symbols are combined, leaving an alphabet with one less symbol. The combined symbol has a probability equal to the sum of the probabilities of the two original symbols. The process is repeated until there are only two symbols. The codeword construction begins allocating the codes 0 and 1 to the two remaining symbols. Conventionally 0 is used to represent the higher priority and 1 the lower priority. Then, each composite symbol is spited by appending 0 and 1 to its code, and the process continues until all the composite symbols have been reduced to original symbols of the alphabet (Symes, 2004).

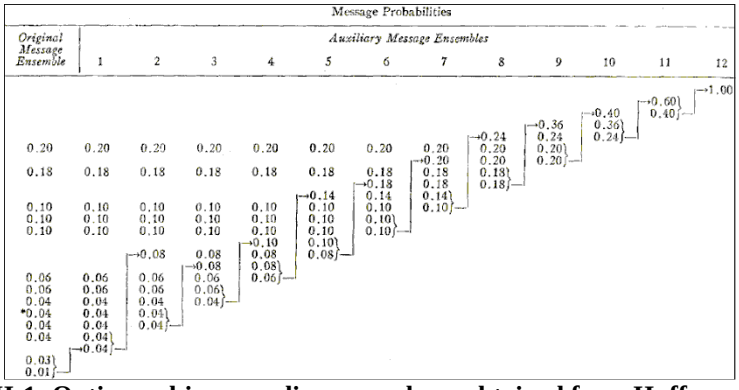

Table III-1: Optimum binary coding procedure, obtained from Huffman (1952).

III.3.2 Run-Length Encodings

Many compression methods are based on run-length encoding (RLE). Imagine a binary string. Let p be the probability that a zero appears and $(1-p)$ the probability that a one appear. If p is large, there will be runs of zeros, suggesting the use of RLE to compress the string. The probability of a run of n zeros is p^n, and the probability of a run of n zeros followed by a 1 is $p^n(1-p)$ indicating that run lengths are distributed geometrically (Salomon, 2007).

Golomb (1966) proposed the following encoding procedure:

Calculate:

$$m = -\frac{\log(2)}{\log(p)}$$

That is $p^m = 1/2$. The results will be most readily applicable for those p such that m is an integer (Golomb, 1966).

By computing:

$$q = \left\lfloor \frac{n}{m} \right\rfloor$$
$$r = n - qm$$
$$c = \lceil \log_2(m) \rceil$$

The code is constructed in two parts; the first is the value of the quotient q, coded in unary; the second is the binary value of the remainder r coded in a special way. The first $2^c - m$ values of r are coded, as unsigned integers, in $(c-1)$ bits each, and the rest are coded in c bits each. The case where m is a power of 2 is special because it does not require $(c-1)$ bit codes. Once a Golomb code is decoded, the relation $n = r - qm$ and the values of q and r can be used to easily reconstruct n (Salomon, 2007).

III.4 DECODER

The video decoder reconstructs a video frame from the compressed bit stream. The coefficients and motion vectors are decoded by an entropy decoder after which the spatial model is decoded to reconstruct a version of the residual frame. “The decoder uses the motion vector parameters, together with one or more previously decoded frames, to create a prediction of the current frame and the frame itself is reconstructed by adding the residual frame to this prediction”. (Richardson, 2003).

Chapter IV

THE H.264 ENCODER (VCL)

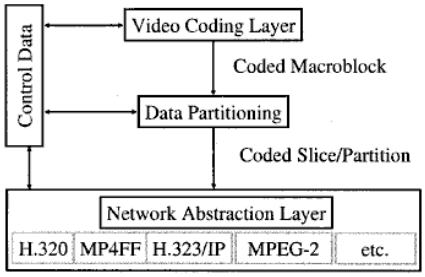

Fig. IV-1: Structure of H.264/AVC video encoder, obtained from Wiegand et al (2003).

According to Wiegand et al. (2003), the H.264/AVC design covers a Video Coding Layer (VCL), which is designed to efficiently represent the video content, and a Network Abstraction Layer (NAL), which formats the VCL representation of the video and provides header information in a manner appropriate for transference by a variety of transport layers or storage media.

In this chapter the encoding function of the VCL is briefly explained. The NAL is out of the scope of this thesis.

IV.1 MACROBLOCKS

A picture is partitioned into fixed size macroblocks that each one covers a rectangular picture area of 16x16 samples of the luma component and 8x8

samples of each of the two chroma components. Macroblocks are the basic building blocks of the standard for which the decoding process is specified. (Wiegand, Sullivan, Bjøtegaard, & Luthra, 2003).

IV.2 SLICES AND SLICE GROUPS

"Slices are a sequence of macroblocks which are processed in the order of a raster scan when not using FMO (Flexible Macroblock Ordering). A picture may be split into one or several slices. A picture is therefore a collection of one or more slices in H.264/AVC. Slices are self-contained in the sense that given the active sequence and picture parameter sets, their syntax elements can be parsed from the bitstream and the values of the samples in the area of the picture that the slice represents can be correctly decoded without use of data from other slices provided that utilized reference pictures are identical at encoder and decoder" (Wiegand, Sullivan, Bjøtegaard, & Luthra, 2003).

According to Wiegand, et al. (2003), each slice can be coded using different coding types as follows:

- I slice: A slice in which all macroblocks of the slice are coded using intra prediction.
- P slice: In addition to the coding types of the I slice, some macroblocks of the P slice can also be coded using inter prediction with at most one motion-compensated prediction signal per prediction block.
- B slice: In addition to the coding types available in a P slice, some macroblocks of the B slice can also be coded using inter prediction with two motion-compensated prediction signals per prediction block.

The above three coding types are very similar to those in previous standards with the exception of the use of reference pictures as described below. The following two coding types for slices are new.

- SP slice: A so-called switching P slice that is coded such that efficient switching between different pre-coded pictures becomes possible.
- SI slice: A so-called switching I slice that allows an exact match of a macroblock in an SP slice for random access and error recovery purposes.

SP-frames make use of motion compensated predictive coding to exploit temporal redundancy in the sequence similar to P-frames. The difference between SP- and P-frames is that SP-frames allow identical frames to be reconstructed

even when they are predicted using different reference frames. Due to this property, SP-frames can be used instead of I-frames in such applications as bitstream switching, splicing, random access, fast forward, fast backward, and error resilience/recovery. At the same time, since SP-frames unlike I-frames are utilizing motion-compensated predictive coding, they require significantly fewer bits than I-frames to achieve similar quality. In some of the mentioned applications, SI-frames are used in conjunction with SP-frames. An SI-frame uses only spatial prediction as an I-frame and still reconstructs identically the corresponding SP-frame, which uses motion-compensated prediction. (Karczewicz & Kurceren, 2003).

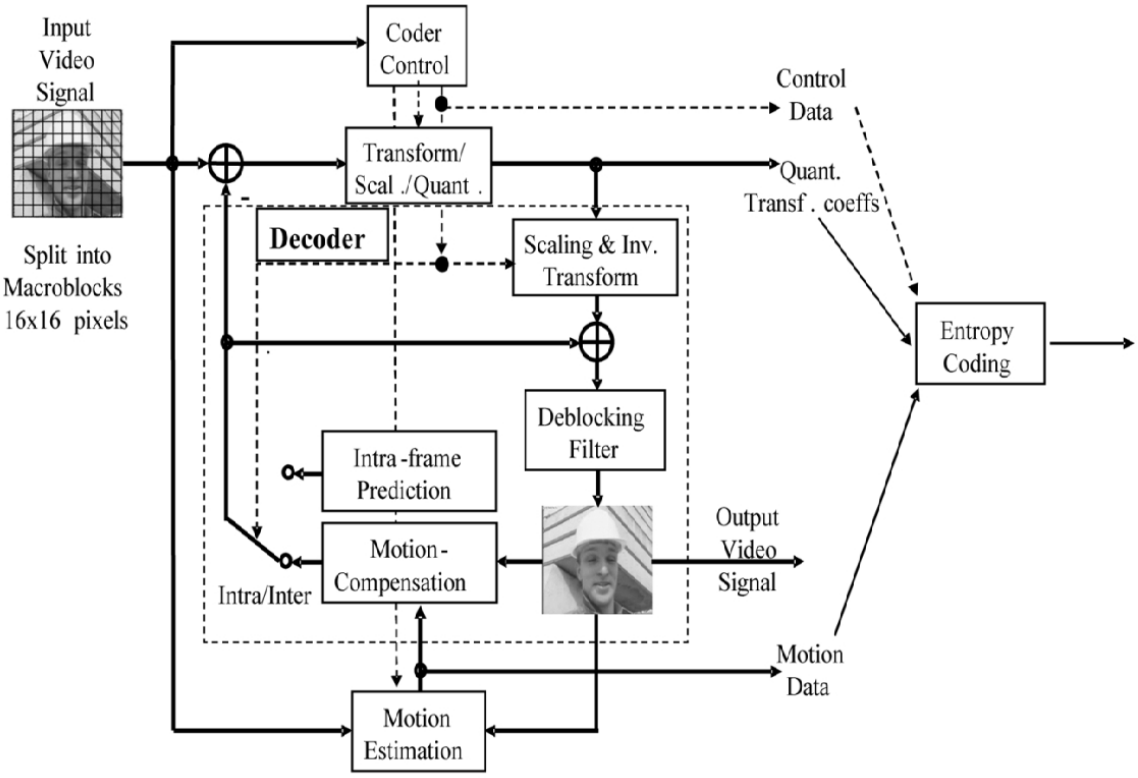

Fig. IV-2: Basic coding structure for H.264/AVC for a macroblock, obtained from Wiegand et al. (2003).

IV.3 MOTION ESTIMATION

Xu & Zhou (2004) state that in the VCL layer of H.264 the block-based displacement from previous frames serves to estimate the inter-frame motion. The estimated Motion Vectors (MVs) can then be predicted from spatially adjacent vectors, thus improving compression efficiency. In the case of the intra pictures, the video compression is achieved through directional prediction in the spatial domain. The motion estimation part of the VCL is out of the scope of this thesis.

IV.4 TRANSFORMATION AND QUANTIZATION

IV.4.1 Transformation

Similar to previous video coding standards, H.264/AVC utilizes transform coding of the prediction residual. Instead of discrete cosine transform (DCT), a separable integer transform with similar properties as DCT is used. This characteristic of the transform in H.264 makes it different than the previous video codecs (Wiegand, Sullivan, Bjøtegaard, & Luthra, 2003).

For the DCT of the luma components the H.264 can use a 4x4 or a 8x8 DCT transform (Schwarz, Marpe, & Wiegand, 2007).

Malvar, Hallapuro, Karczewicz (2002, as cited in Malvar et al. 2003) proposed the following 4x4 transformation for H.264:

> The integer transform used in H.264 is obtained by rounding the scaled entries of the DCT matrix to nearest integers:
>
> H = round { α ADCT }
>
> Where ADCT is the DCT matrix. Setting α = 0.25 leads to the new set of coefficients {a=1, b=2, c=1}

$$\mathbf{H} = \begin{bmatrix} 1 & 1 & 1 & 1 \\ 2 & 1 & -1 & -2 \\ 1 & -1 & -1 & 1 \\ 1 & -2 & 2 & -1 \end{bmatrix}$$

> For the inverse transform, they proposed in **H** the scaling the odd-symmetric basis functions by ½; that is, replacing the rows [2 1 -1 -2] and [1 -2 2 -1] by [1 1/2 -1/2 -1] and [1/2 -1 1 -1/2], respectively. That way, the sum of absolute values of the odd functions is halved to three. The inverse transform matrix is then defined by:

$$\tilde{\mathbf{H}}_{\mathbf{inv}} = \begin{bmatrix} 1 & 1 & 1 & 1/2 \\ 1 & 1/2 & -1 & -1 \\ 1 & -1/2 & -1 & 1 \\ 1 & -1 & 1 & -1/2 \end{bmatrix}$$

Where the tilde indicates that $\tilde{H}_{inv}$ is a scaled inverse of H.

"The multiplications by ½ can be implemented by sign-preserving 1-bit right shifts, so all decoders produce identical results. A key observation is that the small errors caused by the right shifts are compensated by the 2-bit gain in the dynamic range of the input to the inverse transform" (Malvar, Hallapuro, Karczewicz, & Kerofsky, 2003).

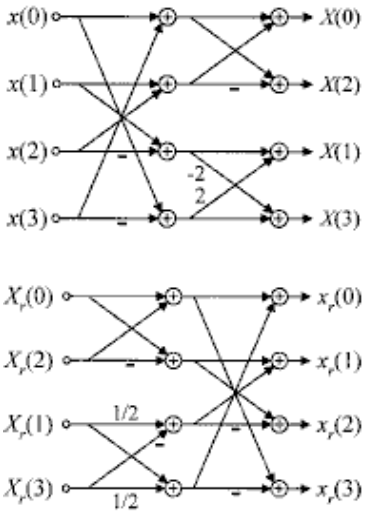

Fig. IV-3: Fast implementation of the H.264 direct transform (top) and inverse transform (bottom), obtained from Malvar et al. (2003)

In a similar way, Bossen (2002) proposed the 8x8 transform for H.264.

1	12/8	1	10/8	1	6/8	½	3/8
1	10/8	1/2	-3/8	-1	-12/8	-1	-6/8
1	6/8	-1/2	-12/8	-1	3/8	1	10/8
1	3/8	-1	-6/8	1	10/8	-1/2	-12/8
1	-3/8	-1	6/8	1	-10/8	-1/2	12/8
1	-6/8	-1/2	12/8	-1	-3/8	1	-10/8
1	-10/8	1/2	3/8	-1	12/8	-1	6/8
1	-12/8	1	-10/8	1	-6/8	½	-3/8

Table IV-1:Inverse 8x8 transform basis, obtained from (Bossen, 2002)

Wien (2003) presents the concept of variable block size transform coding. The scheme is called adaptive block-size transforms (ABT), indicating the adaptation of the transform block size to the block size used for motion compensation.

The large transforms can provide a better energy compaction and a better preservation of detail in a quantized signal than a small transform does. On the

other hand, larger transforms introduce more ringing artifacts caused by quantization than small transforms do. By choosing the transform size according to the signal properties, the tradeoff between energy compaction and preserved detail on the one hand and ringing artifacts on the other can be optimized. (Wien, 2003).

IV.4.2 Quantization

"In lossy compression, quantization is the step that introduces signal loss, for better compression" (Malvar, Hallapuro, Karczewicz, & Kerofsky, 2003). To avoid divisions, the H.264 implements new formulas for quantization:

$$X_q(i,j) = sign\{X(i,j)\}[(|X(i,j)|]A(Q) + f\,2^L) >> L]$$
$$X_r(i,j) = X_q(i,j)B(Q)$$
$$x_r = (H^T X_r + 2^{N-1} e) >> N$$

Where, e = $[1\ 1\ 1\ 1]^T$; Q varies from zero to Q_{max}, and "the association of quantization parameters *A(Q)* and *B(Q)* are such that zero corresponds to the finest quantization and Q_{max} the coarsest quantization" (Malvar, Hallapuro, Karczewicz, & Kerofsky, 2003).

A quantization parameter is used for determining the quantization of transform coefficients in H.264/AVC. The parameter can take 52 values. These values are arranged so that an increase of 1 in quantization parameter means an increase of quantization step size by approximately 12% (an increase of 6 means an increase of quantization step size by exactly a factor of 2 (Wiegand, Sullivan, Bjøtegaard, & Luthra, 2003).

The code of the subroutine used to convert the quantization parameter QP, into the quantizer step size is the following (Sühring, 2007):

```
double QP2Qstep( int QP )
{
 int i;
 double Qstep;
 static const double QP2QSTEP[6] = { 0.625, 0.6875, 0.8125, 0.875, 1.0, 1.125 };
 Qstep = QP2QSTEP[QP % 6];
 for( i=0; i<(QP/6); i++)
  Qstep *= 2;
 return Qstep;
}
```

IV.5 ENTROPY CODING

In H.264/MPEG4-AVC, many syntax elements are coded using the same highly-structured infinite-extent variable-length code (VLC), called a zero-order exponential-Golomb code. A few syntax elements are also coded using simple fixed-length code representations. For the remaining syntax elements, two types of entropy coding are supported, CAVLC and CABAC (Marpe, Wiegand, & Sullivan, 2006).

When using the first entropy-coding configuration, which is intended for lower-complexity implementations, the exponential-Golomb code is used for nearly all syntax elements except those of quantized transform coefficients (Marpe et al., 2006).

“The simpler entropy coding method uses a single infinite-extent codeword table for all syntax elements except the quantized transform coefficients. Thus, instead of designing a different VLC table for each syntax element, only the mapping to the single codeword table is customized according to the data statistics. The single codeword table chosen is an exp-Golomb code with very simple and regular decoding properties” (Wiegand et al. 2003)

IV.5.1 CAVLC

In the Context-adaptive variable length coding (CAVLC) entropy coding method, the number of nonzero quantized coefficients (N) and the actual size and position of the coefficients are coded separately. After zigzag scanning of transform coefficients, their statistical distribution typically shows large values for the low frequency part decreasing to small values later in the scan for the high-frequency part (Wiegand et al., 2003).

When using CAVLC, the encoder switches between different VLC tables for various syntax elements, depending on the values of the previously transmitted syntax elements in the same slice. Since the VLC tables are designed to match the conditional probabilities of the context, the entropy coding performance is improved from that of schemes that do not use context-based adaptivity (Marpe, Wiegand, & Sullivan, 2006).

IV.5.2 CABAC

The Context-based Adaptive Binary Arithmetic Coding (CABAC) design is based on three components: binarization, context modeling, and binary arithmetic coding. Binarization enables efficient binary arithmetic coding by mapping

nonbinary syntax elements to sequences of bits referred to as bin strings. The bins of a bin string can each be processed in either an arithmetic coding mode or a bypass mode. The latter is a simplified coding mode that is chosen for selected bins such as sign information or lesser-significance bins in order to speed up the overall decoding (and encoding) processes. The arithmetic coding mode provides the largest compression benefit, where a bin may be context-modeled and subsequently arithmetic encoded. (Marpe, Wiegand, & Sullivan, 2006).

The compression performance of the arithmetic coded bins is optimized by adaptive estimation of the corresponding (context-conditional) probability distributions. The probability estimation and the actual binary arithmetic coding are conducted using a multiplication-free method that enables efficient implementations in hardware and software (Marpe et al., 2006).

Chapter V

DCT MODELING

V.1 LAPLACE PROBABILITY DENSITY FUNCTION

A random variable X is distributed as Laplacian, or double exponential, if its probability density function (PDF) is given by (Evans, Hastings, & Peacock, 1993):

$$L(x;\mu,\sigma) = \frac{1}{2b} e^{-\left|\frac{x-\mu}{b}\right|}, x \in \mathbb{R}$$

Where $\mu \in \mathbb{R}$, $\sigma > 0$, and $b = \left[\frac{\sigma^2}{2}\right]^{1/2}$.

The C.D.F. is defined by (Evans, Hastings, & Peacock, 1993):

$$F_X(x) = \begin{cases} \frac{1}{2} e^{-\left|\frac{\mu-x}{b}\right|}, & x < \mu \\ 1 - \frac{1}{2} e^{-\left|\frac{x-\mu}{b}\right|}, & x \geq \mu \end{cases}$$

V.2 GENERALIZED GAUSSIAN PROBABILITY DENSITY FUNCTION

A random variable X is distributed as generalized Gaussian if its probability density function (pdf) is given by (Domínguez-Molina, González-Farías, & Rodríguez-Dagnino, 2001):

$$gg(x;\mu,\sigma,p) = \frac{1}{2\Gamma(1+1/p)A(p,\sigma)} e^{-\left|\frac{x-\mu}{A(p,\sigma)}\right|^p}, x \in \mathbb{R}$$

Where $\mu \in \mathbb{R}$, $p,\sigma > 0$, and $A(p,\sigma) = \left[\frac{\sigma^2\Gamma(1/p)}{\Gamma(3/p)}\right]^{1/2}$.

$\Gamma(b)$ is the Gamma function defined as (Abramowitz & Stegun, 1972):

$$\Gamma(b) = \int_0^\infty v^{b-1}e^{-v}\,dv$$

The parameter μ is the mean, the function $A(p,\sigma)$ is a scaling factor which allows that $Var(X) = \sigma^2$, and p is the shape parameter.

When $p = 1$, the G.G. corresponds to a Laplacian distribution, $p = 2$ corresponds to a Gaussian distribution, whereas in the limiting cases $p \to +\infty$ it converges to a uniform distribution in $(\mu - \sqrt{3}\sigma, \mu + \sqrt{3}\sigma)$, and when $p \to 0+$ the distribution becomes a degenerate one in $x = \mu$ (Domínguez-Molina, González-Farías, & Rodríguez-Dagnino, 2001).

Using the following property of the Gamma function:

$$\Gamma(z+1) = \mathrm{z}\Gamma(z)$$

$$gg(x;\mu,\sigma,p) = \frac{p}{2\Gamma(1/p)A(p,\sigma)} e^{-\left|\frac{x-\mu}{A(p,\sigma)}\right|^p}, x \in \mathbb{R}$$

The C.D.F. is defined by (Nadarajah, 2005):

$$F_X(x) = \begin{cases} \dfrac{\Gamma\left(\frac{1}{p}, \left(\frac{\mu - x}{A(p,\sigma)}\right)^p\right)}{2\Gamma\left(\frac{1}{p}\right)}, & x \leq \mu \\ 1 - \dfrac{\Gamma\left(\frac{1}{p}, \left(\frac{x - \mu}{A(p,\sigma)}\right)^p\right)}{2\Gamma\left(\frac{1}{p}\right)}, & x > \mu \end{cases}$$

Where $\Gamma(b,z)$ is the upper incomplete gamma function, defined as (Abramowitz & Stegun, 1972):

$$\Gamma(b,z) = \int_z^\infty v^{b-1} e^{-v}\, dv$$

V.2.1 Parameter Estimation

There are many methods to find the p parameter for the Generalized Gaussian PDF, most of them are either based on the maximum likelihood or on the the moments (Varanasi & Aazhang, 1989); there is also a method based on entropy matching (Aiazzi et al., 1999).

The Maximum Likelihood estimate of the p parameter is the root of the equation:

$$\frac{\psi\left(\frac{1}{p} + 1\right) + \log(p)}{p^2} + \frac{1}{p^2} log\left(\frac{1}{n}\sum_{i=1}^{n} |x_i|^p\right) - \frac{\sum_{i=1}^{n} |x_i|^p log|x_i|}{\sum_{i=1}^{n} |x_i|^p} = 0$$

Where:

$$\psi(\tau) = -\gamma + \int_0^1 (1 - t^{\tau-1})(1-t)^{-1}\, dt$$

and $\gamma = 0.577$ ... denotes the Euler constant (Du, 1991; as cited in Müller, 1993; and in Joshi & Fisher, 1995).

The Entropy-Matching Method (Aiazzi, Alparone, & Baronti, 1999) uses the Entropy of the Generalized Gaussian source:

$$h_{GG} = \frac{1}{pln(2)} - \log_2\left(\frac{p}{2A(p,\sigma)\Gamma\left(\frac{1}{p}\right)}\right)$$

And the zero order entropy obtained after quantization:

$$H_0 = -\sum_i P(iQ) log_2[P(iQ)]$$

Where $P(iQ)$ is the probability that a coefficient is quantized to iQ, where $\{i = 0, \pm 1, \pm 2, \dots\}$ and Q is the quantizer step size.

Then, assuming that the standard deviation $\sigma \gg Q$, the approximation:

$$H_0 \approx h_{GG} - log_2(Q)$$

Can be used and then solve numerically for the parameter p (Aiazzi, Alparone, & Baronti, 1999).

The methods based on Moments consist of equating an appropriate number of sample moments to the corresponding parametric moments of the distribution (Varanasi & Aazhang, 1989).

In general, the nth moment of a random variable X is defined by (León-García, 1994):

$$E[X^n] = \int_{-\infty}^{\infty} x^n f_X(x)\, dx$$

One well-known method based on moments was first proposed by Mallat (1989) and was gradually improved in (Sharifi & León-García, 1995), (Rodríguez-Dagnino & León-García, 1998), (Domínguez-Molina, González-Farías, & Rodríguez-Dagnino, 2001). It can be resumed as follows:

Calculate:

$$M(p) = \frac{\Gamma^2\left(\frac{2}{p}\right)}{\Gamma\left(\frac{1}{p}\right)\Gamma\left(\frac{3}{p}\right)}$$

$$\bar{M}(X) = \frac{(E|X|)^2}{EX^2}$$

Where:

$$(E|X|)^2 = \left(\frac{1}{n}\sum_{i=1}^{n}|X_i - \mu|\right)^2$$

$$EX^2 = \frac{1}{n}\sum_{i=1}^{n}|X_i - \mu|^2$$

Then, by making

$$M(p) = \bar{M}(X)$$

Solve numerically for p (Domínguez-Molina, González-Farías, & Rodríguez-Dagnino, 2001).

Summarizing, the Maximum Likelihood methods are among the most accurate for the estimation of the p parameter, nevertheless, their theoretical formulation and numerical solution make them unsuitable for real-time applications (Aiazzi, Alparone, & Baronti, 1999). The Entropy Matching method proposed in Aiazzi et al. (1999) depends on the assumption $\sigma \gg Q$, which is restricted to small values of the quantizer step size. The methods based on the Moments, in general, are less accurate than the Maximum Likelihood methods; however they have the advantage of being more computationally efficient.

In this thesis, the method for the estimation of the p parameter explained in Domínguez-Molina et al. (2001) was used because of its relative effectiveness and efficiency; also because it has been successfully used in Sun et al. (2005).

V.3 CAUCHY PROBABILITY DENSITY FUNCTION

A random variable X is distributed as Cauchy if its probability density function (PDF) is given by:

$$cauchy(x; a, b) = \frac{b/\pi}{b^2 + (x-a)^2}, x \in \mathbb{R}$$

Where $a \in \mathbb{R}$ and $b > 0$. The parameter a is the location, and b is the scale (Koutrouvelis, 1982).

"The Cauchy distribution is unimodal and symmetric, with much heavier tails than the normal. The probability density function is symmetric about a, with upper and lower quartiles, $a \pm b$" (Evans, Hastings, & Peacock, 1993).

The C.D.F. is defined by (Evans, Hastings, & Peacock, 1993):

$$F_X(x) = \frac{1}{2} + \frac{1}{\pi}\tan^{-1}\left(\frac{x-a}{b}\right)$$

V.3.1 Parameter Estimation

There are many methods to find the scale parameter for the Cauchy PDF, some are based in the maximum likelihood and others on order statistics. For a list of references see (Koutrouvelis, 1982).

The maximum likelihood estimators of a and b are the solutions of the equations:

$$\frac{1}{n}\sum_{i=1}^{n}\frac{2}{1+[(x_i-a)/b]^2} = 1$$

$$\frac{1}{n}\sum_{i=1}^{n}\frac{2x_i}{1+[(x_i-a)/b]^2} = a$$

Where n is the sample size (Krishnamoorthy, 2006).

For the location parameter, “the maximum likelihood estimator is consistent and asymptotically efficient; unfortunately it is difficult to calculate and interpret. The sample median, although inefficient, is the simplest consistent estimator and would probably be used in practice” (Rothenberg, Fisher, & Tilanus, 1964).

Because the moments of the Cauchy PDF doesn’t exist (Krishnamoorthy, 2006), the methods based on moments can’t be applied to estimate the location or scale parameters.

Kamaci et al. (2005) propose a simple and computationally efficient estimation method for the scale parameter, which they used for their experiments on entropy and distortion. It can be resumed as follows:

Let $\hat{F}_X(x)$ be the empirical CDF obtained from the DCT histogram. They claim that this is the CDF of a Cauchy source with location parameter $a = 0$ and scale parameter b.

$$\hat{F}_X(x) \approx F_X(x) = \frac{1}{2} + \frac{1}{\pi}\tan^{-1}\left(\frac{x}{b}\right)$$

Then by letting

$$F_X(|x|) = P(X \leq |x|) = \frac{2}{\pi}\tan^{-1}\left(\frac{x}{b}\right)$$

And solving it for b

$$b = \frac{x}{\tan\left(\frac{\pi}{2}F_X(|x|)\right)}$$

For some threshold x. A proper selection of x would be to set it equal to b, but because it's not known, they experimentally found its range to be in the interval [0,3] and select $x = 2$ (Kamaci et al., 2005).

Although their method is computationally efficient, it is not very accurate. In order to improve it, a few modifications have been made here. First, the use of $F_X(x)$ instead of $F_X(|x|)$, this comes at the cost of processing more elements of the DCT histogram.

$$\hat{F}_X(x) \approx F_X(x) = \frac{1}{2} + \frac{1}{\pi}\tan^{-1}\left(\frac{x}{b}\right)$$

And solving it for b

$$b = \frac{x}{\tan\left(\pi[F_X(x) - 1/2]\right)}$$

The second modification is not selecting a fixed value of the threshold x, instead, selecting the positions of the histogram that make $F_X(x) = [0.7, 0.8, 0.9, 0.999]$, thus obtaining $b\big(F_X(x)\big) = [b(0.7), b(0.8), b(0.9), b(0.999)]$.

It's evident that the Cauchy PDF has its maximum when $x - a = 0$, hence

$$\max\left(cauchy(x; a, b)\right) = \frac{b/\pi}{b^2} = \frac{1}{\pi b}$$

This can be used as a way to select b, which will be the element of $b\big(F_X(x)\big)$ that satisfies $b > 0$ and minimizes:

$$\left|P_h - \frac{1}{\pi b}\right|$$

Where P_h is the peak value of the histogram.

Chapter VI

EXPERIMENTS

VI.1 TEST ENVIRONMENT

The tests were performed using the JM encoder (Sühring, 2007) version 13.2, with the following parameters common to all tests:

Most of the parameters used were the default values for the FREXT (Fidelity Range Extension) Profile (Sühring, 2007), but the transform's size was changed to 8x8 (the default is 4x4).

Three types of GOPs (Group of Pictures) were used. The first one is all intra prediction mode, with the following parameters:
IntraPeriod=1 FrameSkip=0 NumberBFrames=0.

The second type of GOP is I-P-P-P… This GOP is typically used in videoconferencing. The parameters were:
IntraPeriod=0 FrameSkip=0 NumberBFrames=0.

The third type is I-B-B-P-B-B-P with a length of 12 frames.
IntraPeriod=4 FrameSkip=2 NumberBFrames=2.

FramesToBeEncoded (Tourapis, Leontaris, Sühring, & Sullivan, 2007) specifies the number of frames to be coded, excluding B slice frames. If B slices (or Explicit Coding Structure) are to be used (secondary layer) then:

FramesToBeEncoded = int((TotalNumberOfFrames-1)/(NumberBFrames + 1)) + 1

The sequences were encoded and their DCT coefficients were collected and grouped by their position in the 8x8 matrix.

They are not yet scaled (because in the encoder the scaling is absorbed in the quantization process), thus for these experiments the scaling must be made. The scaling factors were obtained from (Sühring, 2007).

With the scaled coefficient data, a histogram is made and then normalized in order to make its total area equal to 1.

VI.1.1 Test sequences

The sequences were obtained from the International Telecommunication Union (2003), the Video Traces Research Group (2007) and Xiph.org (2004). The formats used were the CIF format (Common Intermediate Format, 352x288 pixels) and the QCIF format (Quarter CIF, 176x144 pixels).

For the experiments, the first 121 frames of each sequence were used. The following section shows the sequences used in this thesis and the statistics of their DCT coefficients.

VI.1.1.1 Statistics

Sequence	$C_{0,0}$	$C_{1,1}$	$C_{2,2}$	$C_{3,3}$	$C_{4,4}$	$C_{5,5}$	$C_{6,6}$	$C_{7,7}$
akiyo_qcif	2.086717	1.590254	0.142086	-0.310232	-0.059190	0.040169	-0.041838	0.025059
bus_cif	-1.661079	0.295602	0.057638	-0.024100	0.068945	0.016699	-0.056105	-0.020361
carphone_qcif	-2.888380	-0.420241	0.254001	0.143452	0.118987	-0.072596	-0.058306	-0.048515
claire_qcif	-6.501863	-1.344777	-0.099817	0.207905	0.135529	0.081792	-0.017558	-0.006487
coastguard_qcif	0.620286	-0.711693	-0.181682	0.026823	0.018133	0.072264	-0.036491	-0.028346
container_cif	-4.608557	-0.198365	-0.187613	0.105437	-0.127878	0.034848	0.028559	-0.030402
container_qcif	-3.097911	0.677487	-1.047956	-0.967580	-0.045434	-0.036568	-0.086479	0.032875
flower_cif	-4.653136	-0.590246	0.076459	-0.029807	0.001248	0.058709	-0.060255	-0.014282
foreman_cif	-3.675741	-0.543988	-0.249670	-0.081339	-0.019885	0.053214	-0.065876	-0.028591
foreman_qcif	-6.030702	-0.693296	-0.186270	-0.036082	-0.137149	-0.096460	-0.079305	-0.043624
grandma_qcif	-1.853637	0.731062	-0.475061	-0.079521	0.360268	0.278052	0.055285	-0.037754
hall_cif	-2.433169	-0.428173	0.045587	-0.358540	0.029213	-0.092619	-0.069224	-0.006410
hall_qcif	-9.673669	0.437505	-0.909532	-0.312421	0.533632	-0.045182	0.031915	-0.125306
highway_cif	-0.898291	-0.555644	-0.072453	-0.045357	0.076751	0.058853	-0.045310	-0.030285
highway_qcif	-0.724914	-0.629005	0.165117	0.089743	0.122830	0.094598	-0.025549	-0.030194
miss-america_qcif	0.429640	0.614587	0.055251	-0.069342	0.044565	0.048368	-0.057514	-0.017426
mobile_cif	-3.060984	-0.506081	-0.112044	-0.003616	0.016772	0.055414	-0.046340	-0.023582
mobile_qcif	-3.694267	-1.535062	0.335045	-0.379600	-0.081293	0.059957	-0.044415	-0.022787
mother-daughter_cif	-1.360424	-0.107456	0.104941	-0.003234	0.033299	0.040448	-0.045916	-0.021040
mother-daughter_qcif	-3.985159	0.031763	-0.222220	0.112599	0.183334	0.147132	-0.098476	-0.022815
news_cif	-3.049664	0.753436	-0.407892	-0.003670	-0.005012	-0.065398	-0.092000	-0.034351

news_qcif	-2.233484	1.367358	-1.046850	-0.222587	-0.743554	0.336259	-0.168029	0.023838
paris_cif	0.195083	1.040779	-0.181503	-0.254389	0.053049	0.208428	-0.099713	-0.017628
salesman_qcif	0.372441	0.022167	-0.485885	-0.308124	-0.218427	-0.064065	-0.082745	0.068130
silent_cif	-2.304164	0.574285	-0.555639	0.358604	-0.293090	0.383975	-0.120945	-0.005378
silent_qcif	-4.443211	0.874344	0.474034	0.961649	-0.812304	0.361136	0.010258	-0.054527
stefan_cif	2.725354	0.276966	0.192186	0.126838	0.023504	0.041510	-0.049595	-0.023420
suzie_qcif	-1.999747	0.627622	0.053751	0.165589	-0.016834	0.068837	-0.047365	-0.019204
tempete_cif	1.388582	-0.034748	0.337674	-0.035097	0.076257	0.049034	-0.040136	-0.016037
waterfall_cif	-2.393241	0.135658	-0.016078	-0.071445	0.007938	0.083783	-0.065017	-0.017245

Table VI-1: Mean (GOP: IIIIIII)

Sequence	**$C_{0,0}$**	**$C_{1,1}$**	**$C_{2,2}$**	**$C_{3,3}$**	**$C_{4,4}$**	**$C_{5,5}$**	**$C_{6,6}$**	**$C_{7,7}$**
akiyo_qcif	0.078985	0.439496	-0.001638	-0.107819	-0.058193	0.031242	-0.040430	-0.017119
bus_cif	-1.903319	0.199019	-0.052742	-0.031303	0.042813	0.025185	-0.051819	-0.021022
carphone_qcif	-2.059257	-0.360876	-0.005393	0.117104	0.127455	-0.032489	-0.068673	-0.032393
claire_qcif	-3.685723	-0.472656	-0.011536	0.108166	0.071038	0.043123	-0.017864	-0.021489
coastguard_qcif	-0.815161	-0.316775	-0.126908	0.026425	0.045955	0.076019	-0.043082	-0.023211
container_cif	-2.731526	-0.133425	-0.005838	-0.001305	-0.061119	0.023198	-0.013824	-0.027975
container_qcif	-2.606684	0.173349	-0.310660	-0.256254	-0.038852	0.010363	-0.022960	-0.026448
flower_cif	-2.649997	-0.241844	0.045548	-0.024619	0.032308	0.045316	-0.047572	-0.011974
foreman_cif	-2.715408	-0.369752	-0.217494	-0.069656	-0.013961	0.061211	-0.064899	-0.026136
foreman_qcif	-3.832086	-0.409164	-0.199504	-0.042143	-0.125877	-0.046412	-0.067961	-0.038021
grandma_qcif	-1.755356	0.046117	-0.175044	-0.082810	0.072077	0.073130	-0.005498	-0.025602
hall_cif	-2.432019	-0.310788	-0.018637	-0.237343	0.022858	-0.043667	-0.060393	-0.014312
hall_qcif	-5.444504	0.255896	-0.350717	-0.156578	0.260130	-0.044457	-0.034433	-0.070900
highway_cif	-1.222600	-0.371468	-0.069216	-0.037305	0.074519	0.060439	-0.042331	-0.028832
highway_qcif	-1.426301	-0.424239	0.037714	0.058097	0.068169	0.081380	-0.018161	-0.017989
miss-america_qcif	-0.819791	0.185476	0.023341	-0.035137	0.011825	0.044835	-0.051710	-0.021941
mobile_cif	-2.422457	-0.247708	-0.109920	0.061457	-0.022297	0.088406	-0.044790	-0.020973
mobile_qcif	-2.944330	-0.550775	0.146386	-0.226512	-0.073034	0.028348	-0.047180	-0.011465
mother-daughter_cif	-1.690337	-0.128448	0.011729	-0.011643	0.014692	0.040498	-0.041559	-0.022589
mother-daughter_qcif	-1.983046	-0.041504	-0.169618	0.007706	0.083007	0.063599	-0.067450	-0.027894
news_cif	-1.652915	0.348892	-0.023914	-0.041985	0.019889	-0.006204	-0.054029	-0.030317
news_qcif	-0.490358	0.408743	-0.166294	0.001165	-0.176794	0.136362	-0.053793	-0.016134
paris_cif	-0.794133	0.413788	-0.067256	-0.099948	0.000292	0.101479	-0.064657	-0.013294
salesman_qcif	-0.691909	0.179974	-0.190457	-0.059269	-0.031769	0.001502	-0.033080	-0.015299
silent_cif	-2.438774	0.113114	-0.129766	0.091828	-0.062783	0.137041	-0.051223	-0.024930
silent_qcif	-3.271097	0.379457	-0.221273	0.208078	-0.227896	0.108138	-0.015341	-0.031022
stefan_cif	0.337611	0.139494	0.106068	0.069138	0.002192	0.049492	-0.049934	-0.022190
suzie_qcif	-1.433214	0.343036	0.030088	0.062799	-0.017205	0.045149	-0.037878	-0.019575
tempete_cif	0.002924	-0.072091	0.233770	-0.020148	0.056762	0.052303	-0.036420	-0.021133
waterfall_cif	-2.608339	0.034585	-0.014517	-0.052505	0.010068	0.057962	-0.051657	-0.020789

Table VI-2: Mean (GOP: IBBPBBP_12)

Sequence	**$C_{0,0}$**	**$C_{1,1}$**	**$C_{2,2}$**	**$C_{3,3}$**	**$C_{4,4}$**	**$C_{5,5}$**	**$C_{6,6}$**	**$C_{7,7}$**
akiyo_qcif	0.156349	0.419820	0.001534	-0.039502	-0.093682	0.035740	-0.042936	-0.020069
bus_cif	-1.565650	0.232862	0.060694	-0.039967	0.060272	0.030957	-0.052872	-0.021246
carphone_qcif	-2.025858	-0.504662	-0.012437	0.108456	0.164298	-0.044950	-0.068045	-0.037932
claire_qcif	-2.028592	-0.375646	-0.012400	0.123996	0.085968	0.042375	-0.013409	-0.020062
coastguard_qcif	0.110908	-0.368675	-0.227605	0.046777	0.015882	0.077373	-0.038045	-0.026177
container_cif	-2.685081	-0.303636	-0.037606	0.057649	-0.062702	0.001592	0.000343	-0.029602
container_qcif	-2.358317	0.435344	-0.350470	-0.216977	-0.082000	0.027567	-0.039344	-0.026196
flower_cif	-2.643089	-0.347465	-0.015609	0.009553	0.034834	0.061917	-0.062680	-0.015229
foreman_cif	-2.513557	-0.403024	-0.222150	-0.073331	-0.016639	0.055780	-0.067261	-0.026463
foreman_qcif	-3.401513	-0.521901	-0.255334	-0.019257	-0.129782	-0.067202	-0.069654	-0.038657
grandma_qcif	-1.302842	0.028832	-0.148510	-0.060741	0.095923	0.070814	-0.020068	-0.035670
hall_cif	-2.374791	-0.211218	-0.068774	-0.337108	0.033490	-0.062855	-0.064640	-0.011494
hall_qcif	-6.969097	0.343347	-0.500048	-0.184421	0.377092	-0.056497	-0.028277	-0.088419
highway_cif	-0.918694	-0.473023	-0.068152	-0.043590	0.077153	0.058005	-0.047777	-0.029425
highway_qcif	-0.736174	-0.515065	0.078295	0.045048	0.070691	0.069174	-0.023006	-0.018934
miss-america_qcif	-0.204937	0.313313	0.063553	-0.038585	0.035197	0.048950	-0.049846	-0.023220
mobile_cif	-1.876253	-0.496723	-0.105059	0.002109	0.018273	0.063161	-0.048077	-0.023614
mobile_qcif	-2.235861	-1.015547	0.415279	-0.269392	-0.147477	-0.010438	-0.061684	-0.022490
mother-daughter_cif	-1.055180	-0.141177	0.068883	0.008968	0.015925	0.037966	-0.044212	-0.022427

mother-daughter_qcif	-1.527313	0.016944	-0.227236	0.024147	0.079869	0.087535	-0.062543	-0.032367
news_cif	-1.858238	0.485320	-0.079302	-0.055528	0.042032	-0.027740	-0.055130	-0.030809
news_qcif	0.264173	0.462484	-0.128170	0.054335	-0.224510	0.115806	-0.072457	-0.022993
paris_cif	0.187553	0.427443	0.015551	-0.048165	0.000282	0.072922	-0.064395	-0.014330
salesman_qcif	0.082874	0.205103	-0.154972	-0.023952	-0.016738	0.003565	-0.021623	-0.026650
silent_cif	-1.790511	0.166302	-0.187859	0.126466	-0.089320	0.171082	-0.060374	-0.021088
silent_qcif	-3.214477	0.487363	-0.253406	0.177517	-0.174422	0.104687	-0.011075	-0.035350
stefan_cif	1.478655	0.192951	0.080901	0.099589	0.010694	0.043267	-0.047653	-0.024461
suzie_qcif	-1.090570	0.406537	0.058876	0.088962	-0.018835	0.048763	-0.043451	-0.024596
tempete_cif	1.032841	-0.034499	0.276032	-0.031634	0.062300	0.051410	-0.038945	-0.019239
waterfall_cif	-1.727899	0.071061	-0.042577	-0.051418	0.014398	0.056972	-0.054909	-0.020982

Table VI-3: Mean (GOP: IPPPPPP)

Sequence	**$C_{0,0}$**	**$C_{1,1}$**	**$C_{2,2}$**	**$C_{3,3}$**	**$C_{4,4}$**	**$C_{5,5}$**	**$C_{6,6}$**	**$C_{7,7}$**
akiyo_qcif	0.750000	0.000000	0.000000	0.000000	0.000000	0.000000	0.000000	0.000000
bus_cif	-0.875000	0.000000	0.000000	0.000000	0.000000	0.112091	0.000000	0.000000
carphone_qcif	-2.125000	-0.336273	0.000000	0.000000	0.000000	0.000000	0.000000	0.000000
claire_qcif	-0.250000	0.000000	0.000000	0.000000	0.000000	0.000000	0.000000	0.000000
coastguard_qcif	0.000000	-0.448364	0.000000	-0.112091	0.000000	0.000000	0.000000	0.000000
container_cif	-1.375000	0.000000	0.000000	0.000000	0.000000	0.112091	0.000000	0.000000
container_qcif	-2.250000	0.112091	-0.200790	-0.112091	0.000000	0.000000	0.000000	0.000000
flower_cif	-1.125000	-0.112091	0.000000	0.000000	0.000000	0.000000	0.000000	0.000000
foreman_cif	-2.125000	-0.224182	0.000000	0.000000	0.000000	0.112091	0.000000	0.000000
foreman_qcif	-3.125000	-0.224182	-0.200790	0.000000	0.000000	0.000000	0.000000	0.000000
grandma_qcif	-0.875000	-0.224182	0.000000	0.000000	0.125000	0.000000	0.000000	-0.112091
hall_cif	-2.250000	0.000000	0.000000	-0.112091	0.000000	0.000000	0.000000	0.000000
hall_qcif	-4.250000	0.112091	-0.200790	0.000000	0.125000	0.000000	0.000000	0.000000
highway_cif	-0.750000	0.000000	0.000000	0.000000	0.000000	0.000000	0.000000	0.000000
highway_qcif	-0.375000	-0.336273	0.000000	0.000000	0.000000	0.000000	0.000000	0.000000
miss-america_qcif	-0.250000	-0.112091	0.000000	0.000000	0.000000	0.112091	0.000000	0.000000
mobile_cif	-2.250000	-0.112091	0.000000	0.000000	0.000000	0.112091	0.000000	0.000000
mobile_qcif	-1.875000	-0.560455	-0.200790	-0.224182	0.000000	0.112091	0.000000	0.000000
mother-daughter_cif	-0.625000	0.000000	0.000000	0.000000	0.000000	0.000000	0.000000	0.000000
mother-daughter_qcif	-1.125000	-0.112091	-0.200790	0.000000	0.000000	0.112091	0.000000	0.000000
news_cif	-1.500000	-0.112091	0.000000	0.000000	0.000000	0.000000	0.000000	0.000000
news_qcif	-0.750000	0.112091	-0.200790	-0.224182	0.000000	0.112091	0.000000	0.000000
paris_cif	-1.375000	-0.112091	0.000000	0.000000	0.000000	0.112091	0.000000	0.000000
salesman_qcif	0.625000	-0.112091	-0.401581	-0.448364	0.000000	0.000000	0.000000	0.000000
silent_cif	-1.375000	0.112091	-0.200790	0.000000	0.000000	0.224182	0.000000	0.000000
silent_qcif	-3.750000	0.112091	0.200790	0.336273	-0.125000	0.224182	0.000000	-0.112091
stefan_cif	-0.500000	0.000000	0.000000	0.000000	0.000000	0.000000	0.000000	0.000000
suzie_qcif	-0.250000	0.224182	0.000000	0.000000	0.000000	0.000000	0.000000	0.000000
tempete_cif	0.750000	0.000000	0.000000	0.000000	0.000000	0.112091	0.000000	0.000000
waterfall_cif	-2.250000	0.000000	0.000000	-0.112091	0.000000	0.112091	0.000000	0.000000

Table VI-4: Median (GOP: IIIIIII)

Sequence	**$C_{0,0}$**	**$C_{1,1}$**	**$C_{2,2}$**	**$C_{3,3}$**	**$C_{4,4}$**	**$C_{5,5}$**	**$C_{6,6}$**	**$C_{7,7}$**
akiyo_qcif	-0.125000	0.000000	0.000000	0.000000	0.000000	0.000000	0.000000	0.000000
bus_cif	-2.500000	-0.112091	0.000000	0.000000	0.000000	0.112091	0.000000	0.000000
carphone_qcif	-1.875000	-0.112091	0.000000	0.000000	0.000000	0.000000	0.000000	0.000000
claire_qcif	-2.250000	0.000000	0.000000	0.000000	0.000000	0.000000	0.000000	0.000000
coastguard_qcif	-2.375000	-0.112091	0.000000	0.000000	0.000000	0.112091	0.000000	0.000000
container_cif	-2.000000	0.000000	0.000000	0.000000	0.000000	0.000000	0.000000	0.000000
container_qcif	-1.875000	0.000000	0.000000	0.000000	0.000000	0.000000	0.000000	0.000000
flower_cif	-1.250000	-0.112091	0.000000	0.000000	0.000000	0.112091	0.000000	0.000000
foreman_cif	-2.250000	-0.112091	0.000000	0.000000	0.000000	0.112091	0.000000	0.000000
foreman_qcif	-2.250000	-0.112091	0.000000	0.000000	0.000000	0.000000	0.000000	0.000000
grandma_qcif	-1.625000	-0.112091	0.000000	0.000000	0.000000	0.000000	0.000000	0.000000
hall_cif	-2.000000	0.000000	0.000000	0.000000	0.000000	0.000000	0.000000	0.000000
hall_qcif	-1.750000	0.000000	0.000000	0.000000	0.000000	0.000000	0.000000	0.000000
highway_cif	-1.125000	0.000000	0.000000	0.000000	0.000000	0.000000	0.000000	0.000000
highway_qcif	-1.250000	0.000000	0.000000	0.000000	0.000000	0.000000	0.000000	0.000000
miss-america_qcif	-1.375000	-0.112091	0.000000	0.000000	0.000000	0.000000	0.000000	0.000000
mobile_cif	-2.250000	-0.112091	0.000000	0.000000	0.000000	0.112091	0.000000	0.000000

mobile_qcif	-2.500000	-0.112091	0.000000	-0.112091	0.000000	0.112091	0.000000	0.000000
mother-daughter_cif	-1.625000	0.000000	0.000000	0.000000	0.000000	0.000000	0.000000	0.000000
mother-daughter_qcif	-1.375000	0.000000	0.000000	0.000000	0.000000	0.000000	0.000000	0.000000
news_cif	-0.250000	0.000000	0.000000	0.000000	0.000000	0.000000	0.000000	0.000000
news_qcif	-0.250000	0.000000	0.000000	0.000000	0.000000	0.000000	0.000000	0.000000
paris_cif	-1.625000	-0.112091	0.000000	0.000000	0.000000	0.000000	0.000000	0.000000
salesman_qcif	-0.875000	0.000000	0.000000	-0.112091	0.000000	0.000000	0.000000	0.000000
silent_cif	-1.625000	0.000000	0.000000	0.000000	0.000000	0.000000	0.000000	0.000000
silent_qcif	-1.125000	0.000000	0.000000	0.000000	0.000000	0.000000	0.000000	0.000000
stefan_cif	-1.625000	0.000000	0.000000	0.000000	0.000000	0.000000	0.000000	0.000000
suzie_qcif	-1.500000	0.000000	0.000000	0.000000	0.000000	0.000000	0.000000	0.000000
tempete_cif	-1.875000	0.000000	0.000000	0.000000	0.000000	0.112091	0.000000	0.000000
waterfall_cif	-2.750000	0.000000	0.000000	0.000000	0.000000	0.000000	0.000000	0.000000

Table VI-5: Median (GOP: IBBPBBP_12)

Sequence	**$C_{0,0}$**	**$C_{1,1}$**	**$C_{2,2}$**	**$C_{3,3}$**	**$C_{4,4}$**	**$C_{5,5}$**	**$C_{6,6}$**	**$C_{7,7}$**
akiyo_qcif	0.000000	0.000000	0.000000	0.000000	0.000000	0.000000	0.000000	0.000000
bus_cif	-1.625000	-0.112091	0.000000	0.000000	0.000000	0.112091	0.000000	0.000000
carphone_qcif	-1.000000	-0.112091	0.000000	0.000000	0.000000	0.000000	0.000000	0.000000
claire_qcif	0.000000	0.000000	0.000000	0.000000	0.000000	0.000000	0.000000	0.000000
coastguard_qcif	-1.250000	-0.112091	0.000000	0.000000	0.000000	0.112091	0.000000	0.000000
container_cif	-0.875000	0.000000	0.000000	0.000000	0.000000	0.000000	0.000000	0.000000
container_qcif	-0.375000	0.000000	0.000000	0.000000	0.000000	0.000000	0.000000	0.000000
flower_cif	-0.750000	-0.112091	0.000000	0.000000	0.000000	0.112091	0.000000	0.000000
foreman_cif	-1.375000	-0.112091	0.000000	0.000000	0.000000	0.112091	0.000000	0.000000
foreman_qcif	-1.375000	-0.112091	0.000000	0.000000	0.000000	0.000000	0.000000	0.000000
grandma_qcif	-0.375000	-0.112091	0.000000	0.000000	0.000000	0.000000	0.000000	0.000000
hall_cif	-1.875000	0.000000	0.000000	-0.112091	0.000000	0.000000	0.000000	0.000000
hall_qcif	-1.500000	0.000000	-0.200790	0.000000	0.125000	0.000000	0.000000	0.000000
highway_cif	-0.625000	0.000000	0.000000	0.000000	0.000000	0.000000	0.000000	0.000000
highway_qcif	-0.500000	-0.112091	0.000000	0.000000	0.000000	0.000000	0.000000	0.000000
miss-america_qcif	-0.500000	-0.112091	0.000000	0.000000	0.000000	0.000000	0.000000	0.000000
mobile_cif	-1.125000	-0.112091	0.000000	0.000000	0.000000	0.112091	0.000000	0.000000
mobile_qcif	-0.750000	-0.112091	0.000000	-0.112091	0.000000	0.112091	0.000000	0.000000
mother-daughter_cif	-0.625000	0.000000	0.000000	0.000000	0.000000	0.000000	0.000000	0.000000
mother-daughter_qcif	-0.375000	0.000000	0.000000	0.000000	0.000000	0.000000	0.000000	0.000000
news_cif	-0.125000	0.000000	0.000000	0.000000	0.000000	0.000000	0.000000	0.000000
news_qcif	-0.125000	0.000000	0.000000	0.000000	0.000000	0.000000	0.000000	0.000000
paris_cif	0.000000	0.000000	0.000000	0.000000	0.000000	0.000000	0.000000	0.000000
salesman_qcif	0.000000	0.000000	0.000000	0.000000	0.000000	0.000000	0.000000	0.000000
silent_cif	-0.375000	0.000000	0.000000	0.000000	0.000000	0.000000	0.000000	0.000000
silent_qcif	-0.250000	0.000000	0.000000	0.000000	0.000000	0.000000	0.000000	0.000000
stefan_cif	-0.625000	0.000000	0.000000	0.000000	0.000000	0.000000	0.000000	0.000000
suzie_qcif	-0.625000	0.000000	0.000000	0.000000	0.000000	0.000000	0.000000	0.000000
tempete_cif	-0.875000	0.000000	0.000000	0.000000	0.000000	0.112091	0.000000	0.000000
waterfall_cif	-1.500000	0.000000	0.000000	0.000000	0.000000	0.000000	0.000000	0.000000

Table VI-6: Median (GOP: IPPPPPP)

Sequence	**$C_{0,0}$**	**$C_{1,1}$**	**$C_{2,2}$**	**$C_{3,3}$**	**$C_{4,4}$**	**$C_{5,5}$**	**$C_{6,6}$**	**$C_{7,7}$**
akiyo_qcif	61.736543	24.507318	13.107785	9.052777	5.241058	3.480152	1.725569	0.742873
bus_cif	88.539725	36.458217	26.409668	19.718909	12.933961	6.425340	1.906648	0.630395
carphone_qcif	74.253805	26.301938	15.281913	10.649875	6.550235	4.166385	2.648546	1.691560
claire_qcif	70.695747	21.566631	11.249470	6.650604	3.239524	2.202770	1.385747	0.882926
coastguard_qcif	74.358560	28.948773	19.149477	13.519913	9.208665	6.238692	3.144525	1.330104
container_cif	69.961635	28.455088	20.103732	14.999338	9.484486	5.715847	1.773765	0.714789
container_qcif	85.416328	29.396852	18.147783	13.819524	10.201655	6.823618	3.553404	1.554575
flower_cif	95.334735	50.700864	38.415244	28.638711	19.104901	12.393088	6.132515	2.472474
foreman_cif	45.521769	23.014023	14.056884	9.285712	6.490549	4.679968	2.358464	1.023989
foreman_qcif	68.592633	32.500077	19.362229	14.023807	11.121923	6.657128	2.456723	0.885025
grandma_qcif	50.235137	24.509243	12.779945	8.315201	6.560520	4.404327	2.779349	1.598301
hall_cif	56.345788	30.485846	17.241397	11.659572	7.705993	3.919373	1.265590	0.787908
hall_qcif	77.450774	32.705024	21.796544	15.421775	10.438896	5.972273	3.129190	1.763211
highway_cif	34.699728	13.224974	8.850509	6.668911	5.287142	4.048271	2.965512	2.197397
highway_qcif	59.513582	14.609051	10.188239	7.941889	6.420563	5.444862	4.474263	4.790965

miss-america_qcif	50.112658	16.304233	8.957423	5.194653	2.890568	1.847308	1.027776	0.700618
mobile_cif	103.819964	55.041275	42.381935	35.755879	25.624067	14.687533	4.913242	1.370725
mobile_qcif	112.860597	57.074467	41.114808	30.868841	22.351469	15.351212	8.329999	3.623964
mother-daughter_cif	35.327233	13.662026	8.641356	5.889518	3.262978	1.513598	0.536151	0.404419
mother-daughter_qcif	52.498982	17.713399	11.867775	8.206249	5.459214	3.379026	1.577600	0.676498
news_cif	63.573088	36.005939	21.604890	13.834866	7.396065	3.781815	1.267808	0.538998
news_qcif	78.416531	34.511765	24.547473	18.052193	12.290566	7.971246	2.924150	1.120262
paris_cif	91.920466	34.419384	23.581882	17.307729	10.742208	7.749463	4.794717	2.989186
salesman_qcif	63.664012	26.140399	16.617785	10.944064	7.194184	4.247461	2.616791	1.528526
silent_cif	52.724930	23.353516	14.065528	10.292483	7.114018	4.789055	2.719605	1.290853
silent_qcif	78.243973	29.487435	17.750567	12.749470	7.926034	4.702755	2.096274	0.717887
stefan_cif	91.763915	47.926042	33.990345	23.417392	11.936905	4.760543	1.512055	0.731859
suzie_qcif	49.677263	20.486336	11.895139	7.797429	4.770506	3.283897	2.163288	1.607147
tempete_cif	80.038399	38.747528	25.801832	18.563544	11.816584	6.860651	3.252105	1.782913
waterfall_cif	50.314899	25.660491	18.501565	12.978382	7.505903	3.665549	1.128190	0.474278

Table VI-7: Standard Deviation (GOP: IIIIIII)

Sequence	$C_{0,0}$	$C_{1,1}$	$C_{2,2}$	$C_{3,3}$	$C_{4,4}$	$C_{5,5}$	$C_{6,6}$	$C_{7,7}$
akiyo_qcif	29.815079	14.217397	7.650483	5.364222	3.094598	2.013764	1.050727	0.527767
bus_cif	67.246442	28.397491	20.264200	15.274692	9.914828	5.061966	1.612379	0.612521
carphone_qcif	51.973071	20.692988	11.476268	8.018838	4.947012	3.362949	2.180055	1.507542
claire_qcif	34.354041	14.179159	8.061576	4.747625	2.325388	1.645826	1.050943	0.748512
coastguard_qcif	52.204813	19.953561	13.254116	9.508127	6.757367	4.744605	2.512720	1.139683
container_cif	38.662839	15.658539	10.936715	8.263201	5.323010	3.231551	1.126888	0.588013
container_qcif	37.836234	13.937692	9.043776	6.832842	5.082620	3.480179	1.821581	0.904182
flower_cif	70.871118	37.014070	28.118726	20.910610	14.252203	9.364903	4.785900	2.006996
foreman_cif	35.216477	17.166205	10.205336	6.706685	4.560464	3.384620	1.854239	0.889854
foreman_qcif	50.571036	22.870470	13.640374	9.491054	6.944633	4.206033	1.712215	0.720979
grandma_qcif	27.266388	13.555300	7.208918	4.729337	3.600520	2.566370	1.673647	1.093616
hall_cif	46.033468	24.645813	14.279140	9.594639	6.391673	3.323677	1.127019	0.686266
hall_qcif	57.375059	23.787685	15.911774	11.107593	7.259351	4.315825	2.357474	1.225938
highway_cif	28.789426	11.271562	7.606873	5.802901	4.686806	3.678602	2.791405	2.123991
highway_qcif	44.534158	11.864644	8.512941	6.720867	5.515869	4.763722	4.025067	4.277193
miss-america_qcif	30.241191	10.955111	5.892474	3.497382	2.030217	1.370113	0.892123	0.698575
mobile_cif	79.461941	41.874827	32.192510	27.188807	19.737954	11.551601	4.044936	1.233062
mobile_qcif	78.513017	39.609233	29.006191	21.895379	16.066209	11.203454	6.332261	2.963019
mother-daughter_cif	19.227404	9.105111	5.781692	3.995455	2.369787	1.227781	0.538644	0.438899
mother-daughter_qcif	28.312768	11.494738	7.550449	5.203961	3.504109	2.241156	1.119218	0.596060
news_cif	37.492831	21.714062	12.998777	8.409941	4.499704	2.371454	0.845225	0.446910
news_qcif	40.474633	19.316759	12.708672	9.093914	6.186073	4.012935	1.692137	0.707546
paris_cif	57.961075	24.306769	16.363609	12.040763	7.661823	5.355537	3.307900	2.217367
salesman_qcif	35.015331	15.297894	10.124008	6.541217	4.270185	2.634973	1.653419	1.043352
silent_cif	34.053016	14.411973	8.519989	6.169379	4.344481	3.046295	1.760845	0.915193
silent_qcif	39.919771	17.757894	10.593275	7.243320	4.549981	2.741905	1.238652	0.571145
stefan_cif	70.432450	36.544740	25.913000	17.876370	9.325442	3.896832	1.361875	0.706728
suzie_qcif	35.972179	15.677992	9.215426	6.077811	3.770196	2.635186	1.818995	1.448477
tempete_cif	62.093869	30.336130	20.402373	14.735544	9.541569	5.655600	2.801726	1.636424
waterfall_cif	31.370178	15.666717	11.338015	8.104610	4.853959	2.544833	0.918993	0.492168

Table VI-8: Standard Deviation (GOP: IBBPBBP_12)

Sequence	$C_{0,0}$	$C_{1,1}$	$C_{2,2}$	$C_{3,3}$	$C_{4,4}$	$C_{5,5}$	$C_{6,6}$	$C_{7,7}$
akiyo_qcif	27.197846	13.767375	7.505408	5.087204	3.021556	1.886318	0.968038	0.503951
bus_cif	74.439765	31.179933	22.385551	16.766745	11.040236	5.568001	1.709441	0.618485
carphone_qcif	55.191167	22.365036	12.499170	8.689482	5.346568	3.620020	2.299292	1.547122
claire_qcif	36.018586	14.740893	8.346405	5.008536	2.424589	1.682835	1.091104	0.752412
coastguard_qcif	54.765340	21.827088	14.335131	10.097706	7.118677	4.948281	2.562609	1.163263
container_cif	46.186864	19.072884	13.307910	9.957219	6.253934	3.798782	1.292497	0.628696
container_qcif	43.629353	16.892811	10.967222	8.014823	6.276666	4.159182	2.095042	1.017449
flower_cif	77.892446	40.785018	30.912352	23.065431	15.388567	10.053556	5.050778	2.090349
foreman_cif	36.870106	18.054288	10.788649	7.113854	4.839780	3.532389	1.898055	0.895256
foreman_qcif	52.596781	23.824084	14.222591	9.715400	7.108709	4.270888	1.737367	0.727609
grandma_qcif	30.601590	13.806039	7.349744	4.842494	3.691542	2.611728	1.717105	1.103653
hall_cif	52.011906	27.573681	16.089106	10.733323	7.046169	3.601012	1.189265	0.719579
hall_qcif	65.853973	27.269253	18.354676	12.856620	8.548995	4.993064	2.677369	1.414370

highway_cif	32.572139	12.490177	8.433847	6.401382	5.096311	3.927396	2.904519	2.175093
highway_qcif	54.509884	13.321841	9.358232	7.347369	6.012261	5.125565	4.234764	4.496179
miss-america_qcif	37.763447	12.585584	6.919671	4.083444	2.333112	1.533149	0.929865	0.693388
mobile_cif	87.365987	46.238729	35.288352	29.252079	21.004382	12.237941	4.222757	1.255818
mobile_qcif	95.358304	48.354860	34.682253	26.266783	19.153814	13.200691	7.143319	3.221882
mother-daughter_cif	21.400845	10.798735	6.840230	4.710341	2.707605	1.344435	0.540812	0.423418
mother-daughter_qcif	30.838850	12.074974	8.155031	5.568430	3.713589	2.352399	1.162418	0.604348
news_cif	42.363935	24.680371	15.139964	9.808678	4.978423	2.570950	0.905732	0.457812
news_qcif	39.131073	19.359333	12.931442	8.993939	6.820159	4.106009	1.750685	0.697740
paris_cif	55.585951	24.568623	16.528120	12.023830	7.693398	5.319290	3.206353	2.165390
salesman_qcif	33.096378	15.225769	10.070923	6.376561	4.226578	2.621504	1.628442	1.037341
silent_cif	38.159828	16.077019	9.442782	6.884237	4.822092	3.343638	1.901465	0.961461
silent_qcif	38.553718	17.592258	10.483846	6.962866	4.386793	2.624747	1.193808	0.564701
stefan_cif	77.116866	40.071274	28.530113	19.580387	10.118782	4.140446	1.399124	0.714468
suzie_qcif	40.023249	17.324967	10.141027	6.552717	4.045500	2.776247	1.876318	1.475503
tempete_cif	68.911984	33.515870	22.668511	16.363021	10.482005	6.160295	2.976583	1.692138
waterfall_cif	35.389558	18.022409	12.967343	9.118800	5.409454	2.766539	0.957691	0.489588

Table VI-9: Standard Deviation (GOP: IPPPPPP)

This section shows the estimated parameters of the PDFs. The Laplacian case can be defined using the statistical parameters (mean and standard deviation of the empirical data) shown in the past section.

VI.1.2 Generalized Gaussian

The Generalized Gaussian PDF requires the same parameters as the Laplacian case, plus the p (peakedness) parameter. The following tables show the results of its estimation.

Sequence	$C_{0,0}$	$C_{1,1}$	$C_{2,2}$	$C_{3,3}$	$C_{4,4}$	$C_{5,5}$	$C_{6,6}$	$C_{7,7}$
akiyo_qcif	0.394134	0.483173	0.455411	0.396682	0.406405	0.436122	0.495048	0.759674
bus_cif	0.550202	0.662861	0.618524	0.615892	0.592438	0.612487	0.734979	0.912865
carphone_qcif	0.393910	0.533645	0.453078	0.419758	0.412760	0.458634	0.512938	0.583533
claire_qcif	0.269950	0.348102	0.324361	0.312869	0.375500	0.383256	0.426726	0.514417
coastguard_qcif	0.470338	0.658769	0.662250	0.741181	0.879822	0.921042	1.006556	1.108817
container_cif	0.328250	0.417114	0.425505	0.472060	0.511602	0.481697	0.598151	0.659892
container_qcif	0.335642	0.440915	0.451988	0.476220	0.490150	0.547699	0.565238	0.602196
flower_cif	0.497490	0.547388	0.530843	0.542192	0.545710	0.557899	0.568844	0.617823
foreman_cif	0.483474	0.518073	0.535613	0.564586	0.568786	0.564558	0.658814	0.820451
foreman_qcif	0.536507	0.642396	0.638636	0.596644	0.508122	0.519361	0.618166	0.741491
grandma_qcif	0.465419	0.604408	0.655588	0.648738	0.557374	0.666768	0.669958	0.726064
hall_cif	0.399365	0.346931	0.361063	0.382687	0.410483	0.479177	0.579601	0.450037
hall_qcif	0.502524	0.471694	0.420857	0.441364	0.413166	0.439688	0.477435	0.374747
highway_cif	0.283270	0.394022	0.343320	0.339481	0.360736	0.409157	0.579214	0.681443
highway_qcif	0.267299	0.573205	0.392770	0.348692	0.333455	0.340036	0.382588	0.309589
miss-america_qcif	0.265198	0.368254	0.351959	0.364148	0.409706	0.473977	0.689593	1.058944
mobile_cif	0.634485	0.763841	0.763622	0.749975	0.740216	0.732608	0.768650	0.700670
mobile_qcif	0.783925	0.970478	0.990840	0.992618	1.050105	1.050356	1.054005	1.009655
mother-daughter_cif	0.356361	0.534536	0.545711	0.571958	0.666704	0.859714	1.402411	1.399308
mother-daughter_qcif	0.366472	0.635055	0.580234	0.583535	0.587122	0.618102	0.692183	1.015371
news_cif	0.359795	0.343928	0.326577	0.329440	0.380866	0.393730	0.481167	0.855661
news_qcif	0.463593	0.513435	0.419394	0.367546	0.385935	0.365767	0.460774	0.615812
paris_cif	0.413922	0.582990	0.531376	0.494262	0.520991	0.531543	0.551044	0.558473
salesman_qcif	0.602734	0.937288	0.851862	0.685709	0.691233	0.766064	0.809489	0.831286
silent_cif	0.504200	0.675094	0.677423	0.681087	0.698862	0.818707	0.851991	0.863751
silent_qcif	0.519855	0.855181	0.810805	0.663216	0.657446	0.740709	0.820342	1.157976
stefan_cif	0.531662	0.592602	0.576301	0.590936	0.617295	0.665290	0.805088	0.701471
suzie_qcif	0.502514	0.543517	0.475617	0.451552	0.490369	0.541680	0.591673	0.600099
tempete_cif	0.601314	0.771758	0.671919	0.635395	0.619236	0.629822	0.698579	0.757179
waterfall_cif	0.763209	1.088026	1.100348	1.166825	1.197013	1.257204	1.414931	1.400913

Table VI-10: p Parameter (GOP: IIIIIII)

Sequence	$C_{0,0}$	$C_{1,1}$	$C_{2,2}$	$C_{3,3}$	$C_{4,4}$	$C_{5,5}$	$C_{6,6}$	$C_{7,7}$
akiyo_qcif	0.210558	0.229076	0.233762	0.235880	0.261921	0.297625	0.393531	0.705738
bus_cif	0.370913	0.434729	0.437713	0.462937	0.497211	0.568071	0.741666	1.105482
carphone_qcif	0.294499	0.351968	0.344858	0.344288	0.372338	0.426896	0.535391	0.630748
claire_qcif	0.213074	0.225354	0.229344	0.248708	0.329638	0.385758	0.504377	0.707324
coastguard_qcif	0.306196	0.401366	0.451433	0.535272	0.646764	0.709946	0.859683	1.132096
container_cif	0.199438	0.249013	0.277229	0.319265	0.378494	0.406467	0.617869	1.032509
container_qcif	0.190621	0.219922	0.239478	0.261427	0.297505	0.340177	0.427629	0.667336
flower_cif	0.322019	0.357069	0.363831	0.386616	0.410880	0.448253	0.491671	0.582239
foreman_cif	0.347731	0.365130	0.390097	0.437043	0.499694	0.536569	0.684469	0.967878
foreman_qcif	0.349709	0.395464	0.404675	0.406491	0.392202	0.429840	0.614072	0.957395
grandma_qcif	0.257843	0.285790	0.320042	0.354889	0.372295	0.468993	0.577074	0.761400
hall_cif	0.327210	0.303038	0.329052	0.371143	0.416713	0.513799	0.665248	0.566329
hall_qcif	0.332618	0.322186	0.309747	0.339567	0.348626	0.396804	0.435438	0.457473
highway_cif	0.254206	0.351267	0.337969	0.352722	0.381368	0.444881	0.627432	0.727114
highway_qcif	0.227441	0.407647	0.339102	0.337452	0.337568	0.353541	0.401820	0.328538
miss-america_qcif	0.210548	0.256159	0.279970	0.327215	0.427013	0.583956	0.911399	1.265292
mobile_cif	0.395473	0.463323	0.481712	0.500935	0.529322	0.567416	0.660021	0.703575
mobile_qcif	0.404572	0.474946	0.495738	0.532693	0.587403	0.652822	0.764425	0.886027
mother-daughter_cif	0.318992	0.356250	0.407603	0.499116	0.677800	1.000736	1.537521	1.570733
mother-daughter_qcif	0.268546	0.340979	0.351626	0.383257	0.427865	0.509452	0.727166	1.316196
news_cif	0.225847	0.221472	0.225003	0.236705	0.284503	0.319062	0.481037	0.954500
news_qcif	0.234134	0.249698	0.243870	0.238758	0.255153	0.265414	0.348605	0.630495
paris_cif	0.272216	0.325352	0.325538	0.325820	0.357793	0.396273	0.465679	0.543685
salesman_qcif	0.285716	0.324982	0.326868	0.329418	0.353319	0.414010	0.528133	0.711690
silent_cif	0.289166	0.339281	0.362502	0.388972	0.432538	0.537520	0.639022	0.861062
silent_qcif	0.322744	0.354362	0.352623	0.346990	0.378830	0.446163	0.631638	1.361391
stefan_cif	0.362662	0.405231	0.416994	0.451410	0.514976	0.629802	0.857153	0.834078
suzie_qcif	0.344228	0.358022	0.346092	0.362276	0.426767	0.514063	0.621998	0.651422
tempete_cif	0.420097	0.498534	0.476673	0.481886	0.498770	0.555949	0.676249	0.789094
waterfall_cif	0.333988	0.419256	0.467637	0.543166	0.683242	0.884027	1.360950	1.709152

Table VI-11: p Parameter (GOP: IBBPBBP_12)

Sequence	$C_{0,0}$	$C_{1,1}$	$C_{2,2}$	$C_{3,3}$	$C_{4,4}$	$C_{5,5}$	$C_{6,6}$	$C_{7,7}$
akiyo_qcif	0.198236	0.218384	0.222984	0.229714	0.256394	0.298481	0.407620	0.707021
bus_cif	0.412790	0.488482	0.480920	0.497164	0.508317	0.558788	0.724089	1.039851
carphone_qcif	0.327349	0.390208	0.368529	0.364170	0.384417	0.431253	0.522149	0.609772
claire_qcif	0.211145	0.223653	0.229584	0.246509	0.328198	0.387314	0.500933	0.723426
coastguard_qcif	0.324959	0.421235	0.461066	0.542211	0.645800	0.716430	0.860825	1.110508
container_cif	0.218716	0.261712	0.283839	0.321210	0.375195	0.395165	0.568710	0.928296
container_qcif	0.207814	0.228516	0.238734	0.259405	0.284449	0.323359	0.412210	0.625351
flower_cif	0.356067	0.392996	0.395965	0.414066	0.435173	0.462112	0.497951	0.581591
foreman_cif	0.381590	0.398772	0.420396	0.461796	0.514410	0.544373	0.686896	0.946108
foreman_qcif	0.371506	0.420559	0.424799	0.426160	0.402856	0.440637	0.607591	0.924043
grandma_qcif	0.261455	0.304162	0.338317	0.370931	0.389214	0.488857	0.597210	0.772411
hall_cif	0.376738	0.333924	0.346544	0.380449	0.418528	0.500776	0.619524	0.498455
hall_qcif	0.405169	0.379889	0.349397	0.378328	0.371838	0.413588	0.448943	0.412583
highway_cif	0.272335	0.377363	0.338895	0.341282	0.366371	0.419487	0.595216	0.693550
highway_qcif	0.245049	0.495075	0.372319	0.343598	0.334664	0.345015	0.391910	0.319445
miss-america_qcif	0.217705	0.282690	0.293820	0.327437	0.401937	0.520754	0.818684	1.206893
mobile_cif	0.444694	0.523653	0.538898	0.554951	0.576085	0.601818	0.683675	0.721118
mobile_qcif	0.526437	0.621272	0.646042	0.670291	0.716813	0.760661	0.854138	0.923196
mother-daughter_cif	0.402113	0.416279	0.454264	0.518692	0.665720	0.936294	1.480465	1.501648
mother-daughter_qcif	0.281240	0.365768	0.367885	0.396990	0.439354	0.512033	0.717103	1.289375
news_cif	0.236840	0.232162	0.228383	0.233802	0.284790	0.321682	0.481496	1.034966
news_qcif	0.228071	0.245236	0.240542	0.240854	0.240337	0.261395	0.339664	0.679836
paris_cif	0.269462	0.317347	0.317208	0.319180	0.345722	0.384309	0.460329	0.540734
salesman_qcif	0.284853	0.315875	0.318040	0.324979	0.345938	0.404082	0.522042	0.693987
silent_cif	0.317731	0.374449	0.397171	0.417984	0.457539	0.563137	0.657512	0.852961
silent_qcif	0.337000	0.347384	0.344461	0.346221	0.373453	0.445954	0.636914	1.388510
stefan_cif	0.405203	0.450767	0.455754	0.482520	0.538208	0.638463	0.847679	0.814973
suzie_qcif	0.375237	0.389635	0.369211	0.377472	0.433297	0.513515	0.615479	0.641280

tempete_cif	0.463361	0.560378	0.524041	0.518103	0.529282	0.568045	0.673533	0.773546
waterfall_cif	0.392109	0.487498	0.529100	0.603458	0.729246	0.905112	1.348631	1.648295

Table VI-12: p Parameter (GOP: IPPPPPP)

Note the tendency of the p parameter to augment as the coefficient's number increases.

VI.1.3 Cauchy

The Cauchy PDF requires a location and a scale parameter. For the location, the median of the empirical data is used. The following tables show the results of the estimation of the scale parameter b.

Sequence	$C_{0,0}$	$C_{1,1}$	$C_{2,2}$	$C_{3,3}$	$C_{4,4}$	$C_{5,5}$	$C_{6,6}$	$C_{7,7}$
akiyo_qcif	12.078628	4.438042	1.994797	1.265279	0.806345	0.707086	0.350191	0.269335
bus_cif	22.992363	11.496457	7.931372	5.891759	3.816231	2.193187	0.618573	0.244918
carphone_qcif	6.996109	4.287364	2.341538	1.511774	1.121706	0.887091	0.598122	0.523166
claire_qcif	1.934440	0.468036	0.519285	0.195504	0.426688	0.374722	0.244524	0.191838
coastguard_qcif	18.472506	8.184397	6.926393	5.613541	4.306078	3.081670	1.449019	0.635349
container_cif	7.030017	4.445681	3.255027	3.182243	2.284208	1.506142	0.467857	0.220993
container_qcif	8.060296	4.125725	2.365175	2.245121	2.222249	1.633217	0.917146	0.468321
flower_cif	3.422847	3.994296	2.753361	2.304163	1.682820	1.382022	0.765409	0.532405
foreman_cif	8.567231	5.352024	3.464732	2.468260	1.819630	1.460650	0.725103	0.399849
foreman_qcif	9.937879	9.035332	5.419841	3.928998	2.475825	1.568312	0.673369	0.276204
grandma_qcif	7.154931	4.582249	2.940412	1.978018	1.808943	1.317310	0.907323	0.514911
hall_cif	4.407697	3.652979	2.537336	1.774423	1.501882	0.815457	0.331939	0.196057
hall_qcif	5.626370	5.221872	2.266828	2.126667	1.876006	1.177901	0.756496	0.325469
highway_cif	0.826510	0.311038	1.399248	1.061296	0.950494	0.834996	0.769358	0.649821
highway_qcif	2.844446	3.287451	2.090987	1.322774	1.012747	0.843270	0.777025	0.678647
miss-america_qcif	3.357930	1.704047	1.016933	0.817425	0.599859	0.603716	0.273234	0.308016
mobile_cif	24.547616	18.756020	14.758109	12.333394	8.592550	4.917918	1.605943	0.464967
mobile_qcif	36.993791	20.756268	15.573064	11.434536	8.363056	5.705790	3.025289	1.663454
mother-daughter_cif	4.041258	2.422489	1.878470	1.630492	0.957424	0.481869	0.180325	0.152831
mother-daughter_qcif	6.165791	4.108191	1.618841	1.605462	1.263400	1.060130	0.414760	0.264658
news_cif	4.414965	2.746139	1.994195	1.630408	1.207490	0.833432	0.231195	0.188299
news_qcif	9.284432	6.489951	2.041780	1.525109	1.364531	1.124624	0.633307	0.345618
paris_cif	14.097610	7.795715	4.285587	3.003539	2.304329	1.891774	1.261694	0.839074
salesman_qcif	21.198172	9.864493	5.893688	2.717468	2.165414	1.411346	0.997130	0.628090
silent_cif	11.492223	7.681338	4.245577	3.382455	2.106396	1.773727	1.003656	0.518332
silent_qcif	14.892458	10.904911	6.556110	4.197987	2.062803	1.745225	0.763569	0.272567
stefan_cif	15.437746	7.814923	4.880073	3.638259	2.347308	1.337338	0.486233	0.239706
suzie_qcif	9.553033	5.507778	2.569514	1.676698	1.162786	0.913558	0.566944	0.497723
tempete_cif	24.370935	13.642947	7.924018	5.191253	3.181751	1.988236	1.045991	0.646008
waterfall_cif	19.085517	14.057060	10.151041	7.230226	4.300798	2.221808	0.494074	0.212310

Table VI-13: Scale Parameter (GOP: IIIIIII)

Sequence	$C_{0,0}$	$C_{1,1}$	$C_{2,2}$	$C_{3,3}$	$C_{4,4}$	$C_{5,5}$	$C_{6,6}$	$C_{7,7}$
akiyo_qcif	0.566124	0.241826	0.247420	0.212163	0.221452	0.210221	0.154988	0.148707
bus_cif	8.684357	4.063107	3.361441	3.290933	2.596215	1.686004	0.523520	0.264096
carphone_qcif	2.621680	1.740485	1.285590	1.163743	0.885294	0.768187	0.536789	0.511718
claire_qcif	0.605883	0.343687	0.380505	0.356867	0.306921	0.286756	0.255410	0.206563
coastguard_qcif	4.347126	2.857854	2.718481	2.509321	2.334283	1.881227	0.989936	0.551595
container_cif	1.186543	1.261235	1.278267	1.386455	1.192428	0.897313	0.333960	0.242544
container_qcif	1.080082	0.695343	0.660626	0.725512	0.733250	0.683065	0.395052	0.303643
flower_cif	2.066229	1.308491	1.090456	1.196213	1.030289	1.048368	0.662893	0.573112
foreman_cif	4.954638	2.260245	1.813974	1.527259	1.273407	1.192991	0.619374	0.392921
foreman_qcif	3.080489	1.951366	1.544211	1.494704	1.227232	0.976097	0.467646	0.282318
grandma_qcif	1.248231	0.943852	0.693932	0.683157	0.685749	0.719156	0.482298	0.422054

hall_cif	1.680574	2.703808	1.827150	1.477079	1.293709	1.043715	0.339780	0.209869
hall_qcif	2.064943	2.041098	1.378246	1.380229	1.180590	0.890481	0.488192	0.319208
highway_cif	0.694628	1.708940	1.176660	1.004760	0.905183	0.833304	0.770403	0.651683
highway_qcif	1.161861	1.541356	1.349588	1.054330	0.883056	0.793492	0.739868	0.683418
miss-america_qcif	1.318023	0.799378	0.660452	0.637284	0.535241	0.581591	0.315721	0.333113
mobile_cif	8.445242	4.929449	4.573241	4.749664	4.043196	2.879962	1.230448	0.433102
mobile_qcif	8.980803	4.678161	4.389187	4.120058	4.008626	3.511609	2.302900	1.259372
mother-daughter_cif	0.997351	1.190510	1.013465	0.876994	0.671312	0.561614	0.193370	0.197071
mother-daughter_qcif	2.594951	0.927199	0.954304	0.824873	0.707209	0.658400	0.325464	0.264096
news_cif	0.913277	0.410799	0.389335	0.269845	0.339438	0.350424	0.162819	0.149602
news_qcif	0.978005	0.395512	0.486021	0.284621	0.425586	0.372555	0.246853	0.209380
paris_cif	1.876461	1.205161	1.218129	1.115964	1.041744	1.013209	0.729238	0.669706
salesman_qcif	4.331651	0.805752	0.654729	0.718091	0.590577	0.579467	0.393449	0.380807
silent_cif	3.934510	1.255617	1.404269	1.128510	0.922865	0.962613	0.505669	0.368175
silent_qcif	4.334557	0.914563	0.822090	0.798086	0.749776	0.611187	0.351212	0.252133
stefan_cif	5.700560	3.040182	2.616629	2.419906	1.821507	1.200030	0.452240	0.265768
suzie_qcif	3.082190	1.474664	1.249878	1.112036	0.817675	0.788089	0.524534	0.509827
tempete_cif	5.262189	4.237177	3.027863	2.536403	1.916051	1.515094	0.864876	0.620720
waterfall_cif	5.357169	2.230303	2.174108	2.126521	1.795650	1.230175	0.391198	0.240362

Table VI-14: Scale Parameter (GOP: IBBPBBP_12)

Sequence	$C_{0,0}$	$C_{1,1}$	$C_{2,2}$	$C_{3,3}$	$C_{4,4}$	$C_{5,5}$	$C_{6,6}$	$C_{7,7}$
akiyo_qcif	0.214479	0.214214	0.219553	0.207640	0.196762	0.193484	0.148603	0.135620
bus_cif	7.372813	5.515360	4.229562	3.836969	2.879101	1.831515	0.549895	0.259166
carphone_qcif	4.330351	1.638348	1.556059	1.151534	1.035156	0.795665	0.552393	0.504466
claire_qcif	0.763068	0.384791	0.382069	0.363589	0.321690	0.291767	0.267443	0.211205
coastguard_qcif	3.728310	3.372353	3.039253	2.701959	2.433804	2.006031	1.012803	0.551078
container_cif	1.329135	1.406091	1.401123	1.515769	1.297843	0.937308	0.359391	0.248697
container_qcif	1.082008	0.731342	0.687850	0.734130	0.765202	0.702856	0.405178	0.330416
flower_cif	3.353338	1.474614	1.294701	1.326070	1.148057	1.077537	0.668441	0.536967
foreman_cif	4.062650	2.506503	2.059136	1.706967	1.370836	1.220515	0.631313	0.388260
foreman_qcif	4.080494	2.235331	1.753199	1.643276	1.239177	0.991578	0.468210	0.273263
grandma_qcif	1.944909	1.263185	0.883996	0.740149	0.735298	0.754956	0.495964	0.421884
hall_cif	3.589664	3.359392	2.221641	1.651981	1.416816	1.046808	0.331695	0.197319
hall_qcif	4.771527	2.872371	1.991557	1.669349	1.408442	0.953228	0.543365	0.313510
highway_cif	0.788159	0.305656	1.315293	1.049521	0.943356	0.836979	0.769924	0.652011
highway_qcif	2.840676	2.299648	1.730532	1.194751	0.957695	0.825245	0.762574	0.675264
miss-america_qcif	1.765216	1.050639	0.739574	0.662261	0.549729	0.589384	0.308876	0.319837
mobile_cif	7.479693	7.001543	6.190289	5.963274	4.787865	3.220504	1.320300	0.440328
mobile_qcif	13.224323	9.229038	8.227461	6.605951	5.945262	4.532676	2.504375	1.374662
mother-daughter_cif	1.667240	1.502129	1.341856	1.107517	0.748823	0.599962	0.188095	0.184298
mother-daughter_qcif	1.669964	1.137757	1.170772	1.002378	0.762342	0.702195	0.338900	0.260820
news_cif	0.612062	0.403554	0.442268	0.394267	0.404304	0.388320	0.163755	0.164061
news_qcif	0.277851	0.379400	0.430735	0.443394	0.410287	0.393613	0.236758	0.205466
paris_cif	1.814178	1.281018	1.092420	1.029184	1.122877	0.958019	0.709265	0.661403
salesman_qcif	1.195508	0.806421	1.043247	0.678493	0.566066	0.567380	0.402108	0.370694
silent_cif	2.602452	1.425498	1.260813	1.182117	1.041085	1.074604	0.558836	0.380115
silent_qcif	1.596444	0.912054	0.792900	0.758333	0.690362	0.613408	0.342477	0.248402
stefan_cif	4.755573	3.648172	2.948032	2.674676	1.960826	1.289840	0.463800	0.261794
suzie_qcif	2.396817	1.905886	1.270104	1.180594	0.863464	0.815526	0.530413	0.504266
tempete_cif	9.919085	5.835607	3.988238	2.992882	2.158405	1.630380	0.912587	0.632418
waterfall_cif	3.245408	2.833643	2.712522	2.727066	2.054981	1.366487	0.408767	0.233838

Table VI-15: Scale Parameter (GOP: IPPPPPP)

Note the tendency of b to diminish as the coefficient's number increases.

The following figures show some examples of the DCT modeling. They are presented only as a visual aid, for an objective comparison see the next section.

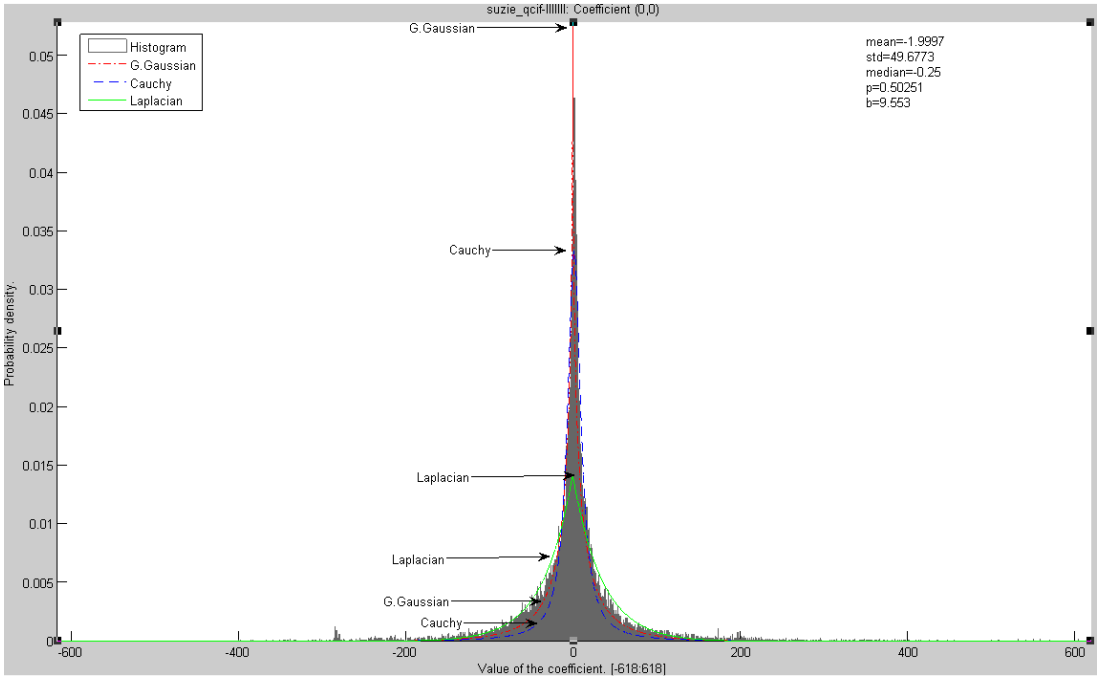

Fig. VI-1: Histogram of Suzie $C_{0,0}$

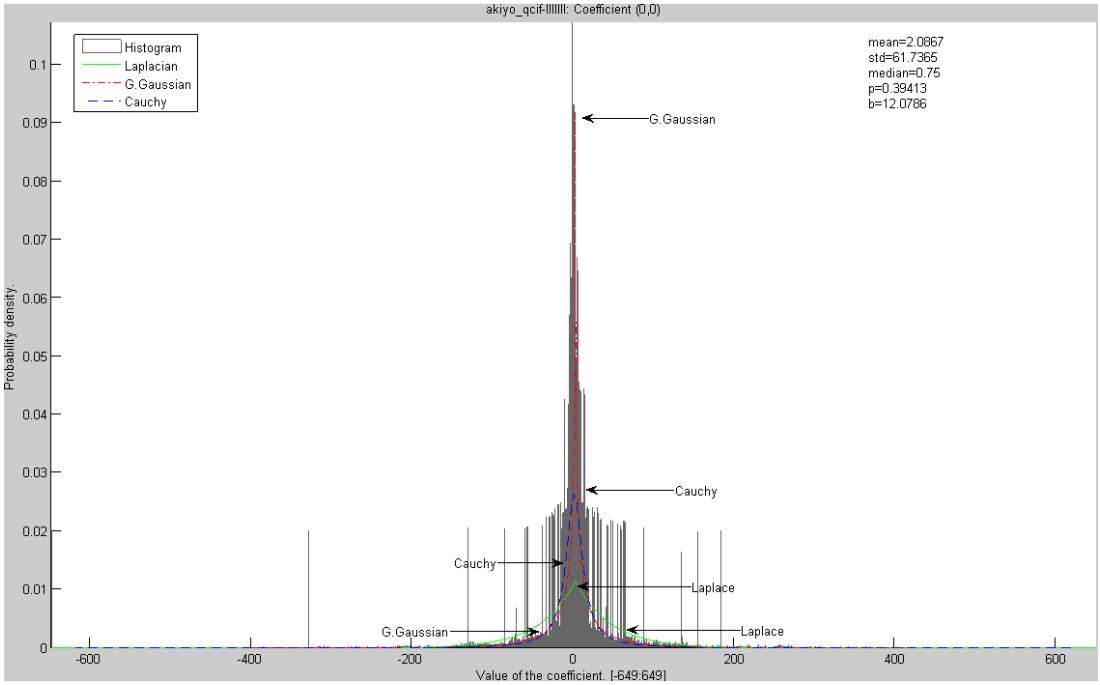

Fig. VI-2: Histogram of Akiyo $C_{0,0}$

Figures VI.1 and VI.2 are examples of the distribution of the DC coefficient (0,0). Fig. VI.1 is a typical case, and Fig. VI.2 is a rare case in which none of the theoretical PDFs used here model it well.

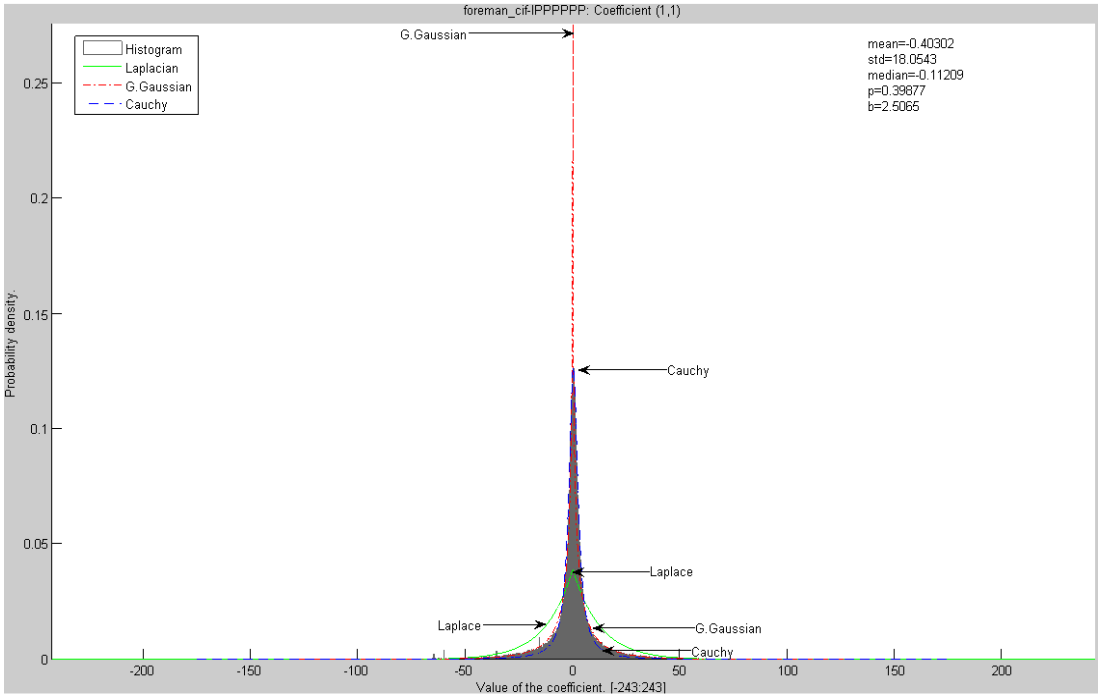

Fig. VI-3: Histogram of Foreman $C_{1,1}$

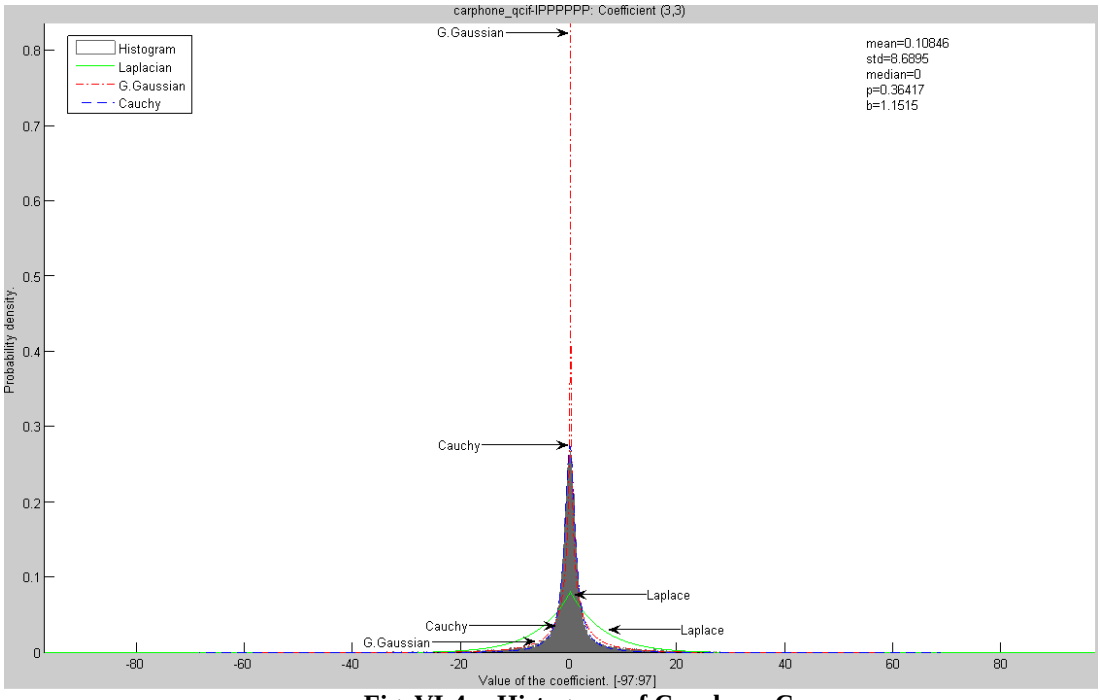

Fig. VI-4: : Histogram of Carphone $C_{3,3}$

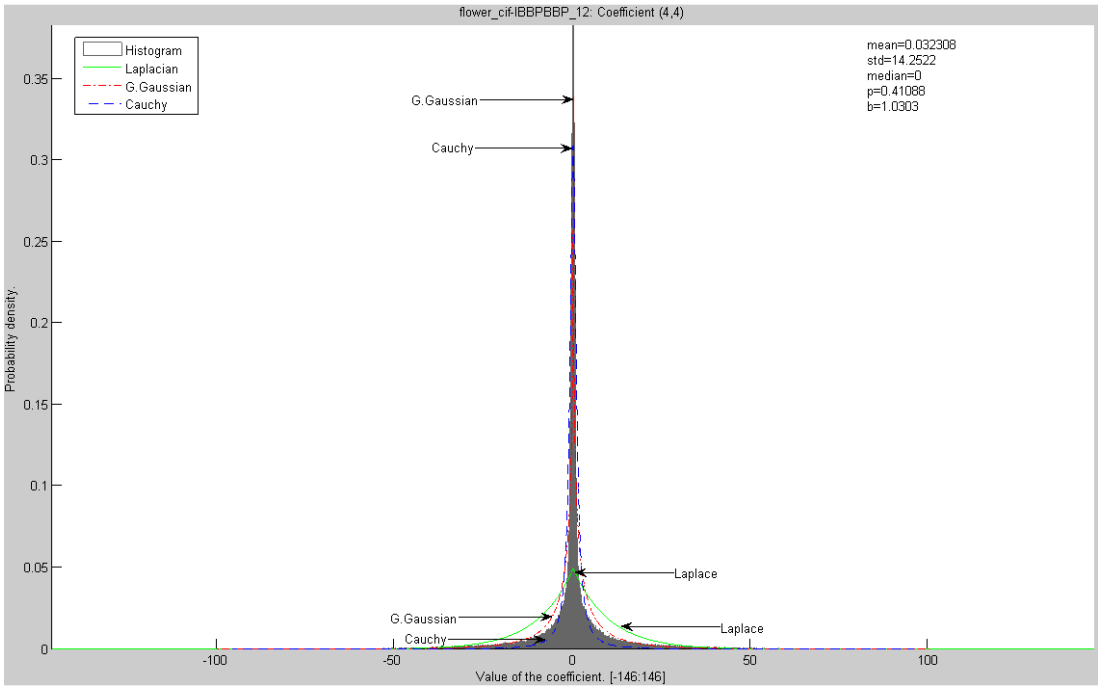

Fig. VI-5: Histogram of Flower $C_{4,4}$

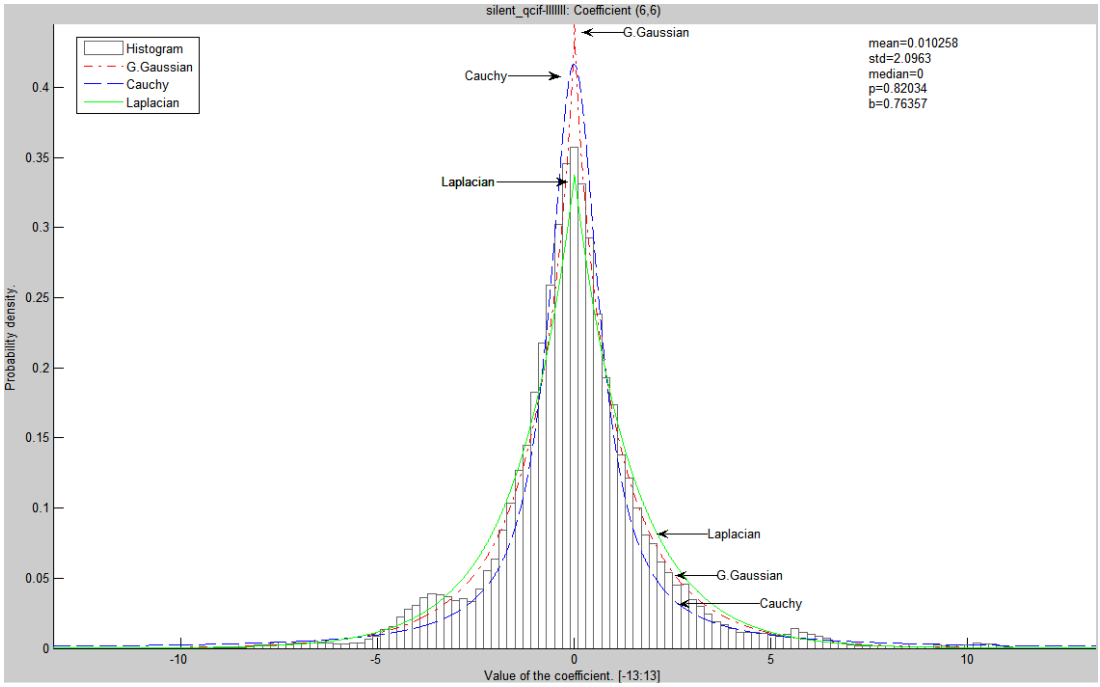

Fig. VI-6: Histogram of Silent $C_{6,6}$

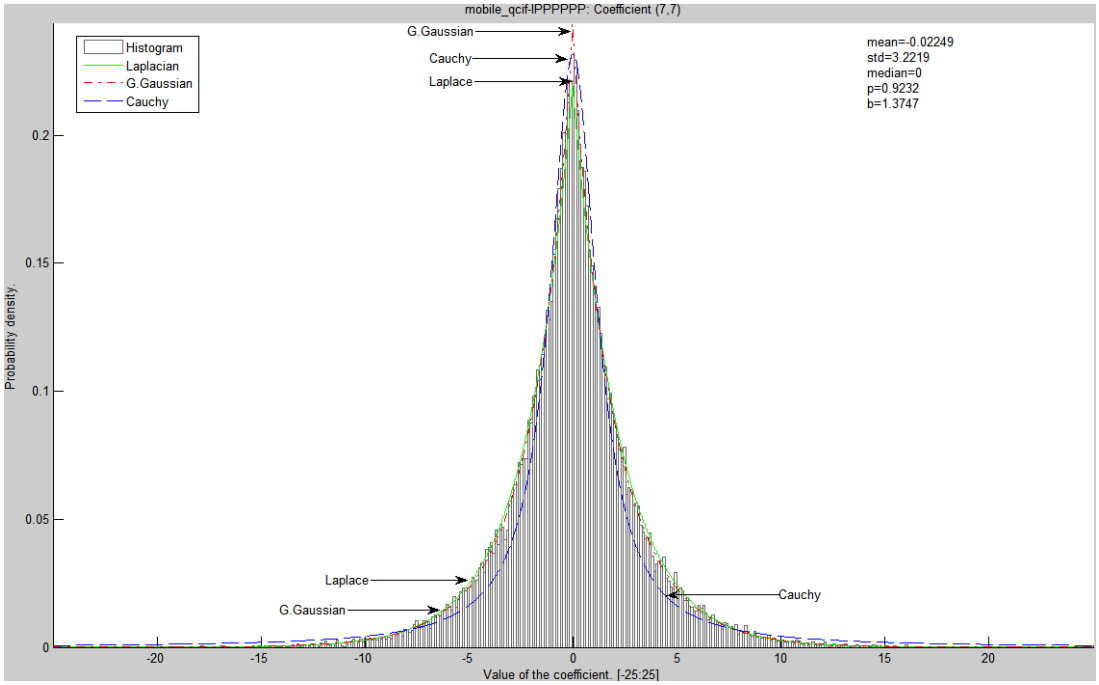

Fig. VI-7: Histogram of Mobile $C_{7,7}$

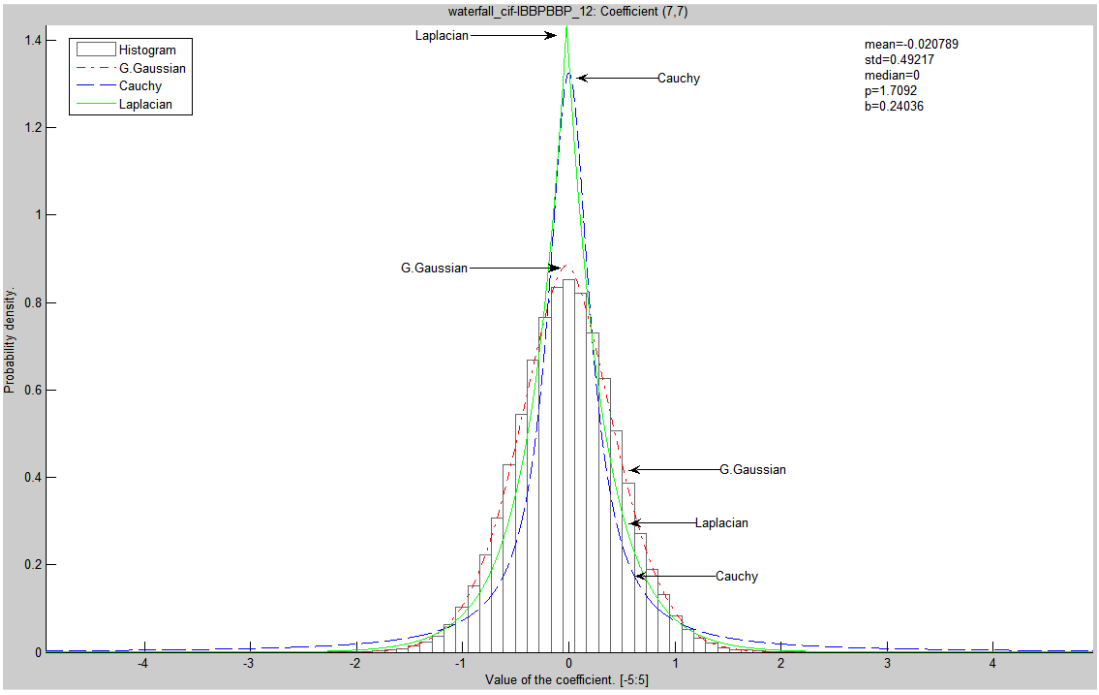

Fig. VI-8: Histogram of Waterfall $C_{7,7}$

Fig. VI.8 is shown as an example of a very rare case as, the distribution of the DCT coefficients seems to be almost Gaussian; note that the value of the p parameter is close to 2. Fig. VI.7 is a more common example of the last coefficient of the DCT (7,7), its distribution seems to be almost Laplacian.

The graphics of the histograms and PDFs are good tools to compare the models with the actual data, but still, an objective measure is needed.

VI.2 THE χ^2 TEST

Pearson (1900; as referenced in Cochran, 1952) proposed the quantity

$$\chi^2 = \sum_{i=1}^{k} \frac{(O_i - E_i)}{E_i}^2$$

In the standard applications of the test, the n observations in a random sample from a population are classified into k mutually exclusive classes. O_i is the number of observations which fall into class i, in other words the observed frequency. $E_i = np_i$ is the expected frequency. p_i is the theoretical probability that a sample belongs to class i (Cochran, 1952), where:

$$\sum_{i=1}^{k} p_i = 1 \qquad \sum_{i=1}^{k} E_i = n$$

The asymptotic distribution of the quantity χ^2 is the chi-square with $k - s - 1$ degrees of freedom, where s is the number of parameters that need to be efficiently estimated from the data (Fisher, 1924; as referenced in Cressie & Read, 1989).

"The χ^2 test compares empirical frequencies with theoretical probabilities and gives therefore a measure of distortion between an empirical and a theoretical PDF" (Müller, 1993).

Cressie & Read (1989) present a discussion of the criteria to choose the cell boundaries. They mention that many authors propose that the cell boundaries should be chosen so the cells are equiprobable, because this choice ensures that the χ^2 test statistic is unbiased. However, they also mention that there are still some disagreements on this issue for certain hypotheses.

Müller (1993) used the χ^2 test to compare the fit of the Laplace and Generalized Gaussian probability density functions for natural images' DCT coefficients. His results showed considerable lower values of the χ^2 for the later. In this section the same test is performed but now using video sequences, and the Cauchy PDF is added.

The criterion to choose the cell boundaries was not the equiprobable one, because that would imply different boundaries for each PDF; the criterion was to have equispaced boundaries, the same for the three PDFs. By taking advantage of the fact that the DCT coefficients in H.264 are integers, albeit multiplied by fractional scale factors (Malvar et al., 2003), the boundaries were chosen to have one cell for each discrete coefficient value.

VI.2.1 Experimental Results

For the video sequences, the test was applied separately to each of the 64 coefficients of the DCT. There is one table per GOP type used. Each row represents one coefficient of the DCT, and the numbers in **bold** denote the minimum χ^2 value, hence the best fit.

In order to establish if the DCT coefficients' modeling with the Generalized Gaussian or the Cauchy distributions is worth the increased complexity in relation to the Laplace distribution, their values of the test statistic χ^2 should be considerably lower than the values of the χ^2 of the latter.

Each result in the table is the weighted mean of the individual sequences' results.

$$\overline{\chi^2} = \frac{1}{K}\sum_{j=1}^{N} {\chi^2}_j k_j$$

Where ${\chi^2}_j$ is the χ^2 test result for the sequence j; k_j is the number of classes into which the sample space of sequence j is divided; N is the number of sequences and K is the sum of all of the k_j.

The k in the tables is simply the mean of the k_j, rounded to the nearest integer.

C.N.	k	Laplace	Laplace μ=0	G.G.	G.G. μ=0	Cauchy	Cauchy b=0
$C_{0,0}$	11792	2.373407E+015	2.444629E+015	3.508254E+005	3.376078E+005	**1.346790E+005**	1.370016E+005
$C_{0,1}$	6678	3.450471E+010	3.542652E+010	8.131983E+004	7.548454E+004	**5.195141E+004**	5.261618E+004
$C_{0,2}$	3780	1.159511E+011	1.263708E+011	6.100044E+004	**4.444225E+004**	7.120664E+004	7.200752E+004
$C_{0,3}$	3886	1.356191E+011	1.307306E+011	4.328117E+004	**3.328111E+004**	4.860848E+004	4.865293E+004
$C_{0,4}$	3002	2.145101E+012	2.158210E+012	5.364961E+004	**3.784569E+004**	5.850302E+004	5.864900E+004
$C_{0,5}$	2525	6.865629E+011	5.860235E+011	7.588034E+004	6.220036E+004	**4.836419E+004**	5.044029E+004
$C_{0,6}$	1330	1.581090E+011	1.826179E+011	3.764930E+004	**2.932602E+004**	5.282825E+004	5.526749E+004
$C_{0,7}$	1178	1.623346E+010	1.307521E+010	2.531871E+004	**1.972889E+004**	4.285262E+004	4.604476E+004
$C_{1,0}$	6599	3.548270E+006	4.054903E+006	4.394518E+004	**3.527317E+004**	7.157551E+004	7.237215E+004
$C_{1,1}$	4433	2.429767E+010	2.578512E+010	3.692821E+004	**3.039750E+004**	7.037139E+004	7.040860E+004
$C_{1,2}$	2791	1.205347E+007	1.188551E+007	2.706057E+004	**2.550554E+004**	3.988687E+004	3.994547E+004
$C_{1,3}$	3107	6.980338E+010	7.153821E+010	2.900912E+004	**2.764824E+004**	4.501874E+004	4.505797E+004
$C_{1,4}$	2366	3.873080E+007	4.002822E+007	3.527749E+004	**3.396216E+004**	3.848425E+004	3.856397E+004
$C_{1,5}$	1964	1.931288E+008	1.968156E+008	3.037369E+004	**2.891999E+004**	3.193678E+004	3.199770E+004
$C_{1,6}$	1013	7.388574E+009	7.689827E+009	3.502200E+004	3.296283E+004	**2.677597E+004**	2.707526E+004
$C_{1,7}$	853	1.140659E+008	1.220224E+008	4.746754E+004	4.790396E+004	**1.909377E+004**	1.938675E+004
$C_{2,0}$	3851	1.797936E+007	1.891476E+007	3.983392E+004	**3.183485E+004**	7.285190E+004	7.321114E+004

$C_{2,1}$	2819	4.888718E+006	4.943707E+006	2.911251E+004	**2.631527E+004**	4.110827E+004	4.112641E+004
$C_{2,2}$	1819	1.063087E+011	1.050852E+011	2.299522E+004	**2.194600E+004**	3.671904E+004	3.674227E+004
$C_{2,3}$	1992	2.620554E+007	2.641334E+007	2.239607E+004	**2.043135E+004**	3.265896E+004	3.266488E+004
$C_{2,4}$	1585	3.070271E+007	3.054517E+007	2.587259E+004	**2.455314E+004**	3.157058E+004	3.158710E+004
$C_{2,5}$	1364	3.270096E+006	3.283828E+006	2.018141E+004	**1.909625E+004**	2.755297E+004	2.756456E+004
$C_{2,6}$	663	4.065795E+008	3.987931E+008	1.253683E+004	**1.211463E+004**	1.938430E+004	1.939412E+004
$C_{2,7}$	562	1.564299E+007	1.577169E+007	2.296677E+004	2.282419E+004	1.622347E+004	**1.621665E+004**
$C_{3,0}$	4226	6.492171E+006	6.451413E+006	4.541342E+004	**3.255338E+004**	6.484747E+004	6.523684E+004
$C_{3,1}$	3083	6.647247E+005	6.659694E+005	2.787471E+004	**2.736082E+004**	5.638623E+004	5.641258E+004
$C_{3,2}$	2044	3.026762E+009	3.003853E+009	2.384998E+004	**2.291450E+004**	3.682006E+004	3.682220E+004
$C_{3,3}$	2286	2.140571E+008	2.163561E+008	2.155788E+004	**2.069877E+004**	3.323769E+004	3.328121E+004
$C_{3,4}$	1797	1.889493E+006	1.892730E+006	1.853725E+004	**1.774500E+004**	2.590294E+004	2.591596E+004
$C_{3,5}$	1547	1.249307E+009	1.264204E+009	1.741014E+004	**1.643884E+004**	2.349811E+004	2.351008E+004
$C_{3,6}$	800	4.178930E+009	4.093476E+009	1.599495E+004	**1.519220E+004**	1.702401E+004	1.702723E+004
$C_{3,7}$	668	6.908253E+007	6.930948E+007	9.061829E+003	**8.676668E+003**	1.164848E+004	1.164848E+004
$C_{4,0}$	3350	6.386162E+006	6.323101E+006	5.428274E+004	**3.086806E+004**	6.670845E+004	6.681593E+004
$C_{4,1}$	2476	1.185815E+006	1.190836E+006	2.723466E+004	**2.581050E+004**	4.876962E+004	4.877623E+004
$C_{4,2}$	1514	5.205710E+008	5.174052E+008	2.168634E+004	**2.121616E+004**	3.493396E+004	3.493547E+004
$C_{4,3}$	1766	3.396728E+009	3.373924E+009	2.044048E+004	**1.973966E+004**	3.106730E+004	3.107124E+004
$C_{4,4}$	1341	2.759393E+007	2.736255E+007	1.711155E+004	**1.630202E+004**	2.455831E+004	2.456438E+004
$C_{4,5}$	1166	1.274246E+008	1.279066E+008	1.290966E+004	**1.261458E+004**	2.062690E+004	2.064048E+004
$C_{4,6}$	601	1.059930E+008	1.092993E+008	9.066610E+003	**8.827139E+003**	1.511287E+004	1.510495E+004
$C_{4,7}$	514	6.819677E+007	6.940912E+007	1.076531E+004	**1.060962E+004**	1.117275E+004	1.117727E+004
$C_{5,0}$	2717	1.628044E+008	1.670685E+008	4.342159E+004	**2.944227E+004**	5.467153E+004	5.471999E+004
$C_{5,1}$	2100	9.492834E+006	9.547131E+006	2.893011E+004	**2.815154E+004**	4.952505E+004	4.956721E+004
$C_{5,2}$	1291	2.174129E+006	2.255435E+006	2.335521E+004	**2.273012E+004**	3.614497E+004	3.620890E+004
$C_{5,3}$	1456	2.778022E+008	2.786387E+008	1.980873E+004	**1.946007E+004**	3.079537E+004	3.084484E+004
$C_{5,4}$	1153	1.752739E+008	1.743671E+008	1.770988E+004	**1.757389E+004**	2.365944E+004	2.371643E+004
$C_{5,5}$	968	6.128057E+007	6.020514E+007	1.347982E+004	**1.316348E+004**	1.846773E+004	1.853801E+004
$C_{5,6}$	487	2.013961E+006	2.033969E+006	**9.149160E+003**	9.149538E+003	1.276101E+004	1.308904E+004
$C_{5,7}$	438	5.502037E+005	5.427470E+005	**6.781946E+003**	7.060347E+003	9.851479E+003	1.004057E+004
$C_{6,0}$	1432	1.665012E+009	1.816427E+009	4.272011E+004	**2.711051E+004**	4.769944E+004	4.787555E+004
$C_{6,1}$	1101	5.669760E+007	5.644835E+007	3.017336E+004	**2.930063E+004**	4.001401E+004	4.002271E+004
$C_{6,2}$	702	1.731911E+007	1.745947E+007	2.297793E+004	**2.205375E+004**	3.708268E+004	3.709869E+004
$C_{6,3}$	737	5.028025E+007	5.077419E+007	1.716160E+004	**1.672685E+004**	3.015610E+004	3.016340E+004
$C_{6,4}$	599	1.612476E+008	1.614666E+008	1.537181E+004	**1.521633E+004**	2.598677E+004	2.601573E+004
$C_{6,5}$	511	1.434798E+009	1.455057E+009	1.273181E+004	**1.261080E+004**	2.176425E+004	2.180315E+004
$C_{6,6}$	263	1.145253E+006	1.167766E+006	**8.561772E+003**	8.816040E+003	1.846328E+004	1.846328E+004
$C_{6,7}$	241	4.804012E+005	4.828484E+005	1.130038E+006	9.049074E+005	1.418346E+004	**1.413829E+004**
$C_{7,0}$	1402	6.110513E+009	6.164156E+009	3.532200E+004	**2.394080E+004**	3.450701E+004	3.476078E+004
$C_{7,1}$	1122	3.280345E+010	3.273775E+010	3.244771E+004	**3.198840E+004**	4.830103E+004	4.830833E+004
$C_{7,2}$	694	8.578144E+009	8.528596E+009	2.654780E+004	**2.599142E+004**	4.192913E+004	4.193631E+004
$C_{7,3}$	711	4.895741E+007	4.945735E+007	1.970688E+004	**1.945876E+004**	3.765292E+004	3.765287E+004
$C_{7,4}$	563	1.884271E+008	1.854936E+008	1.580442E+004	**1.575699E+004**	2.643089E+004	2.645007E+004
$C_{7,5}$	515	1.649264E+008	1.649904E+008	**1.730373E+004**	1.743789E+004	2.078466E+004	2.080843E+004
$C_{7,6}$	284	1.381134E+007	1.407896E+007	1.346610E+005	1.172018E+005	**1.632591E+004**	1.632591E+004
$C_{7,7}$	291	9.265440E+007	9.181694E+007	3.059050E+004	3.094537E+004	**1.548744E+004**	1.549416E+004

Table VI-16: Chi2 results IIIIIII

C.N.	**k**	**Laplace**	**Laplace μ=0**	**G.G.**	**G.G. μ=0**	**Cauchy**	**Cauchy b=0**
$C_{0,0}$	11604	9.398545E+025	1.064279E+026	1.063910E+005	**1.006045E+005**	1.062232E+005	1.325297E+005
$C_{0,1}$	6572	2.005080E+016	1.996889E+016	6.419213E+004	**4.134885E+004**	7.251568E+004	7.522584E+004
$C_{0,2}$	3719	2.245061E+013	2.406304E+013	6.825814E+004	**3.363259E+004**	6.979196E+004	7.094469E+004
$C_{0,3}$	3760	5.550126E+011	5.739162E+011	4.905763E+004	**2.905576E+004**	4.305093E+004	4.309722E+004
$C_{0,4}$	2954	1.710424E+013	1.724297E+013	5.323120E+004	**3.096775E+004**	3.673520E+004	3.674971E+004
$C_{0,5}$	2477	2.519248E+013	2.162762E+013	6.934435E+004	5.237071E+004	**2.607678E+004**	2.960202E+004
$C_{0,6}$	1275	1.131638E+011	1.190593E+011	3.257999E+004	**2.681000E+004**	3.115970E+004	3.467980E+004
$C_{0,7}$	1163	1.005784E+011	8.444299E+010	2.561704E+004	2.190614E+004	**2.027398E+004**	2.310808E+004
$C_{1,0}$	6483	8.201851E+008	8.399624E+008	5.989755E+004	**3.240582E+004**	7.883688E+004	7.898612E+004
$C_{1,1}$	4346	4.866269E+012	5.098438E+012	4.124749E+004	**2.678435E+004**	5.199879E+004	5.202642E+004
$C_{1,2}$	2748	4.038960E+008	4.033907E+008	2.849950E+004	**2.251890E+004**	3.940393E+004	3.942629E+004
$C_{1,3}$	2964	4.931706E+014	4.914301E+014	2.573909E+004	**2.265199E+004**	3.516572E+004	3.522305E+004
$C_{1,4}$	2319	1.259582E+012	1.272955E+012	2.591931E+004	**2.247604E+004**	2.919800E+004	2.923990E+004
$C_{1,5}$	1894	3.870955E+010	3.920558E+010	2.903742E+004	2.685105E+004	**2.325112E+004**	2.330630E+004

$C_{1,6}$	979	2.002354E+012	2.082971E+012	3.177193E+004	2.812051E+004	**1.707608E+004**	1.720820E+004
$C_{1,7}$	829	3.032415E+012	2.903712E+012	7.091989E+004	7.212463E+004	**1.346211E+004**	1.372575E+004
$C_{2,0}$	3763	6.175464E+009	6.135749E+009	3.903109E+004	**2.735225E+004**	6.495830E+004	6.497951E+004
$C_{2,1}$	2743	1.326119E+009	1.354866E+009	2.497555E+004	**2.200924E+004**	3.700084E+004	3.699932E+004
$C_{2,2}$	1771	3.774918E+013	3.726653E+013	2.013668E+004	**1.941634E+004**	3.065773E+004	3.065773E+004
$C_{2,3}$	1940	3.563687E+010	3.650807E+010	1.999120E+004	**1.814394E+004**	2.546037E+004	2.546113E+004
$C_{2,4}$	1557	6.918041E+009	7.113400E+009	2.125729E+004	**1.934208E+004**	2.161478E+004	2.161478E+004
$C_{2,5}$	1320	3.911996E+009	3.912101E+009	1.722737E+004	**1.639814E+004**	1.826855E+004	1.826855E+004
$C_{2,6}$	633	3.161975E+009	3.187196E+009	1.559891E+004	1.555978E+004	**1.327121E+004**	1.327121E+004
$C_{2,7}$	553	3.000841E+009	3.079492E+009	1.077196E+005	1.085944E+005	**1.081865E+004**	1.081865E+004
$C_{3,0}$	4151	6.542207E+010	6.407492E+010	4.682266E+004	**2.766288E+004**	5.521503E+004	5.524617E+004
$C_{3,1}$	2975	7.362839E+008	7.297253E+008	2.436481E+004	**2.280057E+004**	4.910617E+004	4.910419E+004
$C_{3,2}$	1972	1.192275E+011	1.208030E+011	2.016444E+004	**1.855167E+004**	2.534451E+004	2.534451E+004
$C_{3,3}$	2213	1.593318E+010	1.611470E+010	1.852291E+004	**1.784429E+004**	2.462582E+004	2.462482E+004
$C_{3,4}$	1745	5.164599E+008	5.214302E+008	1.635522E+004	**1.542841E+004**	1.756405E+004	1.756503E+004
$C_{3,5}$	1483	1.576018E+010	1.609853E+010	2.087279E+004	1.955541E+004	1.535967E+004	**1.535903E+004**
$C_{3,6}$	775	2.937808E+012	2.891979E+012	2.939318E+004	2.921387E+004	**1.148997E+004**	1.148997E+004
$C_{3,7}$	652	4.272441E+008	4.347108E+008	1.194435E+004	1.176713E+004	**9.215860E+003**	9.215860E+003
$C_{4,0}$	3290	1.033949E+012	1.013019E+012	5.328323E+004	**2.586965E+004**	4.785615E+004	4.786120E+004
$C_{4,1}$	2448	2.327698E+009	2.337947E+009	2.402483E+004	**2.156237E+004**	3.803537E+004	3.803537E+004
$C_{4,2}$	1472	1.321596E+009	1.314777E+009	1.775427E+004	**1.729429E+004**	2.130043E+004	2.130043E+004
$C_{4,3}$	1682	6.767381E+009	6.885992E+009	1.870073E+004	**1.692241E+004**	2.116142E+004	2.116142E+004
$C_{4,4}$	1318	4.762928E+009	4.784220E+009	1.533365E+004	**1.461748E+004**	1.614297E+004	1.614297E+004
$C_{4,5}$	1115	1.723287E+009	1.728590E+009	1.214751E+004	**1.176550E+004**	1.287196E+004	1.287196E+004
$C_{4,6}$	584	2.948349E+010	3.013280E+010	1.043488E+004	1.035951E+004	**9.814964E+003**	9.814964E+003
$C_{4,7}$	499	2.108341E+009	2.136891E+009	1.820117E+004	1.817210E+004	**9.428702E+003**	9.428702E+003
$C_{5,0}$	2648	1.190459E+013	1.193889E+013	3.961181E+004	**2.565517E+004**	3.787246E+004	3.788326E+004
$C_{5,1}$	2071	6.506619E+010	6.479297E+010	2.418631E+004	**2.329901E+004**	3.381205E+004	3.382420E+004
$C_{5,2}$	1247	1.433503E+013	1.424887E+013	1.845195E+004	**1.824229E+004**	1.952710E+004	1.954785E+004
$C_{5,3}$	1422	7.512058E+010	7.493233E+010	1.657780E+004	**1.634392E+004**	1.766523E+004	1.767384E+004
$C_{5,4}$	1122	1.020594E+012	9.744899E+011	1.594846E+004	1.596496E+004	**1.479920E+004**	1.480528E+004
$C_{5,5}$	934	3.429162E+010	3.415118E+010	1.508809E+004	1.465463E+004	**1.197675E+004**	1.199540E+004
$C_{5,6}$	474	1.658944E+009	1.799268E+009	1.745016E+004	1.716912E+004	**9.606319E+003**	9.737883E+003
$C_{5,7}$	420	1.584697E+007	1.612795E+007	2.442383E+004	2.350882E+004	**9.514383E+003**	9.565077E+003
$C_{6,0}$	1412	2.164348E+013	2.134695E+013	4.111231E+004	**2.495952E+004**	2.688970E+004	2.686382E+004
$C_{6,1}$	1076	1.017269E+014	1.022837E+014	2.574643E+004	2.539071E+004	**2.190531E+004**	2.190531E+004
$C_{6,2}$	684	1.643551E+014	1.644683E+014	1.944874E+004	**1.927799E+004**	2.285131E+004	2.285131E+004
$C_{6,3}$	713	1.835281E+011	1.866345E+011	**1.525143E+004**	1.539155E+004	1.825909E+004	1.825932E+004
$C_{6,4}$	583	2.406582E+011	2.384448E+011	1.690622E+004	**1.680817E+004**	1.687437E+004	1.687437E+004
$C_{6,5}$	499	3.656052E+010	3.709132E+010	**1.457492E+004**	1.473692E+004	1.603790E+004	1.603790E+004
$C_{6,6}$	256	3.547437E+007	3.330249E+007	**1.443663E+004**	1.497705E+004	1.543443E+004	1.543443E+004
$C_{6,7}$	236	1.664626E+008	1.681108E+008	1.126106E+008	1.278562E+008	**1.471636E+004**	1.471636E+004
$C_{7,0}$	1385	2.997122E+014	2.848132E+014	3.185304E+004	2.308173E+004	**2.096105E+004**	2.101606E+004
$C_{7,1}$	1089	2.186393E+014	2.210985E+014	2.700021E+004	2.675328E+004	**2.553849E+004**	2.553912E+004
$C_{7,2}$	683	4.185508E+012	4.159143E+012	**2.327132E+004**	2.334563E+004	2.572835E+004	2.572835E+004
$C_{7,3}$	688	1.464112E+015	1.539635E+015	**1.566597E+004**	1.580306E+004	2.213928E+004	2.213928E+004
$C_{7,4}$	547	8.547497E+010	8.276417E+010	**1.707848E+004**	1.719509E+004	1.846368E+004	1.846368E+004
$C_{7,5}$	492	1.362435E+010	1.379392E+010	3.516112E+006	3.813035E+006	**1.553276E+004**	1.553276E+004
$C_{7,6}$	275	3.369263E+008	3.427952E+008	5.621873E+007	6.296729E+007	**1.597077E+004**	1.597077E+004
$C_{7,7}$	280	1.089626E+009	1.092943E+009	1.212935E+008	1.531434E+008	**1.699027E+004**	1.699027E+004

Table VI-17: Chi2 results IBBPBBP_12

C.N.	**k**	**Laplace**	**Laplace μ=0**	**G.G.**	**G.G. μ=0**	**Cauchy**	**Cauchy b=0**
$C_{0,0}$	11655	1.609880E+021	1.726140E+021	1.004407E+005	**5.312771E+004**	1.158775E+005	1.201120E+005
$C_{0,1}$	6622	6.952239E+013	7.084979E+013	6.854671E+004	**4.302392E+004**	9.470747E+004	9.679716E+004
$C_{0,2}$	3743	5.810400E+012	6.316306E+012	7.404112E+004	**3.515129E+004**	6.688468E+004	6.770266E+004
$C_{0,3}$	3818	7.221431E+011	6.916939E+011	5.024464E+004	**3.000890E+004**	4.739292E+004	4.765906E+004
$C_{0,4}$	2959	1.264541E+013	1.273713E+013	5.556402E+004	**3.264310E+004**	4.101532E+004	4.106263E+004
$C_{0,5}$	2477	1.530099E+013	1.310525E+013	6.506460E+004	5.269343E+004	**2.771895E+004**	3.059664E+004
$C_{0,6}$	1306	5.567340E+011	6.456192E+011	3.217750E+004	**2.623428E+004**	3.364577E+004	3.677387E+004
$C_{0,7}$	1168	1.538510E+011	1.431933E+011	2.455768E+004	2.139643E+004	**2.056122E+004**	2.350503E+004
$C_{1,0}$	6542	2.839011E+008	2.827575E+008	5.881684E+004	**3.372632E+004**	8.926179E+004	8.973709E+004
$C_{1,1}$	4405	1.549049E+011	1.634274E+011	4.486895E+004	**2.860447E+004**	8.144862E+004	8.147972E+004
$C_{1,2}$	2756	5.367407E+007	5.360203E+007	2.852816E+004	**2.403927E+004**	4.143044E+004	4.146644E+004

$C_{1,3}$	3082	1.611910E+012	1.611053E+012	2.544503E+004	**2.389877E+004**	4.192989E+004	4.198188E+004
$C_{1,4}$	2333	3.496858E+010	3.573999E+010	2.946909E+004	**2.334836E+004**	3.222028E+004	3.226022E+004
$C_{1,5}$	1940	7.614804E+009	7.720928E+009	3.119964E+004	2.831629E+004	**2.333734E+004**	2.338460E+004
$C_{1,6}$	1004	8.217827E+011	8.561169E+011	3.326204E+004	3.073471E+004	**1.862808E+004**	1.876767E+004
$C_{1,7}$	829	1.375494E+011	1.305419E+011	6.246922E+004	6.366509E+004	**1.330955E+004**	1.357730E+004
$C_{2,0}$	3810	2.503461E+009	2.518225E+009	4.327788E+004	**2.851368E+004**	7.364315E+004	7.381308E+004
$C_{2,1}$	2792	2.837923E+008	2.909727E+008	2.572248E+004	**2.353031E+004**	4.418536E+004	4.418671E+004
$C_{2,2}$	1791	6.303397E+011	6.231783E+011	2.097073E+004	**2.049230E+004**	3.492283E+004	3.491745E+004
$C_{2,3}$	1953	1.178862E+010	1.198816E+010	2.030411E+004	**1.901055E+004**	2.864518E+004	2.864560E+004
$C_{2,4}$	1557	8.818396E+009	9.064211E+009	2.179089E+004	**2.055305E+004**	2.326928E+004	2.326928E+004
$C_{2,5}$	1336	5.926897E+008	6.076717E+008	1.829743E+004	**1.747682E+004**	1.879263E+004	1.879265E+004
$C_{2,6}$	647	1.046654E+008	1.065706E+008	1.272981E+004	**1.268676E+004**	1.380993E+004	1.380993E+004
$C_{2,7}$	552	1.387241E+008	1.394122E+008	3.588909E+004	3.618731E+004	**1.109114E+004**	1.109114E+004
$C_{3,0}$	4171	1.282732E+011	1.289446E+011	5.736320E+004	**2.939937E+004**	6.233908E+004	6.252405E+004
$C_{3,1}$	3024	8.080576E+007	7.969895E+007	2.557672E+004	**2.437855E+004**	5.277316E+004	5.277076E+004
$C_{3,2}$	1980	8.081823E+009	8.098244E+009	2.172515E+004	**1.986273E+004**	2.828030E+004	2.828030E+004
$C_{3,3}$	2256	1.339047E+009	1.360692E+009	1.902081E+004	**1.852675E+004**	2.552531E+004	2.553298E+004
$C_{3,4}$	1743	1.011212E+008	1.006514E+008	1.688555E+004	**1.595558E+004**	1.968268E+004	1.968716E+004
$C_{3,5}$	1497	2.143053E+009	2.136608E+009	1.658776E+004	**1.558823E+004**	1.644339E+004	1.644467E+004
$C_{3,6}$	779	1.209483E+011	1.196816E+011	1.533408E+004	1.485990E+004	**1.166401E+004**	1.166401E+004
$C_{3,7}$	656	3.134875E+008	3.210063E+008	1.199571E+004	1.169645E+004	**9.165141E+003**	9.165141E+003
$C_{4,0}$	3272	9.522366E+011	9.280741E+011	6.203652E+004	**2.762962E+004**	5.394320E+004	5.395318E+004
$C_{4,1}$	2449	3.831052E+008	3.838671E+008	2.519823E+004	**2.300382E+004**	4.040810E+004	4.040810E+004
$C_{4,2}$	1494	2.719373E+009	2.702139E+009	1.955958E+004	**1.875396E+004**	2.629791E+004	2.629799E+004
$C_{4,3}$	1728	1.180376E+010	1.173352E+010	1.896188E+004	**1.794130E+004**	2.256718E+004	2.256718E+004
$C_{4,4}$	1323	2.901716E+008	2.898793E+008	1.621393E+004	**1.541563E+004**	1.696592E+004	1.696671E+004
$C_{4,5}$	1123	5.949882E+008	5.995228E+008	1.274032E+004	**1.241139E+004**	1.361738E+004	1.361738E+004
$C_{4,6}$	586	2.290139E+009	2.332458E+009	1.037425E+004	1.028035E+004	**1.015466E+004**	1.015466E+004
$C_{4,7}$	500	1.175600E+009	1.199882E+009	1.687057E+004	1.680287E+004	**9.449369E+003**	9.449369E+003
$C_{5,0}$	2675	1.601653E+013	1.603449E+013	4.118426E+004	**2.705687E+004**	4.231793E+004	4.233126E+004
$C_{5,1}$	2060	4.434232E+010	4.433106E+010	2.541325E+004	**2.449569E+004**	3.662098E+004	3.664387E+004
$C_{5,2}$	1264	2.882901E+010	2.854666E+010	2.015839E+004	**1.980586E+004**	2.349371E+004	2.352877E+004
$C_{5,3}$	1432	1.603667E+009	1.607649E+009	1.784816E+004	**1.752739E+004**	2.040875E+004	2.041691E+004
$C_{5,4}$	1123	3.891289E+010	3.729526E+010	1.659871E+004	1.646852E+004	1.592381E+004	**1.592289E+004**
$C_{5,5}$	954	3.837293E+009	3.717294E+009	1.537040E+004	1.504803E+004	**1.231583E+004**	1.232903E+004
$C_{5,6}$	475	2.301956E+008	2.462191E+008	1.094031E+004	1.120480E+004	**9.618401E+003**	9.762311E+003
$C_{5,7}$	423	1.685515E+007	1.674857E+007	9.710694E+003	9.868452E+003	**9.428310E+003**	9.503133E+003
$C_{6,0}$	1412	7.436785E+011	7.664650E+011	4.341520E+004	**2.574252E+004**	3.137879E+004	3.138353E+004
$C_{6,1}$	1090	2.217478E+012	2.241705E+012	2.614828E+004	**2.586690E+004**	2.641075E+004	2.641075E+004
$C_{6,2}$	686	2.693129E+012	2.742378E+012	2.016471E+004	**2.007524E+004**	2.595915E+004	2.595915E+004
$C_{6,3}$	727	5.124766E+009	5.301517E+009	**1.535975E+004**	1.540908E+004	2.094802E+004	2.094886E+004
$C_{6,4}$	589	5.353000E+009	5.364062E+009	**1.508779E+004**	1.512293E+004	1.806271E+004	1.806271E+004
$C_{6,5}$	505	3.556140E+009	3.609842E+009	**1.286004E+004**	1.290692E+004	1.668884E+004	1.668884E+004
$C_{6,6}$	259	2.165617E+007	2.167073E+007	1.618749E+004	1.680318E+004	**1.575927E+004**	1.575927E+004
$C_{6,7}$	232	1.539315E+007	1.563612E+007	1.880137E+007	1.513358E+007	**1.476570E+004**	1.476570E+004
$C_{7,0}$	1378	7.249124E+011	7.196072E+011	3.407426E+004	2.391954E+004	**2.355845E+004**	2.366952E+004
$C_{7,1}$	1108	8.836316E+011	8.854912E+011	2.750181E+004	**2.741500E+004**	3.362230E+004	3.362294E+004
$C_{7,2}$	679	9.135410E+012	9.280964E+012	**2.293619E+004**	2.298692E+004	2.870418E+004	2.870418E+004
$C_{7,3}$	705	2.573759E+011	2.671274E+011	**1.773557E+004**	1.795874E+004	2.432824E+004	2.434288E+004
$C_{7,4}$	555	6.843683E+009	6.611888E+009	**1.571875E+004**	1.579884E+004	1.989978E+004	1.989978E+004
$C_{7,5}$	507	1.183257E+009	1.185828E+009	4.136356E+005	4.342491E+005	1.663204E+004	**1.662787E+004**
$C_{7,6}$	278	6.288743E+007	6.405347E+007	4.939948E+007	4.679052E+007	**1.569093E+004**	1.569093E+004
$C_{7,7}$	283	6.062739E+008	5.957302E+008	1.295263E+007	1.554219E+007	**1.698741E+004**	1.698741E+004

Table VI-18: Chi2 results IPPPPPP

It can be seen that, in general, the test statistic χ^2 is considerably lower for the G. G. and the Cauchy distributions than the Laplace distribution; in some coefficients even by various orders of magnitude.

The G.G. and the Cauchy PDFs are the best models for the DCT coefficients. Whereas G.G. PDF is the one with the smallest χ^2 in many cases, the Cauchy PDF is very consistent, its results are almost always smaller than 10^5 (except for $C_{0,0}$ and a few rare cases, which are less than 10^6). In the G.G. case there are a few results bigger than 10^6.

With respect to the location parameter, the test gives better results using it for the Laplacian and Cauchy cases. In the Generalized Gaussian case, setting $\mu = 0$ yields better results.

VI.3 ENTROPY MODELS OF QUANTIZED SOURCES

Assume that the DCT coefficients are uniformly quantized with a quantization step size Q. Let $P(iQ)$ be the probability that a coefficient is quantized to iQ, where $\{i = 0, \pm 1, \pm 2, \dots\}$. Then the entropy of the quantized DCT coefficients is computed as (Kamaci, Altunbasak, & Mersereau, 2005):

$$H(Q) = -\sum_{i=-\infty}^{\infty} P(iQ) log_2[P(iQ)]$$

Where:

$$P(iQ) = \int_{\left(i-\frac{1}{2}\right)Q}^{\left(1+\frac{1}{2}\right)Q} f_X \, dx$$

If the Probability Density Function is symmetrical and centered in 0, $H(Q)$ can be expressed as:

$$H(Q) = -P(0Q) log_2[P(0Q)] - 2\sum_{i=1}^{\infty} P(iQ) log_2[P(iQ)]$$

VI.3.1 Laplace

As found in (Syu, 2005)

$$P(iQ) = \begin{cases} 1 - \mathrm{e}^{-\mathrm{r}}, & i = 0 \\ \mathrm{e}^{-\frac{|\mathrm{i}|\mathrm{Q}}{\mathrm{b}}} \sinh(\mathrm{r}), & i \neq 0 \end{cases}$$

Where $r = \frac{\mathrm{Q}}{2\mathrm{b}}$

$$H(Q) = -(1 - \mathrm{e}^{-\mathrm{r}}) log_2(1 - \mathrm{e}^{-\mathrm{r}}) - 2 \sum_{i=1}^{\infty} \mathrm{e}^{-\frac{|\mathrm{i}|\mathrm{Q}}{\mathrm{b}}} \sinh(\mathrm{r})\, log_2\left(\mathrm{e}^{-\frac{|\mathrm{i}|\mathrm{Q}}{\mathrm{b}}} \sinh(\mathrm{r})\right)$$

$$H(Q) = \frac{1}{\ln(2)}\left[-(1 - \mathrm{e}^{-\mathrm{r}})\ln(1 - \mathrm{e}^{-\mathrm{r}}) + \frac{\mathrm{r}}{\sinh(\mathrm{r})} - \mathrm{e}^{-\mathrm{r}} \ln(\sinh(\mathrm{r}))\right]$$

VI.3.2 Cauchy

As found in (Kamaci, Altunbasak, & Mersereau, 2005). M is the last level of the quantizer.

$$P(iQ) = \begin{cases} \frac{2}{\pi}\tan^{-1}\left(\frac{\mathrm{Q}}{2\mathrm{b}}\right), & i = 0 \\ \frac{1}{\pi}\tan^{-1}\left(\frac{\mathrm{bQ}}{\mathrm{b}^2 + \left(\mathrm{i}^2 - \frac{1}{4}\right)\mathrm{Q}^2}\right), & i \neq 0 \end{cases}$$

$$H(Q) = -\frac{2}{\pi}\tan^{-1}\left(\frac{\mathrm{Q}}{2\mathrm{b}}\right) log_2\left[\frac{2}{\pi}\tan^{-1}\left(\frac{\mathrm{Q}}{2\mathrm{b}}\right)\right] - \frac{2}{\pi}\sum_{i=1}^{M} \tan^{-1}\left(\frac{\mathrm{bQ}}{\mathrm{b}^2 + \left(\mathrm{i}^2 - \frac{1}{4}\right)\mathrm{Q}^2}\right) log_2\left[\frac{1}{\pi}\tan^{-1}\left(\frac{\mathrm{bQ}}{\mathrm{b}^2 + \left(\mathrm{i}^2 - \frac{1}{4}\right)\mathrm{Q}^2}\right)\right]$$

VI.3.3 Generalized Gaussian

See appendix VII.1 for the procedure.

$$H(Q) = -G\left(\frac{1}{p}, \left(\frac{Q}{2A}\right)^p\right) log_2\left(G\left(\frac{1}{p}, \left(\frac{Q}{2A}\right)^p\right)\right) - \sum_{i=1}^{M}\left[G\left(\frac{1}{p}, L_2\right) - G\left(\frac{1}{p}, L_1\right)\right]\left[log_2\left(G\left(\frac{1}{p}, L_2\right) - G\left(\frac{1}{p}, L_1\right)\right) - 1\right]$$

Where $G(b,z)$ is the lower regularized incomplete gamma function, defined as:

$$G(b,z) = \frac{\gamma(b,z)}{\Gamma(b)} = \frac{\int_0^z v^{b-1}e^{-v}\,dv}{\Gamma(b)}$$

VI.3.4 Experimental Results

The actual bit/pixel ratio was obtained from the frame statistics of the encoded sequences. The sum of the bits/frame was divided by the total number of frames. The result was divided by the number of pixels per frame (101376 for the CIF sequences, 24768 for the QCIF sequences).

The entropy of the models was calculated separately for each of the 64 subbands of the DCT, the sum of the results was then divided by 64.

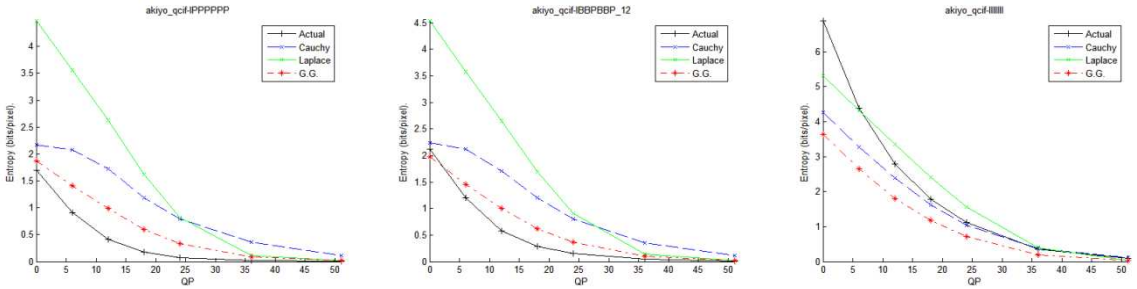

Fig. VI-9: Entropy of akiyo_qcif

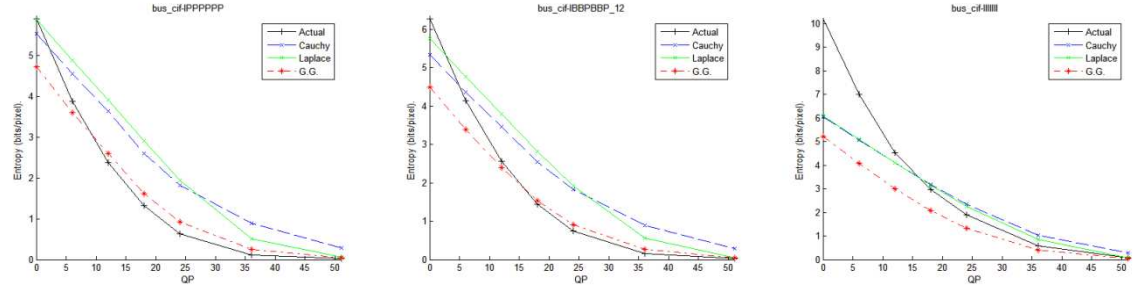

Fig. VI-10: Entropy of bus_cif

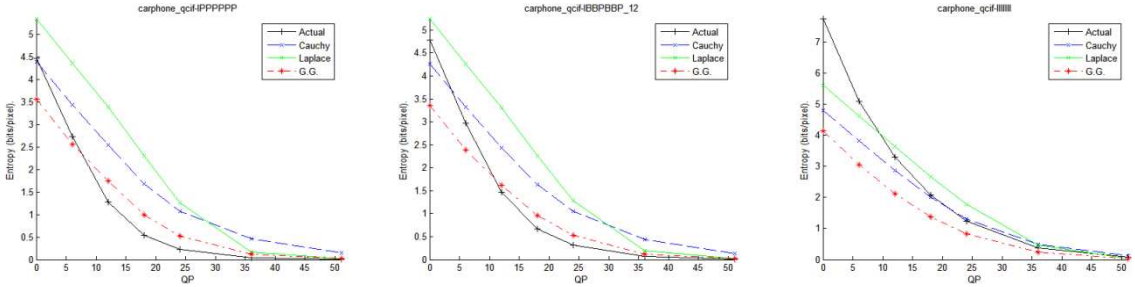

Fig. VI-11: Entropy of carphone_qcif

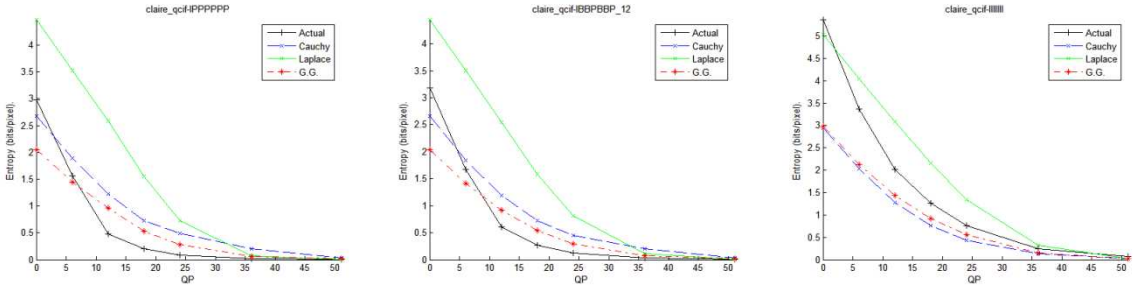

Fig. VI-12: Entropy of claire_qcif

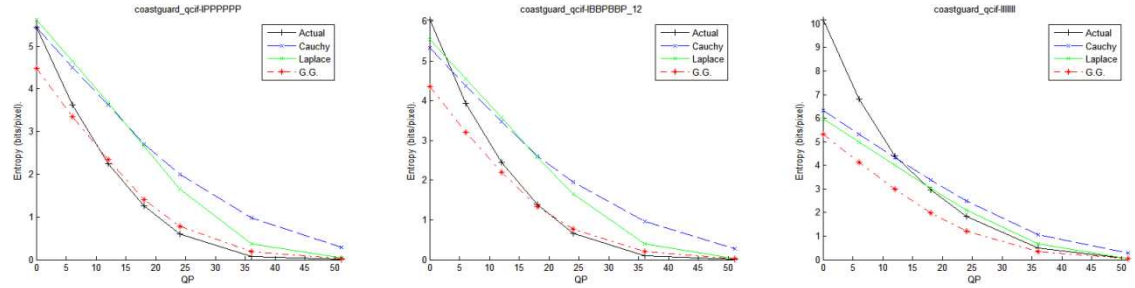

Fig. VI-13: Entropy of coastguard_qcif

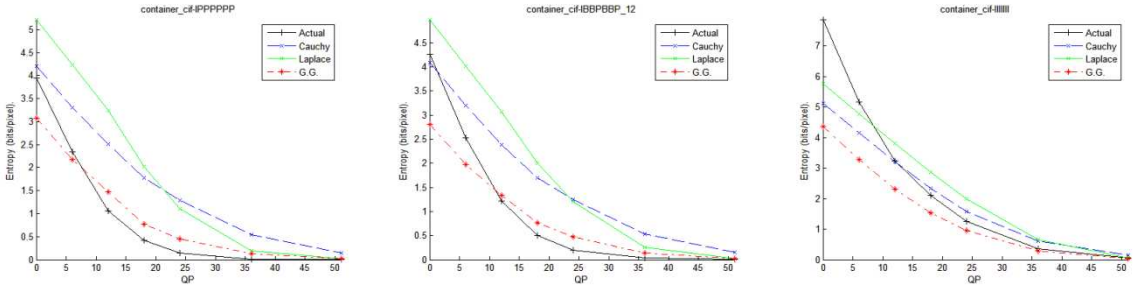

Fig. VI-14: Entropy of container_cif

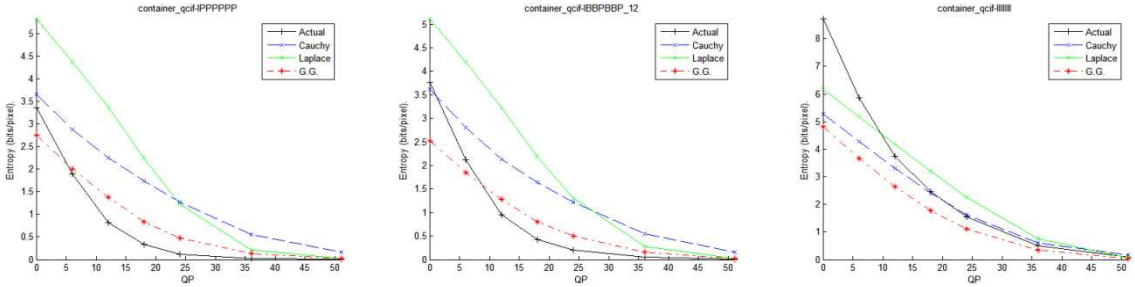

Fig. VI-15: Entropy of container_qcif

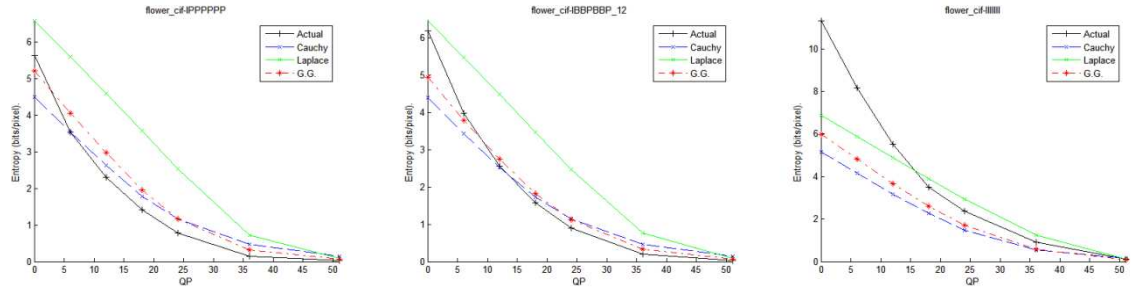

Fig. VI-16: Entropy of flower_cif

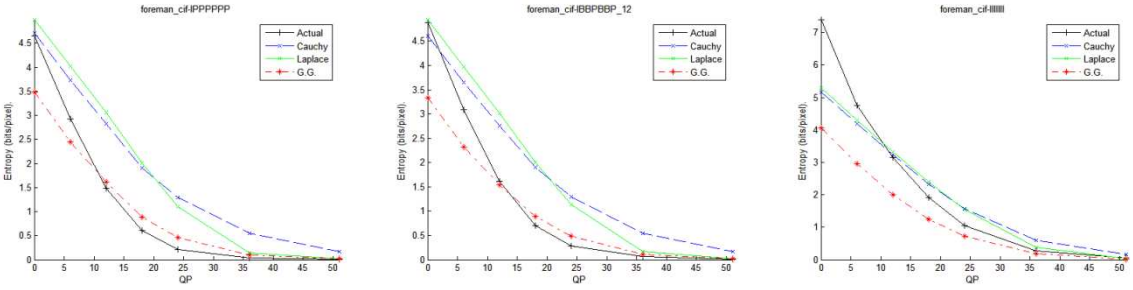

Fig. VI-17: Entropy of foreman_cif

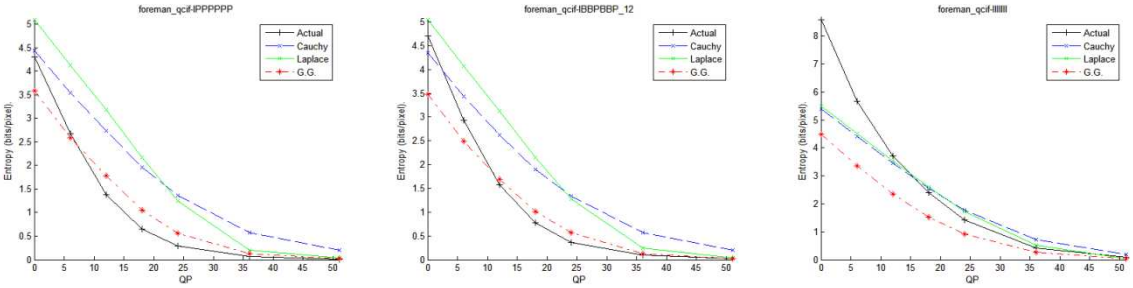

Fig. VI-18: Entropy of foreman_qcif

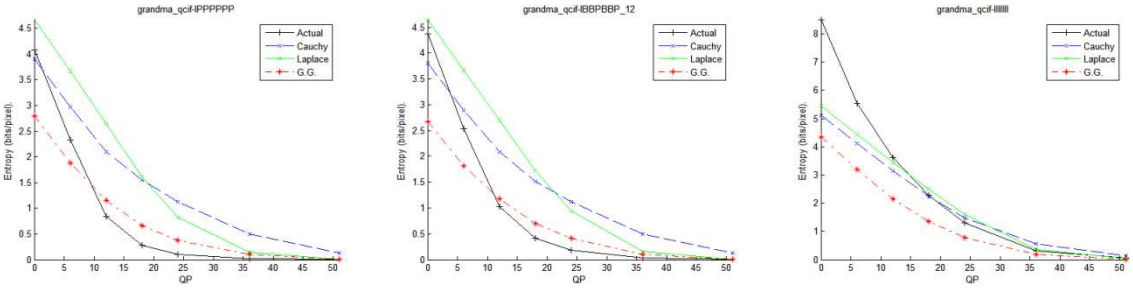

Fig. VI-19: Entropy of grandma_qcif

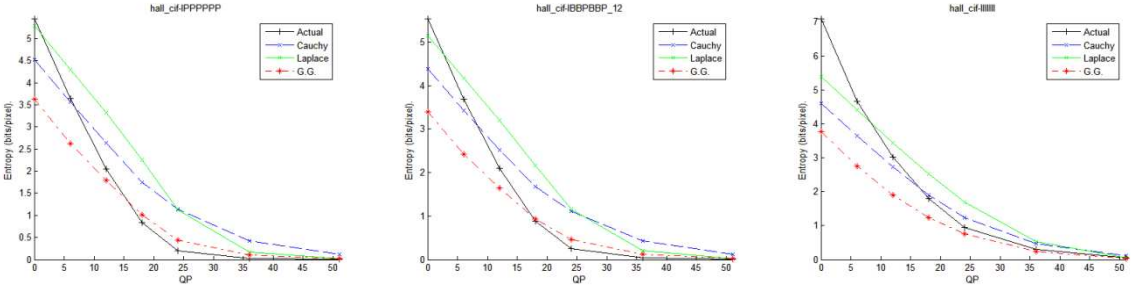

Fig. VI-20: Entropy of hall_cif

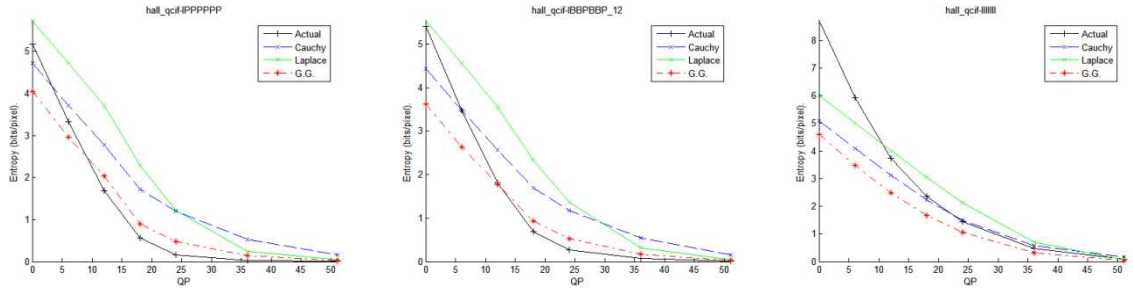

Fig. VI-21: Entropy of hall_qcif

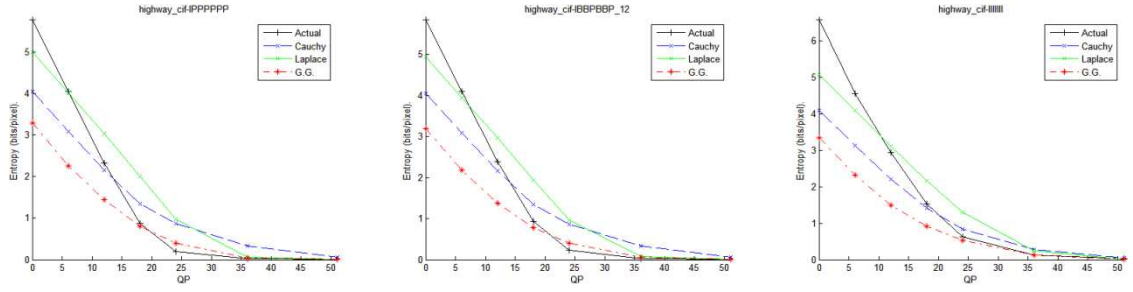

Fig. VI-22: Entropy of highway_cif

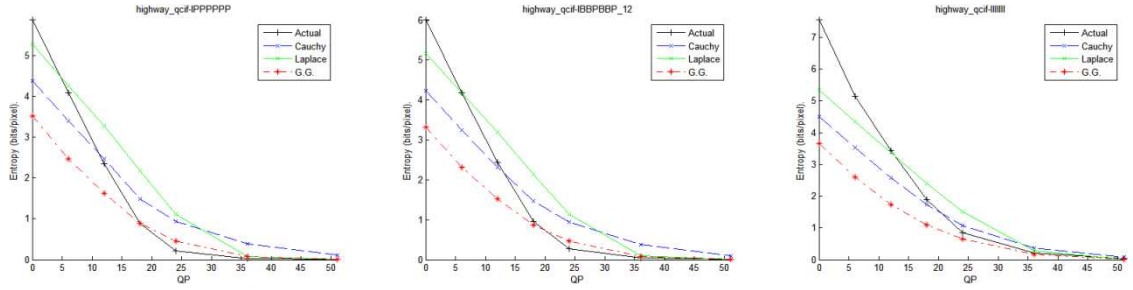

Fig. VI-23: Entropy of highway_qcif

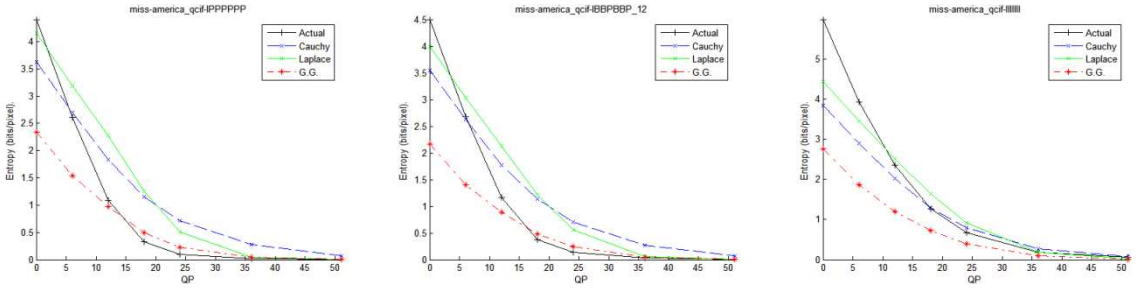

Fig. VI-24: Entropy of miss-america_qcif

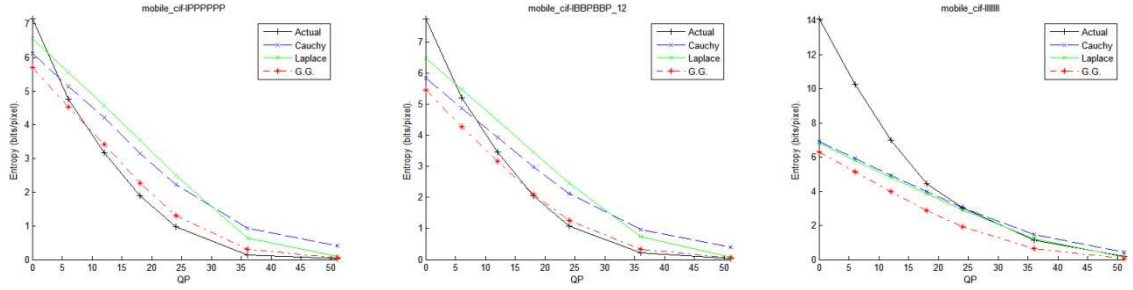

Fig. VI-25: Entropy of mobile_cif

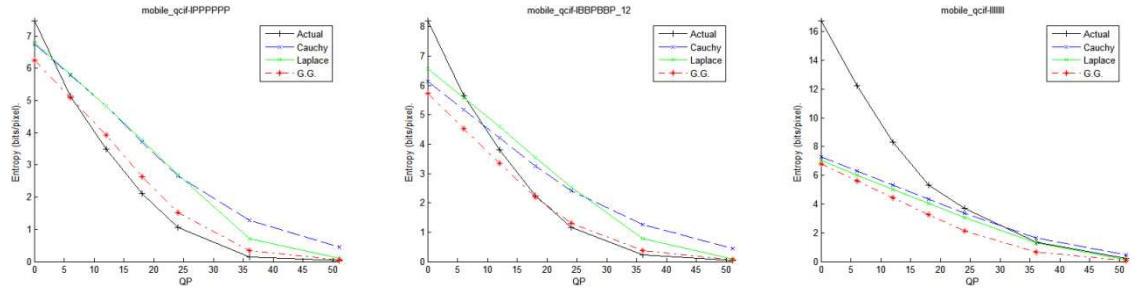

Fig. VI-26: Entropy of mobile_qcif

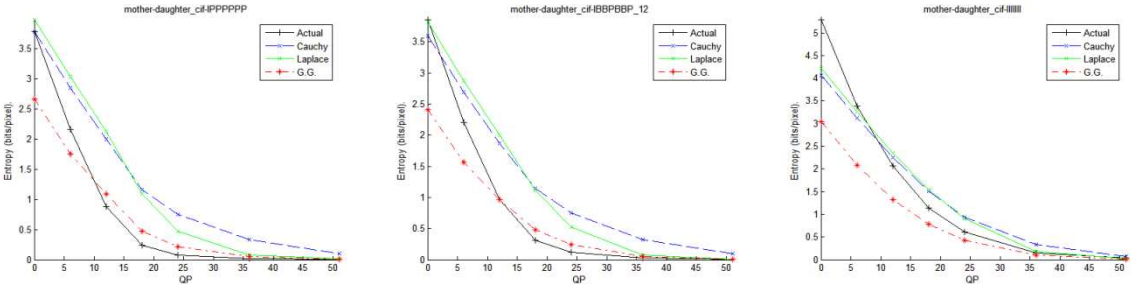

Fig. VI-27: Entropy of mother-daughter_cif

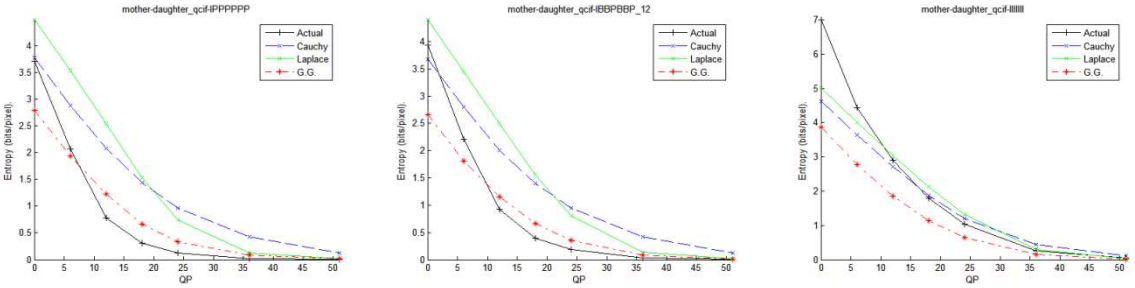

Fig. VI-28: Entropy of mother-daughter_qcif

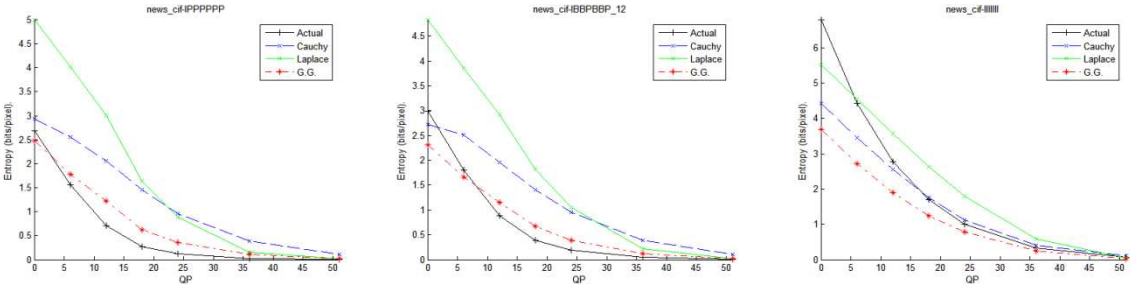

Fig. VI-29: Entropy of news_cif

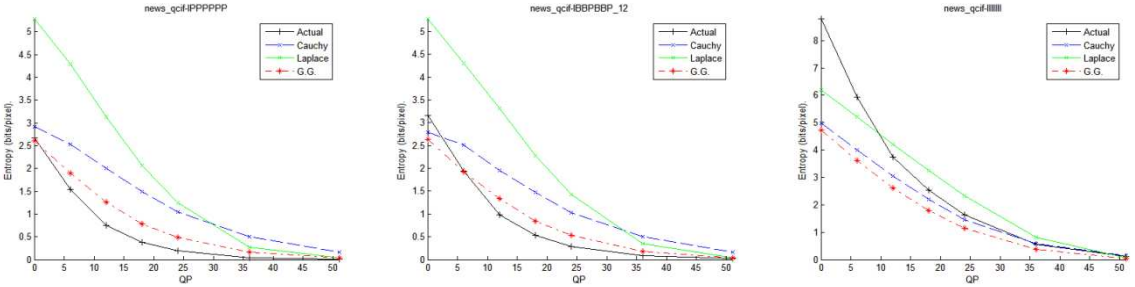

Fig. VI-30: Entropy of news_qcif

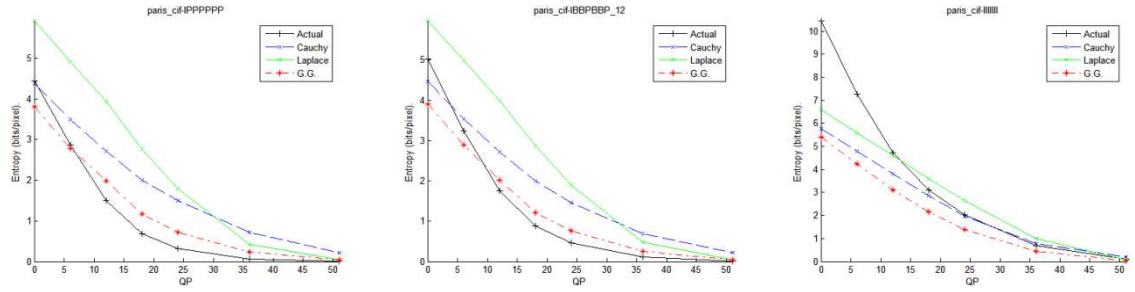

Fig. VI-31: Entropy of paris_cif

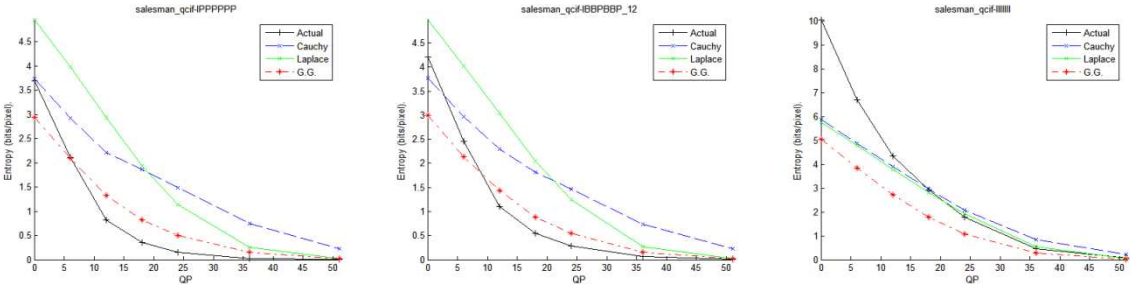

Fig. VI-32: Entropy of salesman_qcif

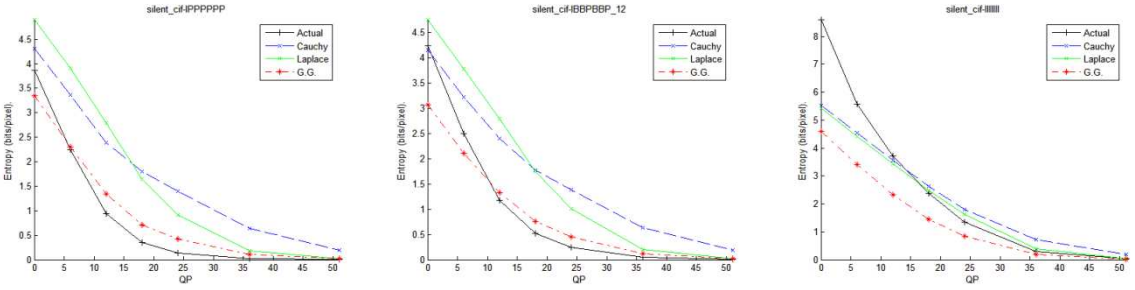

Fig. VI-33: Entropy of silent_cif

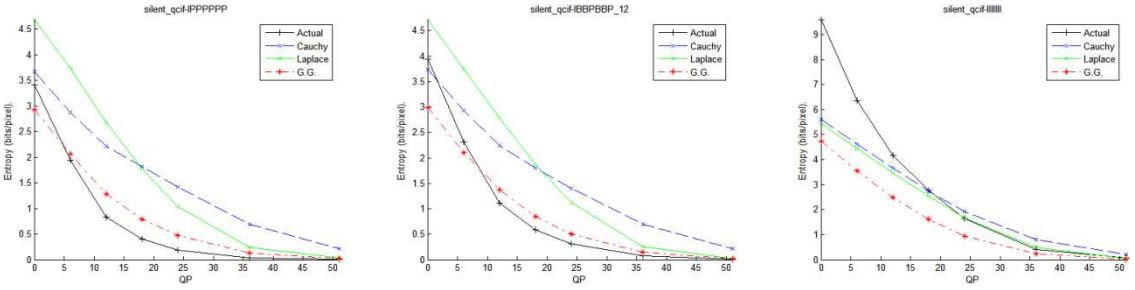

Fig. VI-34: Entropy of silent_qcif

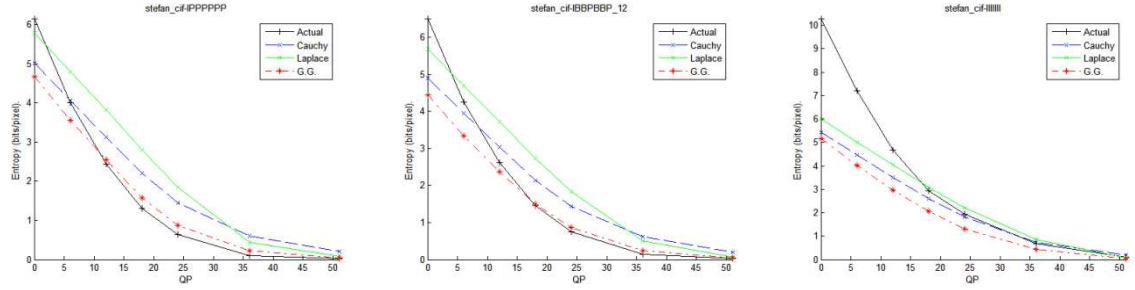

Fig. VI-35: Entropy of stefan_cif

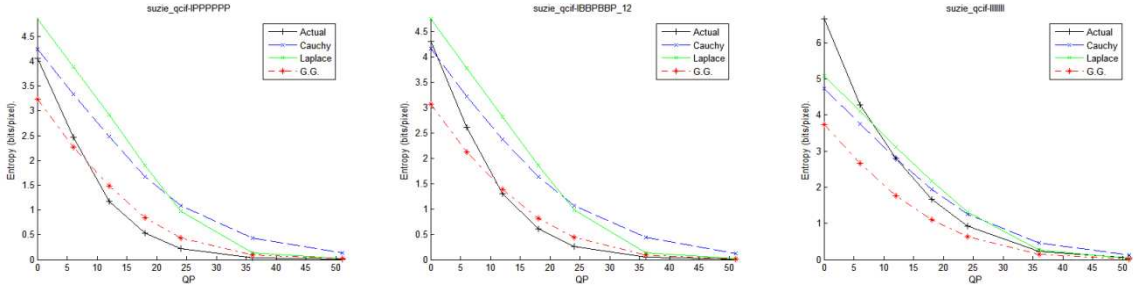

Fig. VI-36: Entropy of suzie_qcif

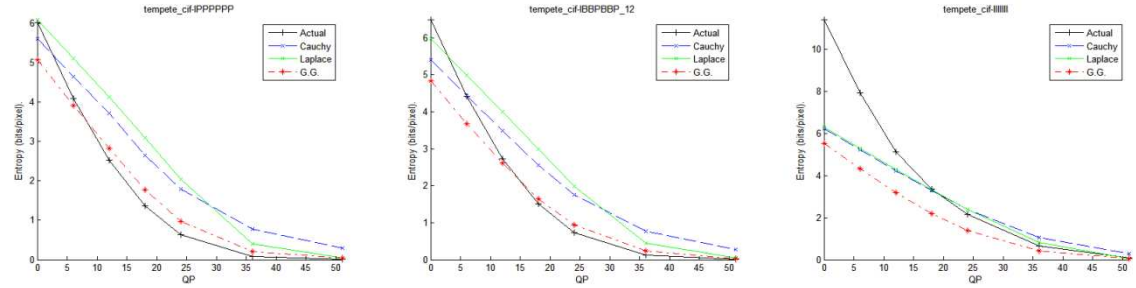

Fig. VI-37: Entropy of tempete_cif

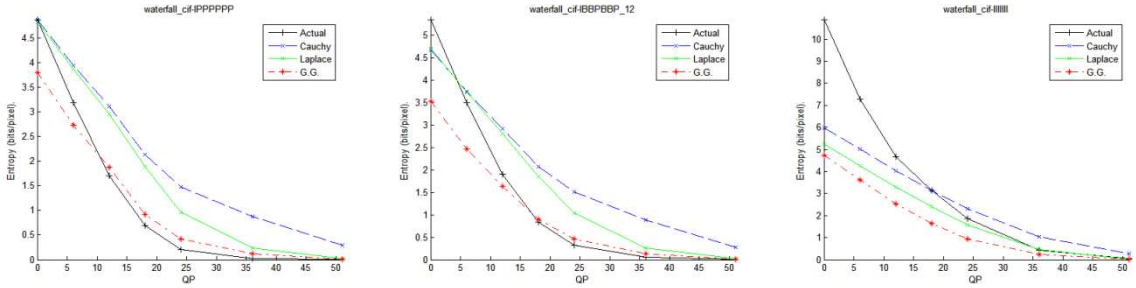

Fig. VI-38: Entropy of waterfall_cif

It can be seen from the figures that, in general, for the IPPPPP… and IBBPBBP… GOPs the Generalized Gaussian model is the most accurate when the QP is greater than 6, and the Cauchy model is better when QP is equal or smaller than 6. The IIII… GOP is a special case, because it uses spatial prediction only and doesn't take advantage of the temporal redundancy between frames, hence has worse compression efficiency (requires more bits) than the other GOPs. For it, Cauchy and Laplace models offer a better estimation (being the Cauchy model slightly better than the Laplace).

VI.4 DISTORTION MODELS OF QUANTIZED SOURCES

The quality of the reproduction can be measured by the goodness of the resulting reproduction in comparison to the original. One way of accomplishing this is to define a nonnegative distortion measure $d(x,\hat{x})$ that quantifies cost or distortion resulting from reproducing input x as $\hat{x}$, and to consider the average

distortion as a measure of the quality of a system, with smaller average distortion meaning higher quality (Gray & Neuhoff, 1998).

"Ideally, one would like a distortion measure that is easy to compute, useful in analysis, and perceptually meaningful in the sense that small (large) distortion means good (poor) perceived quality. No single distortion measure accomplishes all three goals, but the common squared-error distortion satisfies the first two. The squared error is defined as" (Gray & Neuhoff, 1998):

$$d(x, \hat{x}) = |x - \hat{x}|^2$$

In practice, the average will be a sample average when the quantizer is applied to a sequence of real data, but the theory views the data as sharing a common probability density function (PDF) $f(x)$ corresponding to a generic random variable X and the average distortion becomes an expectation (Gray & Neuhoff, 1998).

$$D(q) = E\big[d\big(X, q(X)\big)\big] = \sum_i \int_{S_i} d(x, y_i) f(x)\, dx$$

VI.4.1 Laplace

For a Laplace source with $\mu = 0$, the distortion caused by an in an uniform quantizer with step size Q is given by (Syu, 2005):

$$\mathrm{D(Q)} = 2b^2 \left(1 - \frac{r}{\sinh r}\right)$$

Where $r = \frac{Q}{2b}$ and $b = \left[\frac{\sigma^2}{2}\right]^{1/2}$

VI.4.2 Cauchy

For a Cauchy source with $a = 0$, the distortion caused by quantization is given by (Kamaci, Altunbasak, & Mersereau, 2005):

$$D(Q) = 2\sum_{i=1}^{M}\left[\frac{bQ}{\pi} - \frac{ibQ}{\pi}\ln\left(\frac{b^2 + \left(i+\frac{1}{2}\right)^2 Q^2}{b^2 + \left(i-\frac{1}{2}\right)^2 Q^2}\right) - \left(\frac{b^2 - i^2Q^2}{\pi}\right)\tan^{-1}\left(\frac{bQ}{b^2 + \left(i^2 - \frac{1}{4}\right)Q^2}\right)\right] + \left[\frac{bQ}{\pi} - \frac{2b^2}{\pi}\tan^{-1}\left(\frac{Q}{2b}\right)\right]$$

Where Q is the quantizer step size and M is the maximum level of the quantizer. (Kamaci, Altunbasak, & Mersereau, 2005).

VI.4.3 Generalized Gaussian

For the distortion model we will consider a G.G. with $\mu = 0$. For a generalized Gaussian source $f_X(x) = gg(x; 0, \sigma, p)$, in an uniform quantizer with step size Q, and levels i, the distortion caused by quantization is given by:

$$D(Q) = \sigma^2 G\left(3/p, \left(\frac{(M+1/2)Q}{A}\right)^p\right) + \sum_{i=1}^{M}\left[(iQ)^2\left[G\left(\frac{1}{p}, \left(\frac{(i+1/2)Q}{A}\right)^p\right) - G\left(\frac{1}{p}, \left(\frac{(i-1/2)Q}{A}\right)^p\right)\right] - \frac{2iQA\Gamma\left(\frac{2}{p}\right)}{\Gamma\left(\frac{1}{p}\right)}\left[G\left(\frac{2}{p}, \left(\frac{(i+1/2)Q}{A}\right)^p\right) - G\left(\frac{2}{p}, \left(\frac{(i-1/2)Q}{A}\right)^p\right)\right]\right]$$

Where $G(b, z)$ is the lower regularized incomplete gamma function, defined as:

$$G(b, z) = \frac{\gamma(b, z)}{\Gamma(b)} = \frac{\int_0^z v^{b-1} e^{-v}\, dv}{\Gamma(b)}$$

See the appendix for the procedure to obtain the model.

VI.4.4 Experimental Results

The actual distortion was calculated with the PSNR of the encoded sequences by using the following equation (Richardson, 2003):

$$MSE = \frac{(2^n - 1)^2}{10^{\left(\frac{PSNR_{db}}{10}\right)}}$$

The vertical axis of the plots is in logarithmic scale.

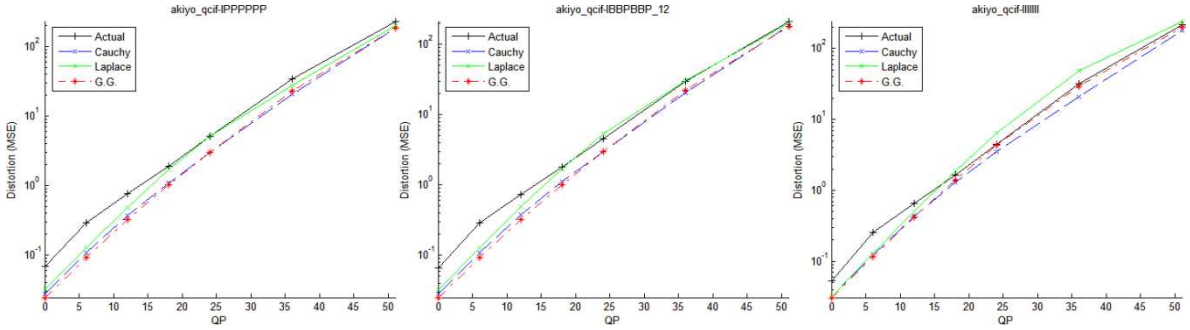

Fig. VI-39: Distortion of akiyo_qcif

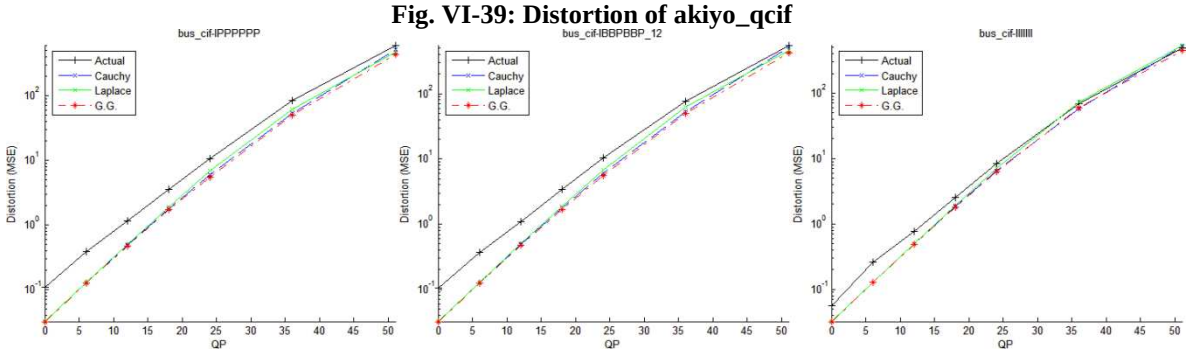

Fig. VI-40: Distortion of bus_cif

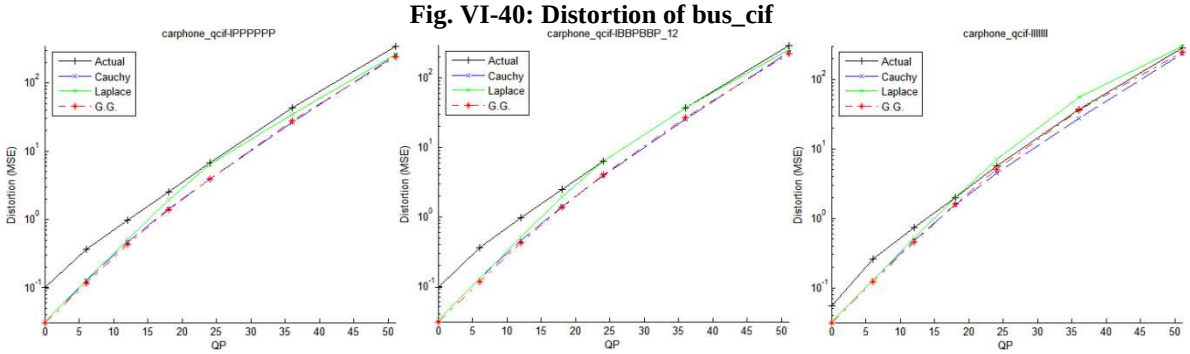

Fig. VI-41: Distortion of carphone_qcif

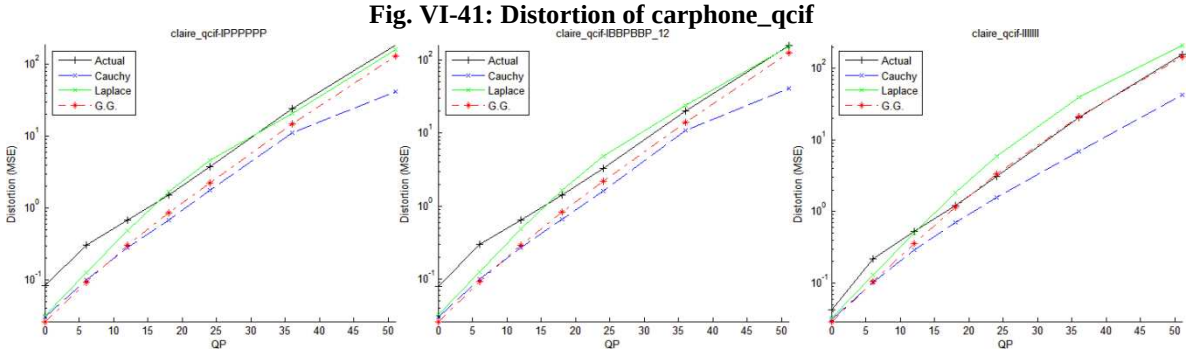

Fig. VI-42: Distortion of claire_qcif

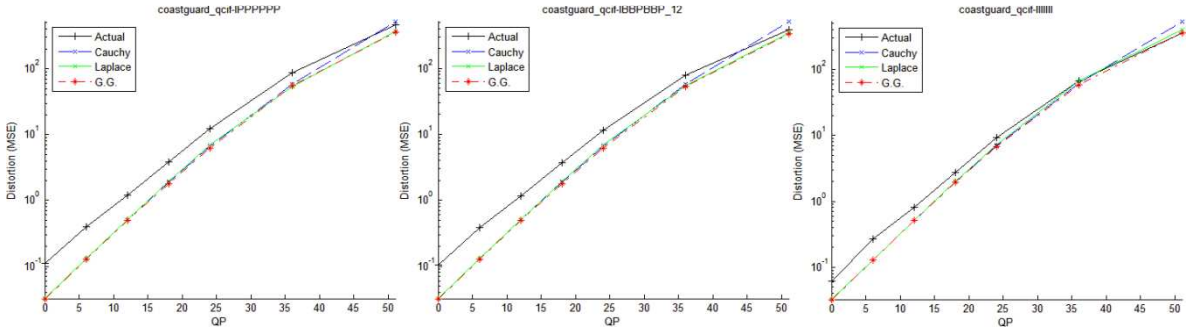

Fig. VI-43: Distortion of coastguard_qcif

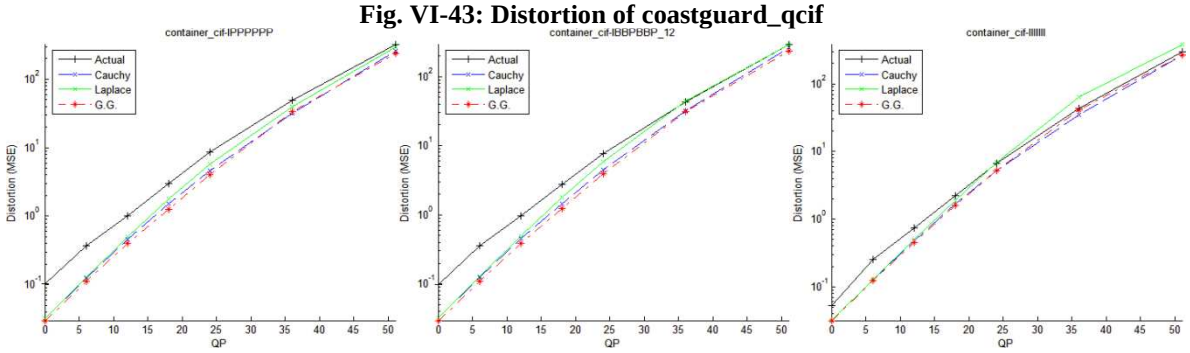

Fig. VI-44: Distortion of container_cif

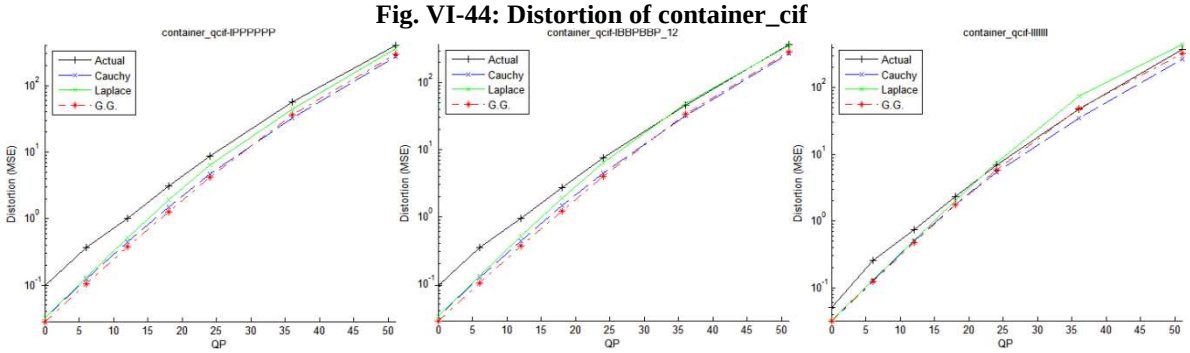

Fig. VI-45: Distortion of container_qcif

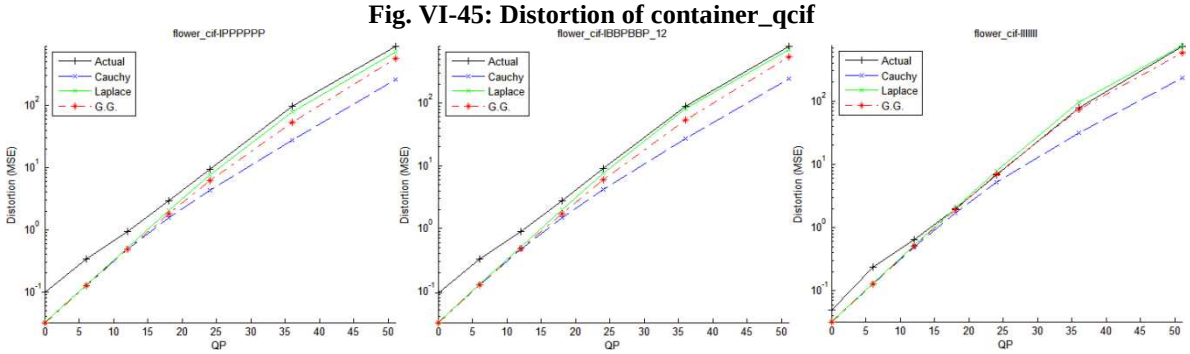

Fig. VI-46: Distortion of flower_cif

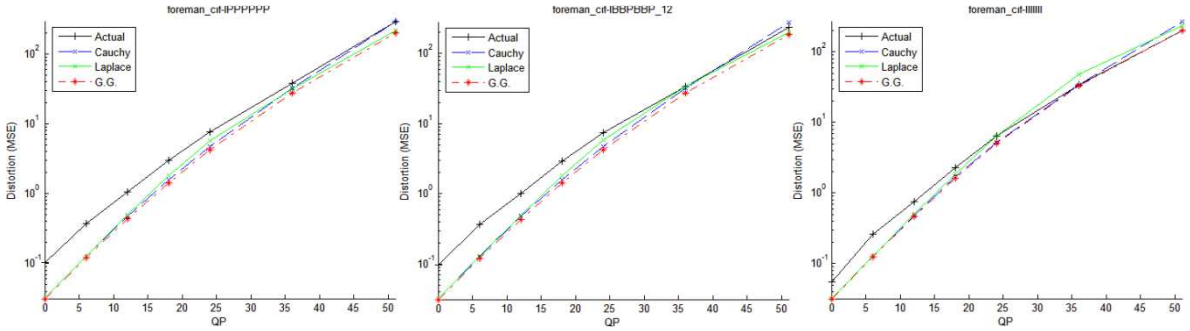

Fig. VI-47: Distortion of foreman_cif

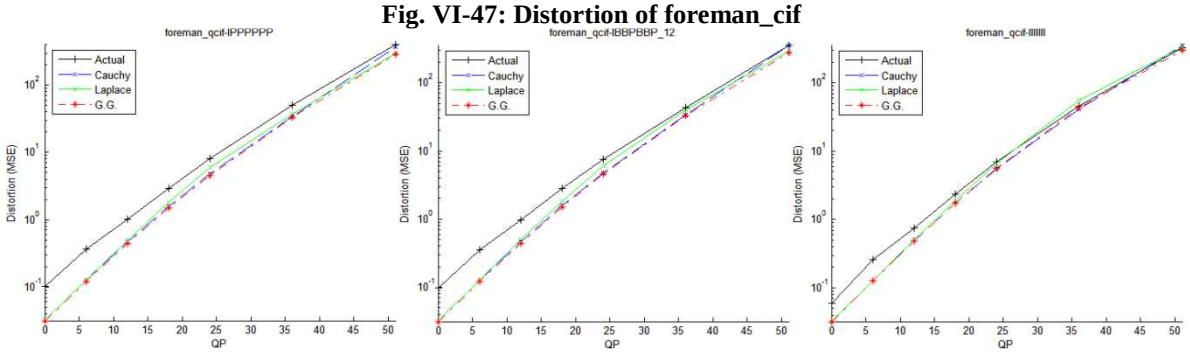

Fig. VI-48: Distortion of foreman_qcif

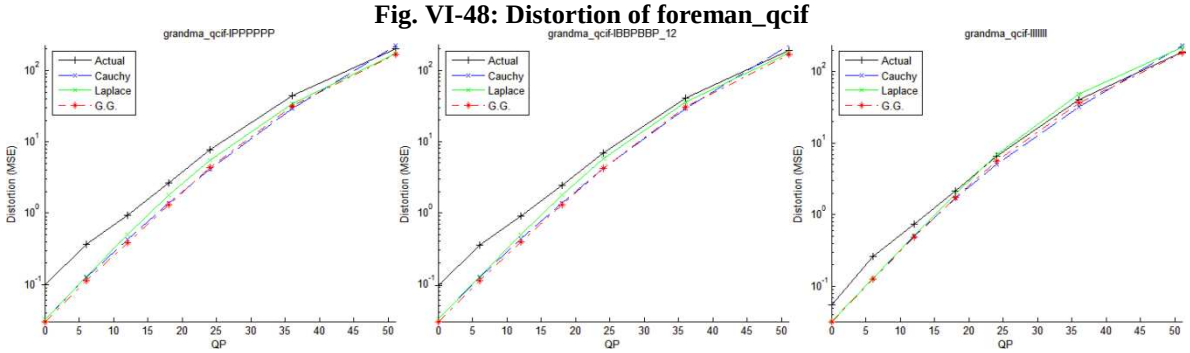

Fig. VI-49: Distortion of grandma_qcif

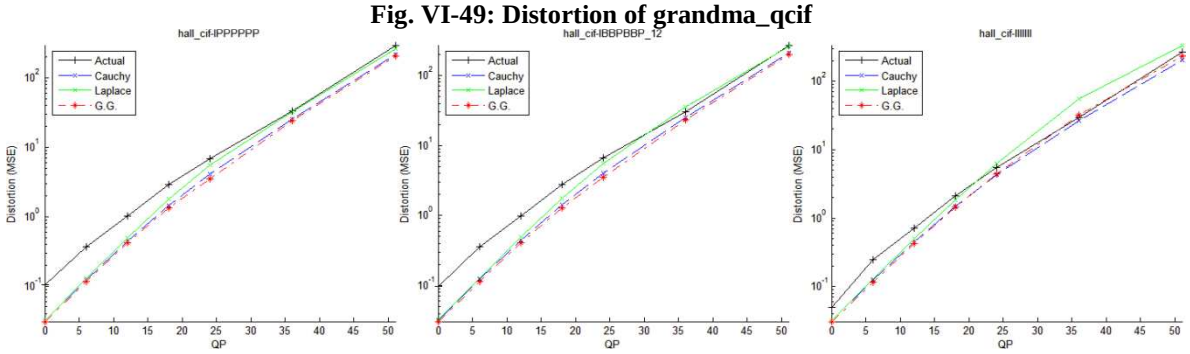

Fig. VI-50: Distortion of hall_cif

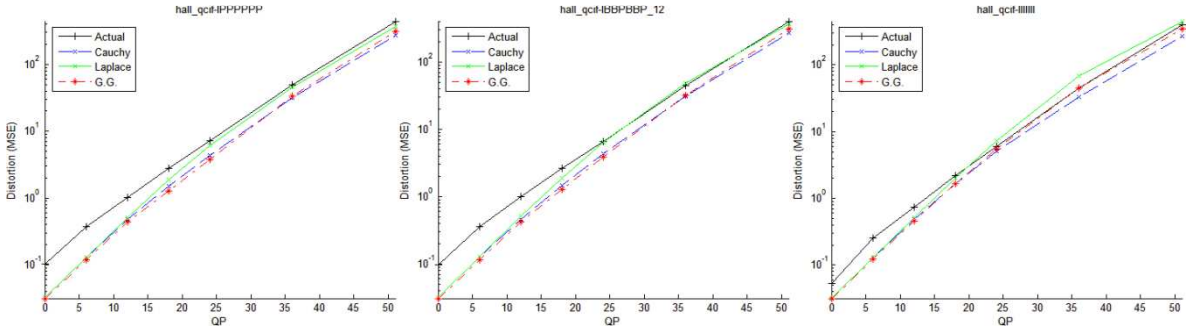

Fig. VI-51: Distortion of hall_qcif

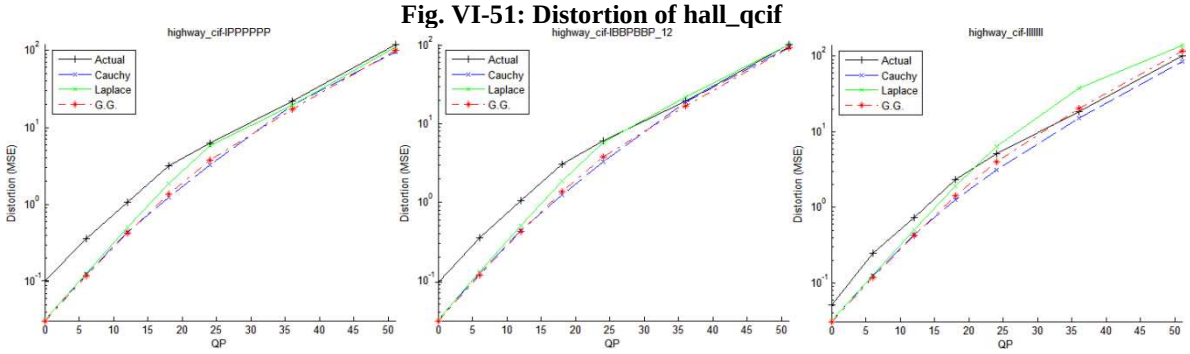

Fig. VI-52: Distortion of highway_cif

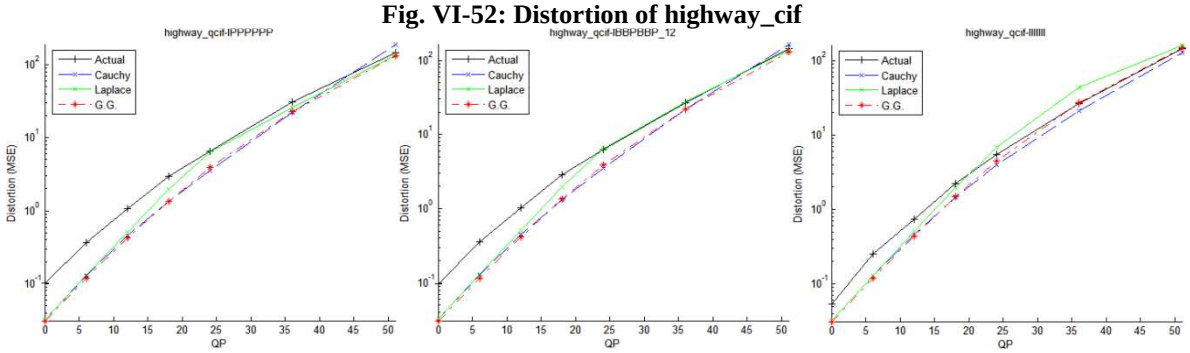

Fig. VI-53: Distortion of highway_qcif

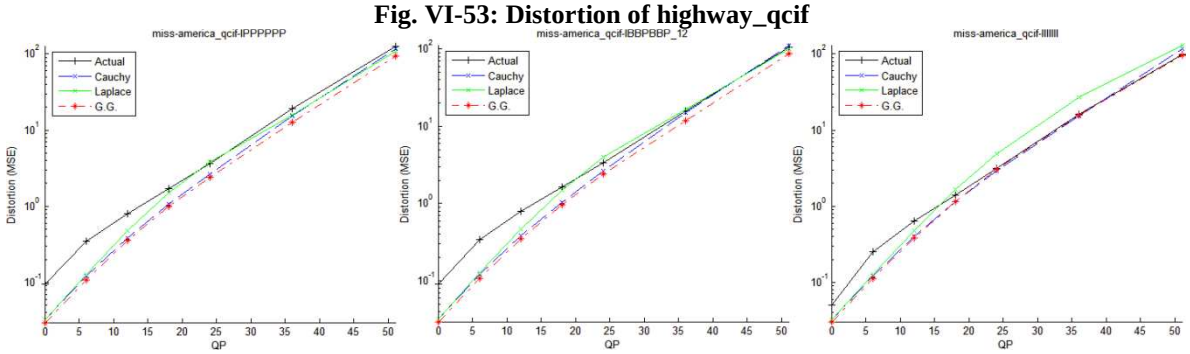

Fig. VI-54: Distortion of miss-america_qcif

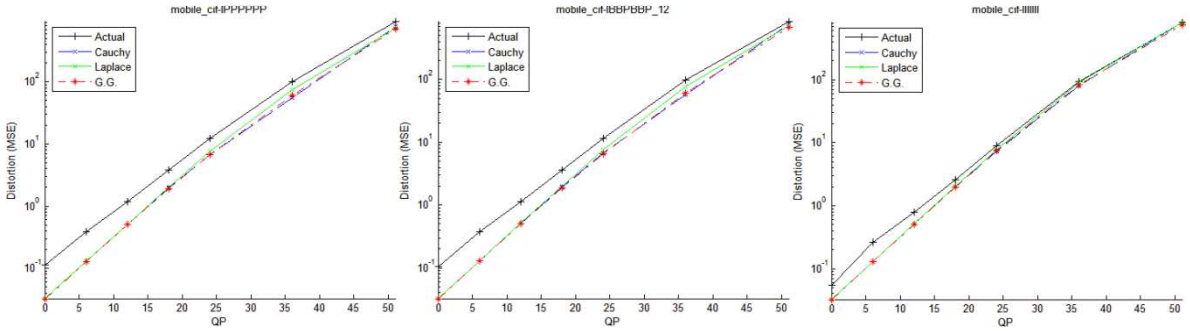

Fig. VI-55: Distortion of mobile_cif

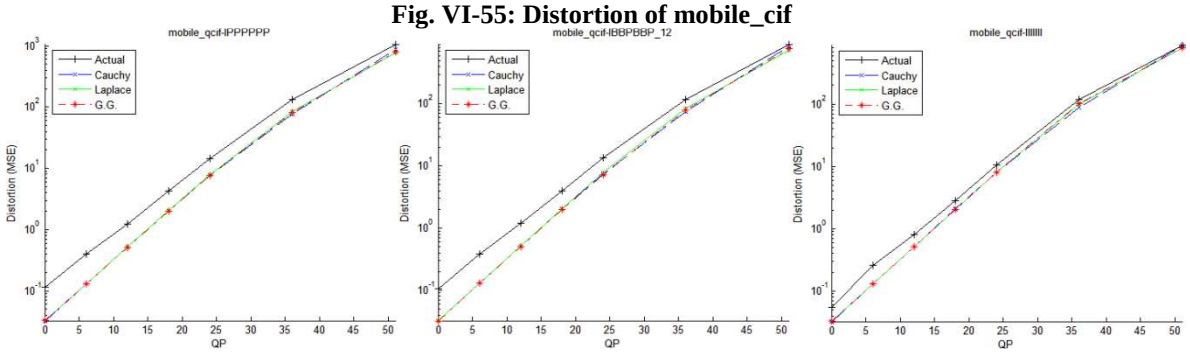

Fig. VI-56: Distortion of mobile_qcif

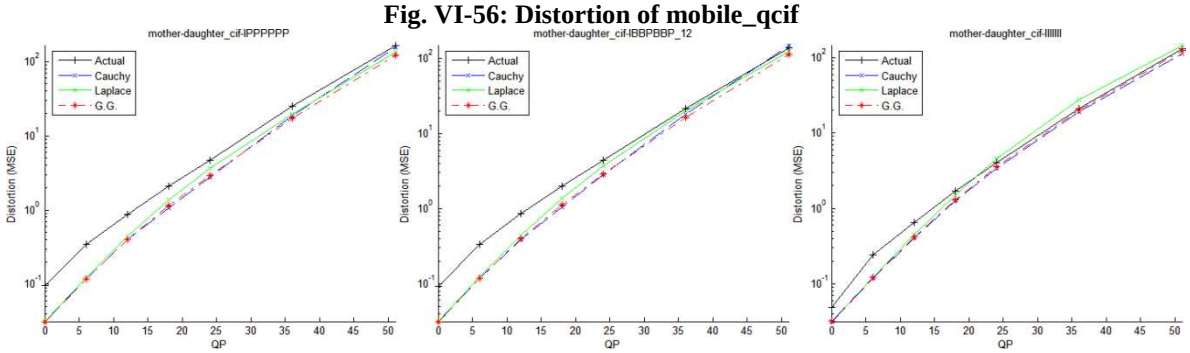

Fig. VI-57: Distortion of mother-daughter_cif

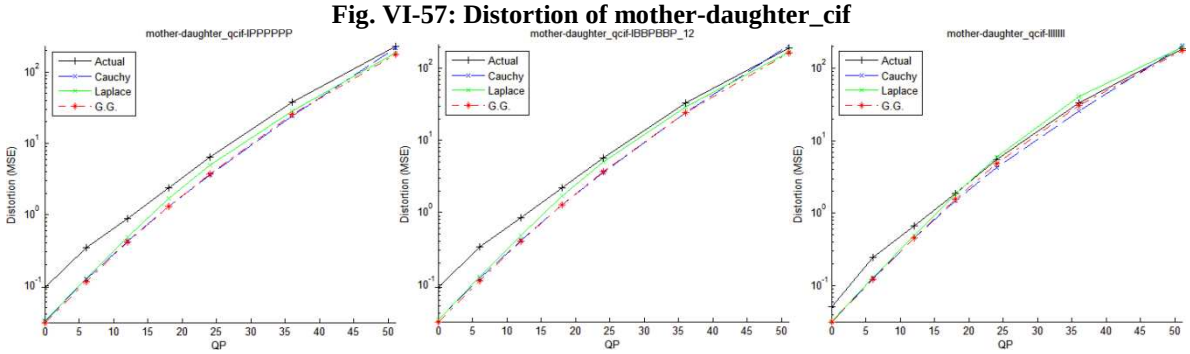

Fig. VI-58: Distortion of mother-daughter_qcif

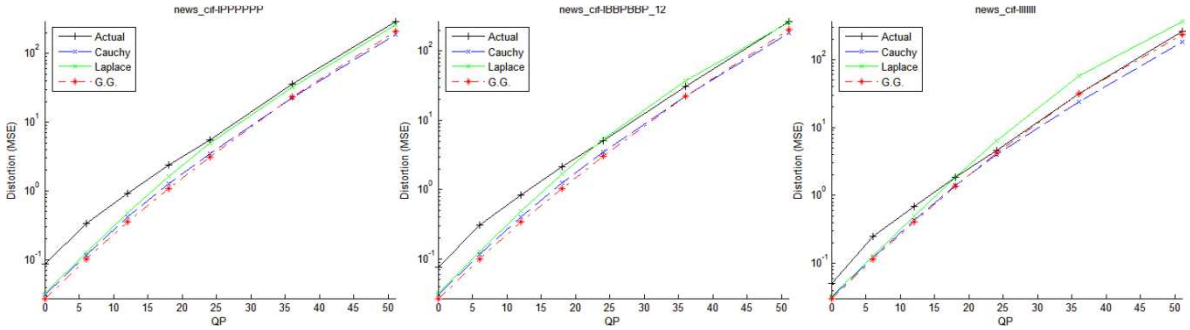

Fig. VI-59: Distortion of news_cif

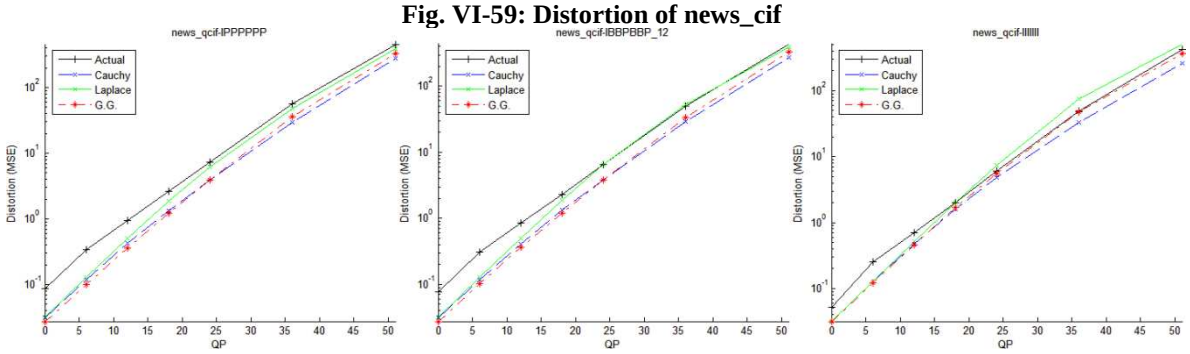

Fig. VI-60: Distortion of news_qcif

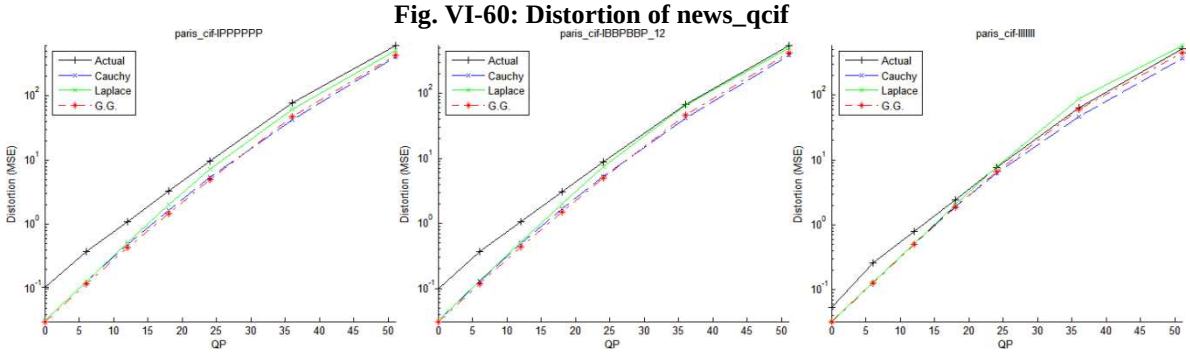

Fig. VI-61: Distortion of paris_cif

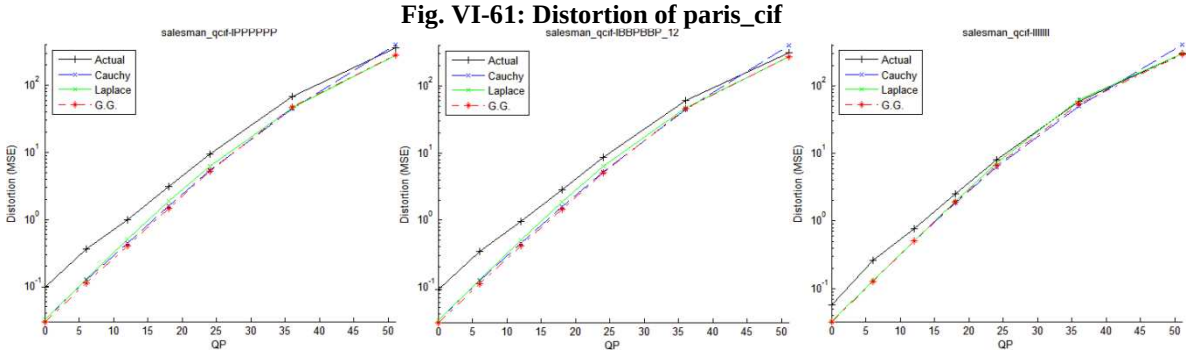

Fig. VI-62: Distortion of salesman_qcif

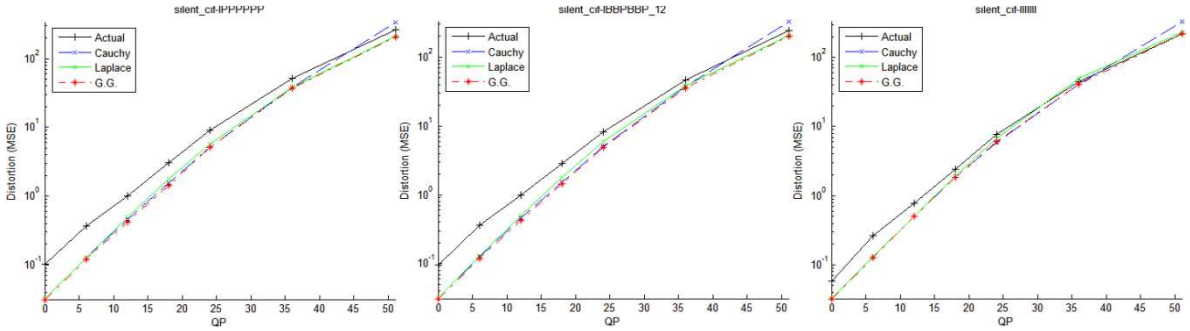

Fig. VI-63: Distortion of silent_cif

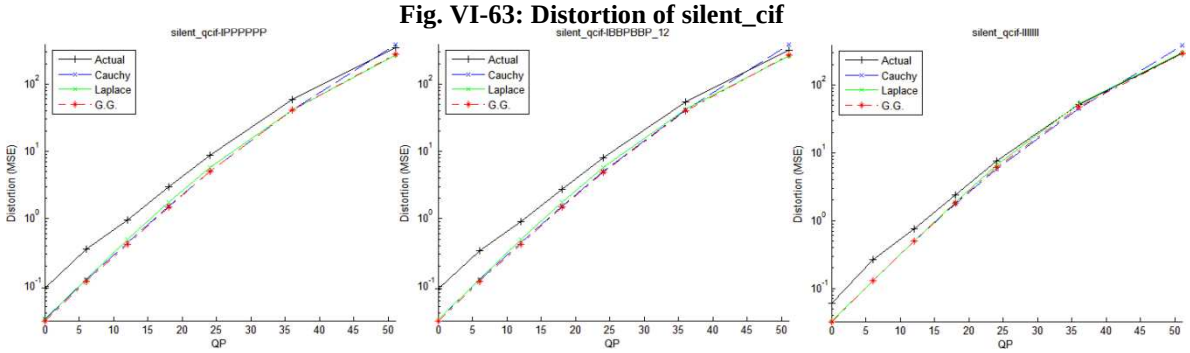

Fig. VI-64: Distortion of silent_qcif

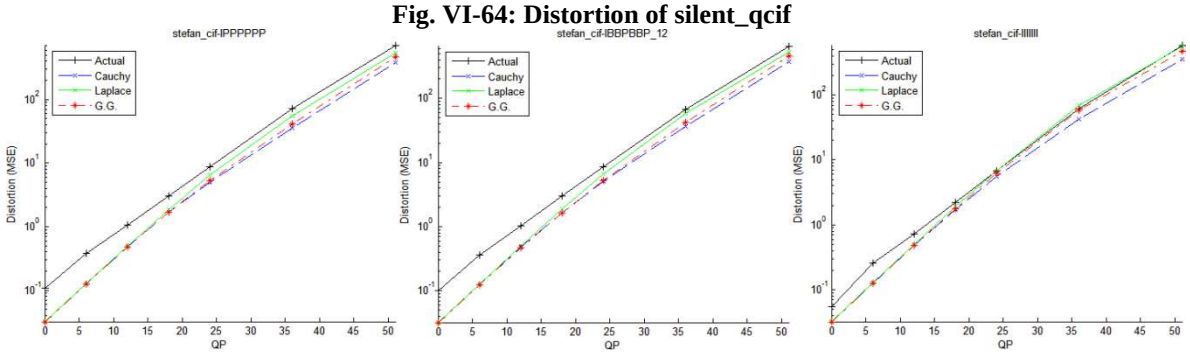

Fig. VI-65: Distortion of stefan_cif

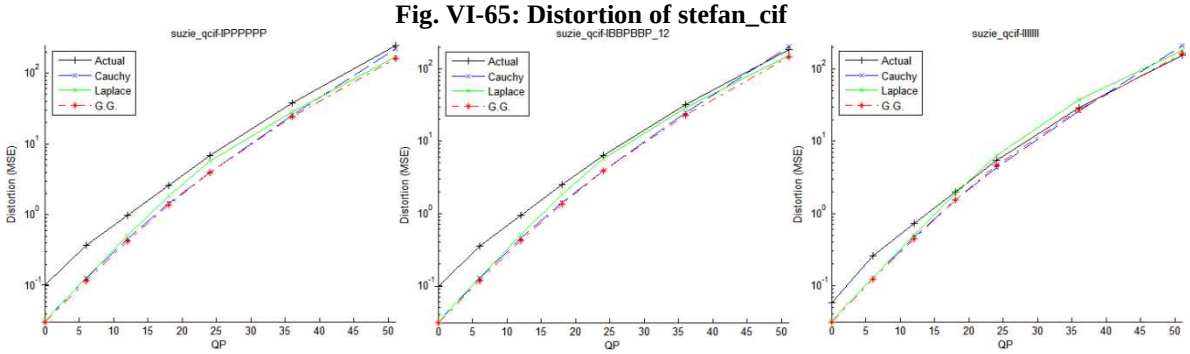

Fig. VI-66: Distortion of suzie_qcif

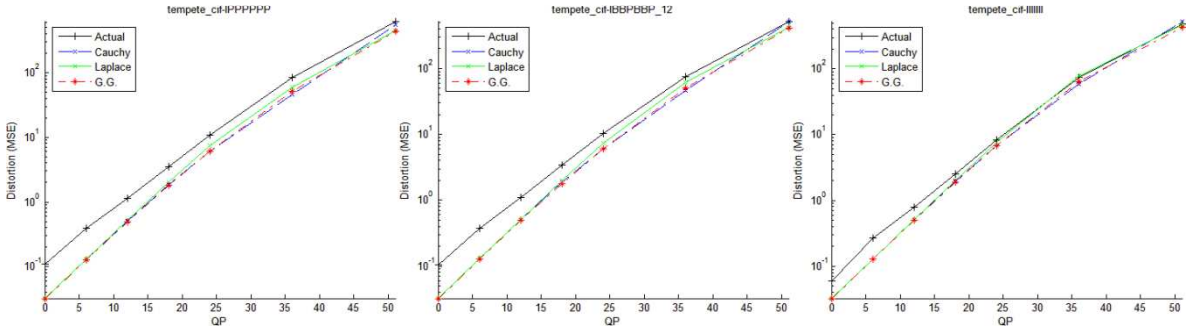

Fig. VI-67: Distortion of tempete_cif

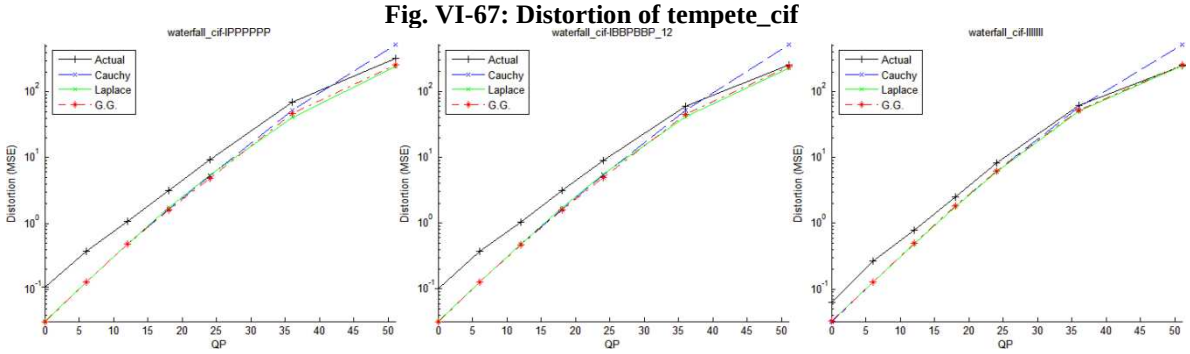

Fig. VI-68: Distortion of waterfall_cif

The Laplacian model is the most simple, and contrary to what one should expect, is in general the most accurate for the IPPPPP… and IBBPBBP… GOPs . The Generalized Gaussian is in general the most accurate for the IIIIII… GOP. In the other cases the model gives an "optimistic" distortion, that is, usually predicts a smaller distortion than the actual. The Cauchy model ranges between greater and smaller distortions. It is important to mention that for small QPs (less than 12) the predictions of the three models are almost the same.

VI.5 CONCLUSIONS AND FURTHER WORK

Summarizing, I compared three Probability Density Functions (Laplace, Cauchy and Generalized Gaussian) in order to find which one is the most accurate representation of the DCT coefficients. The Laplace PDF is the most widely used, mostly because of its simplicity (Kamaci et al., 2005). The two types of comparisons (the graphical and the analytical) executed here, demonstrate that both the Generalized Gaussian and Cauchy PDFs outperform the Laplace function, especially in the coefficients of the DCT with lower index (i,j).

Another comparison that I made in this thesis is how well the models based on the mentioned PDFs can predict the actual rate of the coded video. For the entropy tests, the Generalized Gaussian model is in general the most accurate when interprediction is used (GOP types IPPPP.. and IBBPBBP…) and the quantization

parameter QP is greater than 6. For the case where QP is less or equal than 6, the Cauchy model is in general the most accurate. For the case when only interprediction is used, the Cauchy and Laplace models offer a better estimation (being the Cauchy model slightly better than the Laplace).

The Laplacian distortion model is the most simple, and contrary to what one should expect, is in general the most accurate for the IPPPPP… and IBBPBBP… GOPs . The Generalized Gaussian is in general the most accurate for the IIIIII… GOP. One important detail worth noting is that for small QPs (less than 12) the predictions of the three models are almost the same, thus in those cases, the simplest model (Laplace) can be used disregarding the type of GOP.

I haven't found in the literature exact analytical models based on the Generalized Gaussian PDF to predict the entropy or the distortion. Under the best of my knowledge, they are first proposed in this thesis.

A very important factor is the computational cost of each distribution (which includes the parameters' estimation) and the computational cost its models.

It can be seen from chapter V that the Cauchy PDF uses only simple arithmetic operations. The Laplace PDF uses only simple arithmetic operations and the exponential function. The G. Gaussian, basically uses the same types of operations as the Laplacian (although its number of operations is greater) plus the Gamma function.

The parameter estimation for the Laplace PDF is very simple because it only requires the calculation of the mean and standard deviation of the empirical data. The parameter estimation for the G. Gaussian involves the same as the Laplacian plus the estimation of the p parameter, which has a method with very good effectiveness/cost ratio (see chapter V for details). The parameter estimation of the Cauchy PDF is its weak spot, due to the fact that it does not have moments, the methods based on them (which generally are the choice for real-time applications due to their good effectiveness/cost ratio) cannot be used. I selected the method used in (Kamaci et al., 2005) because of its simplicity and computational efficiency (ideal for practical applications), however its effectiveness was not that good; therefore, I modified it to make it more accurate, but obviously in order to do that I had to increase its computational cost (see chapter V for details).

The Laplace entropy model involves exponential, logarithmic and hyperbolic functions. The Cauchy entropy model involves mostly trigonometric and logarithmic functions. The G. Gaussian entropy model involves exponential, gamma, and incomplete gamma functions; being the most computationally expensive of the three.

The Laplace distortion model involves a hyperbolic function. The Cauchy distortion model involves mostly trigonometric and logarithmic functions. The G.

Gaussian distortion model involves exponential, gamma, and incomplete gamma functions; again, being the most computationally expensive of the three.

The Laplace entropy and distortion models have an extra advantage over the others. Their summatories have been simplified using the properties of the exponential function, for the complete procedure see (Syu, 2005); hence their evaluation does not require a loop.

By taking into consideration both the cost (mentioned in the last paragraphs) and the experimental results in this thesis, I can conclude that the Laplace PDF is the wisest choice when the video encoding is done with scarce computational resources (such as those of a cell phone or PDA).

If the video encoding is done with sufficient computational resources (such as those of a personal computer) the Generalized Gaussian or the Cauchy PDF should be used to model the DCT coefficients and to do the rate prediction. Which one of the two will depend on the expected quantization parameters that the application will use (if they are bigger than 6 use the G. Gaussian, else use the Cauchy). If they are not known in advance (as in the case of Rate Control), I suggest to use the Generalized Gaussian because, considering the whole range of QP, it is the most accurate. For the distortion prediction, however, I suggest to use the Laplace model, regardless of which PDF was chosen for the rate prediction.

Suppose a Cauchy - Laplace combination, where the former is used for the modeling and the rate prediction and the latter is used for the distortion prediction. Compared to an “all Cauchy” approach, the combination will have the disadvantage of computing the Laplace’s parameters, but will have the advantage of fewer computations for distortion prediction, and yet it will be more accurate.

Now suppose a Generalized Gaussian - Laplace combination, where the former is used for the modeling and the rate prediction and the latter is used for the distortion prediction. Compared to an “all Generalized Gaussian” approach, the combination will be still obtaining good results in the distortion prediction, and will have the advantage of much fewer computations for it; and being the Laplace a particular case of the G. Gaussian, they will use the same parameters (except for p, of course).

In my opinion, the G. Gaussian models that I presented here need to be studied further, because simplifications or improvements could be found, that would reduce its costs thus making them more attractive. This research could also be extended by including the 4x4 transform size.

Chapter VII

APPENDIXES

VII.1 GENERALIZED GAUSSIAN ENTROPY MODEL

Assume that the DCT coefficients are uniformly quantized with a quantization step size Q. Let $P(iQ)$ be the probability that a coefficient is quantized to iQ, where $\{i = 0, \pm 1, \pm 2, \dots\}$. Then the entropy of the quantized DCT coefficients is computed as (Kamaci, Altunbasak, & Mersereau, 2005):

$$H(Q) = -\sum_{i=-\infty}^{\infty} P(iQ) log_2[P(iQ)]$$

Where:

$$P(iQ) = \int_{\left(i-\frac{1}{2}\right)Q}^{\left(1+\frac{1}{2}\right)Q} f_X \, dx$$

Due to the fact that the Generalized Gaussian PDF is symmetrical, and in this particular case, centered at 0, $H(Q)$ can be expressed as:

$$H(Q) = -P(0Q) log_2[P(0Q)] - 2\sum_{i=1}^{\infty} P(iQ) log_2[P(iQ)]$$

Where:

$$P(iQ) = \int_{\left(i-\frac{1}{2}\right)Q}^{\left(i+\frac{1}{2}\right)Q} \frac{\left(\frac{p}{A}\right)}{\Gamma\left(\frac{1}{p}\right)} e^{-\left|\frac{x}{A}\right|^p} dx = \frac{1}{2}\left[\frac{\gamma\left(\frac{1}{p}, \left(\left(i+\frac{1}{2}\right)Q/A\right)^p\right)}{\Gamma\left(\frac{1}{p}\right)} - \frac{\gamma\left(\frac{1}{p}, \left(\left(i-\frac{1}{2}\right)Q/A\right)^p\right)}{\Gamma\left(\frac{1}{p}\right)}\right]$$

This integral can be easily solved using the definition of the Generalized Gaussian CDF; or in this case, by noting that is a particular case or the integrals that appear in the distortion model (see the next appendix). Thus:

$$P(iQ) = \begin{cases} \dfrac{\gamma\left(\frac{1}{p}, \left(\frac{Q}{2A}\right)^p\right)}{\Gamma\left(\frac{1}{p}\right)}, & i = 0 \\ \dfrac{\left[\gamma\left(\frac{1}{p}, L_2\right) - \gamma\left(\frac{1}{p}, L_1\right)\right]}{2\Gamma\left(\frac{1}{p}\right)}, & i \neq 0 \end{cases}$$

Where:

$$L_2 = \left(\left(i+\frac{1}{2}\right)Q/A\right)^p$$
$$L_1 = \left(\left(i-\frac{1}{2}\right)Q/A\right)^p$$

$$H(Q) = -\frac{\gamma\left(\frac{1}{p}, \left(\frac{Q}{2A}\right)^p\right)}{\Gamma\left(\frac{1}{p}\right)} log_2\left[\frac{\gamma\left(\frac{1}{p}, \left(\frac{Q}{2A}\right)^p\right)}{\Gamma\left(\frac{1}{p}\right)}\right] - \frac{2}{2\Gamma\left(\frac{1}{p}\right)} \sum_{\mathrm{i}=1}^{\mathrm{M}} \left[\gamma\left(\frac{1}{p}, L_2\right) - \gamma\left(\frac{1}{p}, L_1\right)\right] log_2\left[\frac{\gamma\left(\frac{1}{p}, L_2\right) - \gamma\left(\frac{1}{p}, L_1\right)}{2\Gamma\left(\frac{1}{p}\right)}\right]$$

Expressing $D(Q)$ in terms of the lower normalized incomplete gamma function:

$$G(b,z) = \frac{\gamma(b,z)}{\Gamma(b)}$$

$$H(Q) = -G\left(\frac{1}{p},\left(\frac{Q}{2A}\right)^p\right) log_2\left(G\left(\frac{1}{p},\left(\frac{Q}{2A}\right)^p\right)\right) - \sum_{\mathrm{i}=1}^{\mathrm{M}}\left[G\left(\frac{1}{p},L_2\right) - G\left(\frac{1}{p},L_1\right)\right]\left[log_2\left(\mathrm{G}\left(\frac{1}{p},L_2\right) - G\left(\frac{1}{p},L_1\right)\right) - 1\right]$$

VII.2 GENERALIZED GAUSSIAN DISTORTION MODEL

For a generalized Gaussian source $f_X(x) = gg(x;0,\sigma,p)$, in an uniform quantizer with step size Q, and levels i, the distortion caused by quantization is given by:

$$D(Q) = \sum_{i=-\infty}^{\infty} \int_{\left(i-\frac{1}{2}\right)Q}^{\left(i+\frac{1}{2}\right)Q} |x - iQ|^2 \frac{p}{2\Gamma(1/p)A} e^{-\left|\frac{x}{A}\right|^p} dx$$

Note that, because of the symmetry of the GG distribution,

$$gg(x;0,\sigma,p) = gg(-x;0,\sigma,p)$$

so $D(Q)$ can be expressed as:

$$D(Q) = \int_{-\frac{1}{2}Q}^{\frac{1}{2}Q} |x|^2 \frac{p}{2\Gamma(1/p)A} e^{-\left|\frac{x}{A}\right|^p} dx + \sum_{i=-\infty}^{-1} \int_{\left(i-\frac{1}{2}\right)Q}^{\left(i+\frac{1}{2}\right)Q} |x - iQ|^2 \frac{p}{2\Gamma(1/p)A} e^{-\left|\frac{x}{A}\right|^p} dx + \sum_{i=1}^{\infty} \int_{\left(i-\frac{1}{2}\right)Q}^{\left(i+\frac{1}{2}\right)Q} |x - iQ|^2 \frac{p}{2\Gamma(1/p)A} e^{-\left|\frac{x}{A}\right|^p} dx$$

For $i = 0$:

$$\int_{-\frac{1}{2}Q}^{\frac{1}{2}Q} |x|^2 \frac{p}{2\Gamma(1/p)A} e^{-\left|\frac{x}{A}\right|^p} dx = \int_{-\frac{1}{2}Q}^{0} |x|^2 \frac{p}{2\Gamma(1/p)A} e^{-\left|\frac{x}{A}\right|^p} dx + \int_{0}^{\frac{1}{2}Q} |x|^2 \frac{p}{2\Gamma(1/p)A} e^{-\left|\frac{x}{A}\right|^p} dx$$

Because of the symmetry of the GG distribution and because $|x|^2 = |-x|^2$, it's easy to see that

$$\int_{-\frac{1}{2}Q}^{0} |x|^2 \frac{p}{2\Gamma(1/p)A} e^{-\left|\frac{x}{A}\right|^p} dx = \int_{0}^{\frac{1}{2}Q} |x|^2 \frac{p}{2\Gamma(1/p)A} e^{-\left|\frac{x}{A}\right|^p} dx$$

And for $i \neq 0$

$$\sum_{i=-\infty}^{-1} \int_{\left(i-\frac{1}{2}\right)Q}^{\left(i+\frac{1}{2}\right)Q} |x - iQ|^2 \frac{p}{2\Gamma(1/p)A} e^{-\left|\frac{x}{A}\right|^p} dx + \sum_{i=1}^{\infty} \int_{\left(i-\frac{1}{2}\right)Q}^{\left(i+\frac{1}{2}\right)Q} |x - iQ|^2 \frac{p}{2\Gamma(1/p)A} e^{-\left|\frac{x}{A}\right|^p} dx$$

It can be rewritten as:

$$\sum_{i=1}^{\infty} \left[\int_{-\left(i+\frac{1}{2}\right)Q}^{-\left(i-\frac{1}{2}\right)Q} |x - (-i)Q|^2 \frac{p}{2\Gamma(1/p)A} e^{-\left|\frac{x}{A}\right|^p} dx + \int_{\left(i-\frac{1}{2}\right)Q}^{\left(i+\frac{1}{2}\right)Q} |x - iQ|^2 \frac{p}{2\Gamma(1/p)A} e^{-\left|\frac{x}{A}\right|^p} dx \right]$$

Again, because of the symmetry of the GG distribution, $gg(x; 0, \sigma, p) = gg(-x; 0, \sigma, p)$; and because $|x - iQ|^2 = |(-x) - (-i)Q|^2$,

$$\int_{-\left(i+\frac{1}{2}\right)Q}^{-\left(i-\frac{1}{2}\right)Q} |x - (-i)Q|^2 \frac{p}{2\Gamma(1/p)A} e^{-\left|\frac{x}{A}\right|^p} dx = \int_{\left(i-\frac{1}{2}\right)Q}^{\left(i+\frac{1}{2}\right)Q} |x - iQ|^2 \frac{p}{2\Gamma(1/p)A} e^{-\left|\frac{x}{A}\right|^p} dx$$

Thus, $D(Q)$ can be rewritten as:

$$D(Q) = 2 \int_{0}^{\frac{1}{2}Q} |x|^2 \frac{p}{2\Gamma(1/p)A} e^{-\left|\frac{x}{A}\right|^p} dx + \sum_{i=1}^{\infty} 2 \int_{\left(i-\frac{1}{2}\right)Q}^{\left(i+\frac{1}{2}\right)Q} |x - iQ|^2 \frac{p}{2\Gamma(1/p)A} e^{-\left|\frac{x}{A}\right|^p} dx$$

Let M be the maximum level of the quantizer. If we algebraically manipulate $D(Q)$:

$$D(Q) = \int_0^{\frac{1}{2}Q} x^2 \frac{p}{\Gamma(1/p)A} e^{-\left|\frac{x}{A}\right|^p} dx + \sum_{i=1}^{M} \int_{\left(i-\frac{1}{2}\right)Q}^{\left(i+\frac{1}{2}\right)Q} (x^2 - 2xiQ + i^2Q^2) \frac{p}{\Gamma(1/p)A} e^{-\left|\frac{x}{A}\right|^p} dx$$

$$D(Q) = \int_0^{\frac{1}{2}Q} \frac{px^2}{\Gamma(1/p)A} e^{-\left|\frac{x}{A}\right|^p} dx + \sum_{i=1}^{M} \int_{\left(i-\frac{1}{2}\right)Q}^{\left(i+\frac{1}{2}\right)Q} \frac{px^2}{\Gamma(1/p)A} e^{-\left|\frac{x}{A}\right|^p} dx + \sum_{i=1}^{M} \int_{\left(i-\frac{1}{2}\right)Q}^{\left(i+\frac{1}{2}\right)Q} (-2xiQ + i^2Q^2) \frac{p}{\Gamma(1/p)A} e^{-\left|\frac{x}{A}\right|^p} dx$$

Note that for $i = 1,2, \dots M$:

$$\sum_{i=1}^{M} \int_{\left(i-\frac{1}{2}\right)Q}^{\left(i+\frac{1}{2}\right)Q} \frac{px^2}{\Gamma(1/p)A} e^{-\left|\frac{x}{A}\right|^p} dx$$

$$= \int_{\left(1-\frac{1}{2}\right)Q}^{\left(1+\frac{1}{2}\right)Q} \frac{px^2}{\Gamma(1/p)A} e^{-\left|\frac{x}{A}\right|^p} dx + \int_{\left(2-\frac{1}{2}\right)Q}^{\left(2+\frac{1}{2}\right)Q} \frac{px^2}{\Gamma(1/p)A} e^{-\left|\frac{x}{A}\right|^p} dx + \cdots$$

$$+ \int_{\left(M-\frac{1}{2}\right)Q}^{\left(M+\frac{1}{2}\right)Q} \frac{px^2}{\Gamma(1/p)A} e^{-\left|\frac{x}{A}\right|^p} dx = \int_{\frac{1}{2}Q}^{\left(M+\frac{1}{2}\right)Q} \frac{px^2}{\Gamma(1/p)A} e^{-\left|\frac{x}{A}\right|^p} dx$$

Thus:

$$D(Q) = \int_0^{\frac{1}{2}Q} \frac{px^2}{\Gamma(1/p)A} e^{-\left|\frac{x}{A}\right|^p} dx + \int_{\frac{1}{2}Q}^{\left(M+\frac{1}{2}\right)Q} \frac{px^2}{\Gamma(1/p)A} e^{-\left|\frac{x}{A}\right|^p} dx + \sum_{i=1}^{M} \int_{\left(i-\frac{1}{2}\right)Q}^{\left(i+\frac{1}{2}\right)Q} (-2xiQ + i^2Q^2) \frac{p}{\Gamma(1/p)A} e^{-\left|\frac{x}{A}\right|^p} dx$$

$$D(Q) = \int_{0}^{\left(M+\frac{1}{2}\right)Q} \frac{px^2}{\Gamma(1/p)A} e^{-\left|\frac{x}{A}\right|^p} dx + \sum_{i=1}^{M} \left[-2iQ \int_{\left(i-\frac{1}{2}\right)Q}^{\left(i+\frac{1}{2}\right)Q} \frac{px}{\Gamma(1/p)A} e^{-\left|\frac{x}{A}\right|^p} dx + i^2Q^2 \int_{\left(i-\frac{1}{2}\right)Q}^{\left(i+\frac{1}{2}\right)Q} \frac{p}{\Gamma(1/p)A} e^{-\left|\frac{x}{A}\right|^p} dx \right]$$

In order to solve the integrals above, we will use a technique found in López-Esquivel (2000) that he employed to calculate the moments of a random variable $Y = |X|$, where in his case X was a generalized Gaussian random variable.

If X is a GG with $\mu = 0$. Then:

$$E[X^n] = \int_{-\infty}^{\infty} x^n \frac{p}{2\Gamma(1/p)A(p,\sigma)} e^{-\left|\frac{x}{A}\right|^p} dx$$

López-Esquivel (2000) used the following transformation:

$$f_Y(y) = f_X(-y)\left|\frac{dy}{dx}\right| + f_X(y)\left|\frac{dy}{dx}\right| = f_X(-y)|-1| + f_X(y)|1| = \frac{p}{2\Gamma(1/p)A} e^{-\left|\frac{y}{A}\right|^p} + \frac{p}{2\Gamma(1/p)A} e^{-\left|\frac{y}{A}\right|^p} = \frac{p}{\Gamma(1/p)A} e^{-\left|\frac{y}{A}\right|^p}$$

and calculated the moments of Y

$$E[Y^n] = \int_{0}^{\infty} y^n \frac{p}{\Gamma(1/p)A} e^{-\left|\frac{y}{A}\right|^p} dy$$

Solving that integral by noticing the resemblance with the generalized Gamma probability density function defined by (Stacy, 1962):

$$f(x;a,d,p) = \frac{\left(\frac{p}{a^d}\right)x^{d-1}}{\Gamma\left(\frac{d}{p}\right)} e^{-\left(\frac{x}{a}\right)^p}, x \geq 0$$

for positive values of the parameters a, d, and p. And the cumulative function:

$$F(x;a,d,p) = \frac{\gamma\left(\frac{d}{p}, \left(\frac{x}{a}\right)^p\right)}{\Gamma\left(\frac{d}{p}\right)}$$

Where $\gamma(b,z)$ is the lower incomplete gamma function, defined as (Abramowitz & Stegun, 1972):

$$\gamma(b,z)=\int_0^z v^{b-1}e^{-v}\,dv$$

It is important to emphasize the generalized Gaussian PDF exists for $x\in\mathbb{R}$, whereas the generalized Gamma only exists for $x\geq 0$; that is why López-Esquivel (2000) had to work with the random variable $Y=|X|$.

Note that, because we have exploited the symmetry of both the quantizer and the generalized Gaussian PDF, in our case i is always positive, and hence, $x\geq 0$. Therefore we don't need to use the random variable $Y=|X|$.

$$D(Q)=\int_0^{\left(M+\frac{1}{2}\right)Q}\frac{px^2}{\Gamma(1/p)A}e^{-\left|\frac{x}{A}\right|^p}\,dx+\sum_{i=1}^{M}\left[-2iQ\int_{\left(i-\frac{1}{2}\right)Q}^{\left(i+\frac{1}{2}\right)Q}\frac{px}{\Gamma(1/p)A}e^{-\left|\frac{x}{A}\right|^p}\,dx+i^2Q^2\int_{\left(i-\frac{1}{2}\right)Q}^{\left(i+\frac{1}{2}\right)Q}\frac{p}{\Gamma(1/p)A}e^{-\left|\frac{x}{A}\right|^p}\,dx\right]$$

As we know, the CDF of Z can be obtained by integrating the PDF (León-García, 1994)

$$F_Z(z)=\int_{-\infty}^{z}f_Z(x)\,dx$$

If Z is a generalized Gamma random variable, then:

$$F_Z(z)=\int_0^z f_Z(x)\,dx$$

$$\frac{\gamma\left(\frac{d}{p},\left(\frac{x}{a}\right)^p\right)}{\Gamma\left(\frac{d}{p}\right)}=\int_0^z\frac{\left(\frac{p}{a^d}\right)x^{d-1}}{\Gamma\left(\frac{d}{p}\right)}e^{-\left(\frac{x}{a}\right)^p}\,dx$$

Integrating the three terms separately:

$$i^2Q^2\int_{\left(i-\frac{1}{2}\right)Q}^{\left(i+\frac{1}{2}\right)Q}\frac{(p/A)}{\Gamma(1/p)}e^{-\left|\frac{x}{A}\right|^p}\,dx=i^2Q^2\left[\int_0^{\left(i+\frac{1}{2}\right)Q}\frac{(p/A)}{\Gamma(1/p)}e^{-\left|\frac{x}{A}\right|^p}\,dx-\int_0^{\left(i-\frac{1}{2}\right)Q}\frac{(p/A)}{\Gamma(1/p)}e^{-\left|\frac{x}{A}\right|^p}\,dx\right]$$

If we let $a = A$, $d = 1$, we could use

$$\frac{\gamma\left(\frac{d}{p}, \left(\frac{x}{a}\right)^p\right)}{\Gamma\left(\frac{d}{p}\right)} = \int_0^z \frac{\left(\frac{p}{a^d}\right) x^{d-1}}{\Gamma\left(\frac{d}{p}\right)} e^{-\left(\frac{x}{a}\right)^p}\, dx$$

Thus:

$$i^2Q^2 \int_{\left(i-\frac{1}{2}\right)Q}^{\left(i+\frac{1}{2}\right)Q} \frac{\left(\frac{p}{A}\right)}{\Gamma\left(\frac{1}{p}\right)} e^{-\left|\frac{x}{A}\right|^p}\, dx = i^2Q^2 \left[\frac{\gamma\left(\frac{1}{p}, \left(\left(i+\frac{1}{2}\right)Q/A\right)^p\right)}{\Gamma\left(\frac{1}{p}\right)} - \frac{\gamma\left(\frac{1}{p}, \left(\left(i-\frac{1}{2}\right)Q/A\right)^p\right)}{\Gamma\left(\frac{1}{p}\right)}\right]$$

For the term:

$$\int_{\left(i-\frac{1}{2}\right)Q}^{\left(i+\frac{1}{2}\right)Q} (-2xiQ) \frac{p}{\Gamma(1/p)A} e^{-\left|\frac{x}{A}\right|^p}\, dx = \frac{-2iQ\Gamma(2/p)A}{\Gamma(1/p)} \int_{\left(i-\frac{1}{2}\right)Q}^{\left(i+\frac{1}{2}\right)Q} \frac{\left(\frac{p}{A^2}\right)x}{\Gamma(2/p)} e^{-\left|\frac{x}{A}\right|^p}\, dx$$

Letting $a = A$, $d = 2$

$$\frac{-2iQ\Gamma\left(\frac{2}{p}\right)A}{\Gamma\left(\frac{1}{p}\right)} \int_{\left(i-\frac{1}{2}\right)Q}^{\left(i+\frac{1}{2}\right)Q} \frac{\left(\frac{p}{A^2}\right)x}{\Gamma\left(\frac{2}{p}\right)} e^{-\left|\frac{x}{A}\right|^p}\, dx$$
$$= \frac{-2iQA}{\Gamma(1/p)}\left[\gamma\left(\frac{2}{p}, \left(\left(i+\frac{1}{2}\right)Q/A\right)^p\right) - \gamma\left(\frac{2}{p}, \left(\left(i-\frac{1}{2}\right)Q/A\right)^p\right)\right]$$

And for the term:

$$\int_0^{\left(M+\frac{1}{2}\right)Q} \frac{px^2}{\Gamma(1/p)A} e^{-\left|\frac{x}{A}\right|^p}\, dx = \frac{\Gamma(3/p)A^2}{\Gamma(1/p)} \int_{\left(i-\frac{1}{2}\right)Q}^{\left(i+\frac{1}{2}\right)Q} \frac{\left(\frac{p}{A^3}\right)x^2}{\Gamma(3/p)} e^{-|ax|^p}\, dx$$

If we let $a = A$, $d = 3$

$$\frac{\Gamma\left(\frac{3}{p}\right)A^2}{\Gamma\left(\frac{1}{p}\right)}\int_0^{\left(M+\frac{1}{2}\right)Q}\frac{\left(\frac{p}{A^3}\right)x^2}{\Gamma\left(\frac{3}{p}\right)}e^{-\left|\frac{x}{A}\right|^p}\,dx=\frac{A^2}{\Gamma\left(\frac{1}{p}\right)}\left[\gamma\left(\frac{3}{p},\left(\left(M+\frac{1}{2}\right)Q/A\right)^p\right)\right]$$

Substituting in $D(Q)$

$$D(Q)=\frac{A^2}{\Gamma\left(\frac{1}{p}\right)}\gamma\left(3/p,\left(\frac{(M+1/2)Q}{A}\right)^p\right)$$
$$+\frac{1}{\Gamma\left(\frac{1}{p}\right)}\sum_{i=1}^{M}\left[(iQ)^2\left[\gamma\left(1/p,\left(\frac{(i+1/2)Q}{A}\right)^p\right)-\gamma\left(\frac{1}{p},\left(\frac{(i-1/2)Q}{A}\right)^p\right)\right]\right.$$
$$\left.-2iQA\left[\gamma\left(2/p,\left(\frac{(i+1/2)Q}{A}\right)^p\right)-\gamma\left(\frac{2}{p},\left(\frac{(i-1/2)Q}{A}\right)^p\right)\right]\right]$$

Expressing $D(Q)$ in terms of the normalized incomplete gamma function:

$$G(b,z)=\frac{\gamma(b,z)}{\Gamma(b)}$$

$$D(Q)=\frac{A^2\Gamma\left(\frac{3}{p}\right)}{\Gamma\left(\frac{1}{p}\right)}G\left(3/p,\left(\frac{(M+1/2)Q}{A}\right)^p\right)$$
$$+\sum_{i=1}^{M}\left[(iQ)^2\left[G\left(1/p,\left(\frac{(i+1/2)Q}{A}\right)^p\right)-G\left(\frac{1}{p},\left(\frac{(i-1/2)Q}{A}\right)^p\right)\right]\right.$$
$$\left.-\frac{2iQA\Gamma\left(\frac{2}{p}\right)}{\Gamma\left(\frac{1}{p}\right)}\left[G\left(2/p,\left(\frac{(i+1/2)Q}{A}\right)^p\right)-G\left(\frac{2}{p},\left(\frac{(i-1/2)Q}{A}\right)^p\right)\right]\right]$$

$$A(p,\sigma) = \left[\frac{\sigma^2\Gamma(1/p)}{\Gamma(3/p)}\right]^{1/2}$$

$$D(Q) = \sigma^2 G\left(3/p, \left(\frac{(M+1/2)Q}{A}\right)^p\right) + \sum_{i=1}^{M}\left[(iQ)^2\left[G\left(1/p, \left(\frac{(i+1/2)Q}{A}\right)^p\right) - G\left(\frac{1}{p}, \left(\frac{(i-1/2)Q}{A}\right)^p\right)\right] - \frac{2iQA\Gamma\left(\frac{2}{p}\right)}{\Gamma\left(\frac{1}{p}\right)}\left[G\left(2/p, \left(\frac{(i+1/2)Q}{A}\right)^p\right) - G\left(\frac{2}{p}, \left(\frac{(i-1/2)Q}{A}\right)^p\right)\right]\right]$$

Chapter VIII

REFERENCES

"Advanced video coding for generic audiovisual services". (2005). *ITU-T Recommendation H.264, Version 4* . International Telecommunication Union - Telecommunication Standardization Sector. ITU-T Rec. H.264 ISO/IEC 14496-10, March 2005.

Abramowitz, M., & Stegun, I. A. (Eds.). (1972). *Handbook of Mathematical Functions with Formulas, Graphs, and Mathematical Tables* (9th ed.). New York, United States of America: Dover Publications.

Abramson, N. (1963). *Information Theory and Coding* (1st ed.). New York, United States of America: McGraw-Hill.

Ahmed, N., Natarajan, T., & Rao, K. R. (1974). "Discrete Cosine Transform". *IEEE Transactions on Computers , Vol. C-23* (Iss. 1), pp. 90-93.

Aiazzi, B., Alparone, L., & Baronti, S. (1999). "Estimation based on entropy matching for generalized Gaussian PDF modeling". *IEEE Signal Processing Letters , Vol. 6* (Iss. 6), pp. 138-140.

Altunbasak, Y., & Kamaci, N. (2004). "An analysis of the DCT coefficient distribution with the H.264 video coder". *Proceedings of the IEEE International Conference on Acoustics, Speech, and Signal Processing, Vol. 3*, pp. 177-180.

Birney, K. A., & Fischer, T. R. (1995). "On the modeling of DCT and subband image data for compression". *IEEE Transactions on Image Processing , Vol. 4* (Iss. 2), pp. 186-193.

Bossen, F. (2002). *"ABT cleanup and complexity reduction" in Joint Video Team (JVT) of ISO/IEC MPEG & ITU-T VCEG Meeting: Geneva, Switzerland, October, 2002.* Retrieved September 2, 2007, from JVT site: http://ftp3.itu.ch/av-arch/jvt-site/2002_10_Geneva/JVT-E087.doc

Britanak, V. (2001). "Discrete Cosine and Sine Transforms". In K. R. Rao, & P. C. Yip, *"The Transform and Data Compression Handbook", Chapter 4* (1st ed.). Boca Raton, United States of America: CRC Press LLC.

Chang, J.-H., Shin, J. W., Kim, N. S., & Mitra, S. K. (2005). "Image Probability Distribution Based on Generalized Gamma Function". *IEEE Signal Processing Letters , Vol. 12* (Iss. 4), pp. 325-328.

Choe, J., & Lee, C. (2007). "Estimation of the peak signal-to-noise ratio for compressed video based on generalized Gaussian modeling". *SPIE Journal of Optical Engineering , Vol. 46* (Iss. 10), pp. 1-9.

Cochran, W. G. (1952). "The $\chi 2$ Test of Goodness of Fit". *The Annals of Mathematical Statistics , Vol. 23* (Iss. 3), pp. 315-345.

Cressie, N., & Read, T. R. (1989). "Pearson's X2 and the Loglikelihood Ratio Statistic G2 : A Comparative Review". *International Statistical Review / Revue Internationale de Statistique , Vol. 57* (Iss. 1), pp. 19-43.

Domínguez-Molina, J. A., González-Farías, G., & Rodríguez-Dagnino, R. M. (2001). *"A practical procedure to estimate the shape parameter in the generalized Gaussian distribution", Technique Report I-01-18 (PE).* Retrieved from Centro de Investigación en Matemáticas, A.C.: http://www.cimat.mx/reportes/enlinea/I-01-18_eng.pdf

Easterling, R. G. (1976). "Goodness of Fit and Parameter Estimation". *Technometrics , Vol. 18* (Iss. 1), pp. 1-9.

Evans, M., Hastings, N., & Peacock, B. (1993). *Statistical Distributions* (2nd ed.). New York, United States of America: John Wiley & Sons.

Ghanbari, M. (2003). *Standard Codecs: Image Compression to Advanced Video Coding* (2nd ed.). London, United Kingdom: Institution of Electrical Engineers.

Gish, H., & Pierce, J. N. (1968). "Asymptotically efficient quantizing". *IEEE Transactions on Information Theory , Vol. 14* (Iss. 5), pp. 676-683.

Golomb, S. W. (1966). "Run-length encodings". *IEEE Transactions on Information Theory , Vol. 12* (Iss. 3), pp. 399-401.

González-López, D. (2006). *"Codiseño de un Decodificador de Video para el Estándar MPEG". Tesis.* Instituto Tecnológico y de Estudios Superiores de Monterrey, Campus Monterrey.

Gray, R. M., & Neuhoff, D. L. (1998). "Quantization". *IEEE Transactions on Information Theory , Vol. 44* (Iss. 6), pp. 2325-2383.

Huffman, D. A. (1952). "A Method for the Construction of Minimum-Redundancy Codes". *Proceedings of the IRE , Vol. 40* (Iss. 9), pp. 1098-1101.

International Telecommunication Union. (2003, May 1). *Sequences*. Retrieved June 6, 2007, from ITU Video Site: http://ftp3.itu.ch/av-arch/video-site/sequences/

Joshi, R. L., & Fischer, T. R. (1995). "Comparison of generalized Gaussian and Laplacian modeling in DCT image coding". *IEEE Signal Processing Letters , Vol. 2* (Iss. 5), pp. 81-82.

Kamaci, N., & Altunbasak, Y. (2005). " Frame Bit Allocation for H.264 Using Cauchy-Distribution Based Source Modelling". *Proceedings of the IEEE International Conference on Acoustics, Speech, and Signal Processing, Vol. 2*, pp. 57-60.

Kamaci, N., Altunbasak, Y., & Mersereau, R. M. (2005). "Frame bit allocation for the H.264/AVC video coder via Cauchy-density-based rate and distortion models". *IEEE Transactions on Circuits and Systems for Video Technology , Vol. 15* (Iss. 8), pp. 994-1006.

Karczewicz, M., & Kurceren, R. (2003). "The SP- and SI-frames design for H.264/AVC". *IEEE Transactions on Circuits and Systems for Video Technology , Vol. 13* (Iss. 7), pp. 637-644.

Koutrouvelis, I. A. (1982). "Estimation of Location and Scale in Cauchy Distributions Using the Empirical Characteristic Function". *Biometrika , Vol. 69* (Iss. 1), pp. 205-213.

Krishnamoorthy, K. (2006). *Handbook of statistical distributions with applications* (1st ed.). Boca Raton, United States of America: Chapman & Hall CRC.

Lam, E. Y., & Goodman, J. W. (2000). "A mathematical analysis of the DCT coefficient distributions for images". *IEEE Transactions on Image Processing , Vol. 9* (Iss. 10), pp. 1661-1666.

León-García, A. (1994). *Probability and Random Processes for Electrical Engineering* (2nd ed.). Reading, MA, United States of America: Addison-Wesley.

López-Esquivel, J. A. (2000). *"Una metodología de investigación en la estimación del parámetro de forma de la distribución gaussiana generalizada". Tesis.* Instituto Tecnológico y de Estudios Superiores de Monterrey, Campus Monterrey.

Luther, A. (1997). *Principles of Digital Audio and Video* (1st ed.). United States of America: Artech House.

Mallat, S. G. (1989). "A theory for multiresolution signal decomposition: the wavelet representation". *IEEE Transactions on Pattern Analysis and Machine Intelligence , Vol. 11* (Iss. 7), pp. 674-693.

Malvar, H. S., Hallapuro, A., Karczewicz, M., & Kerofsky, L. (2003). "Low-complexity transform and quantization in H.264/AVC". *IEEE Transactions on Circuits and Systems for Video Technology , Vol. 13* (Iss. 7), pp. 598-603.

Marpe, D., Wiegand, T., & Sullivan, G. J. (2006). "The H.264/MPEG4 advanced video coding standard and its applications". *IEEE Communications Magazine , Vol. 44* (Iss. 8), pp. 134-143.

Müller, F. (1993). "Distribution shape of two-dimensional DCT coefficients of natural images". *IEEE Electronics Letters , Vol. 29* (Iss. 22), pp. 1935-1936.

Nadarajah, S. (2005). "A generalized normal distribution". *Journal of Applied Statistics , Vol. 32* (Iss. 7), pp. 685-694.

Pu, I. M. (2006). *Fundamental Data Compression* (1st ed.). Oxford, Great Britain: Butterworth-Heinemann.

Ramírez-Velarde, R. V. (2004). *"Performance Analysis of a VBR Video Server With Self Similar Gamma Distributed MPEG-4 Data". Doctoral dissertation.* Instituto Tecnológico y de Estudios Superiores de Monterrey, Campus Monterrey.

Reiningek, R. C., & Gibson, J. D. (1983). "Distributions of the Two-Dimensional DCT Coefficients for Images". *IEEE Transactions on Communications , Vol. 31* (Iss. 6), pp. 835-839.

Richardson, I. E. (2003). *"H.264 and MPEG-4 Video Compression: Video Coding for Next-generation Multimedia"* (1st ed.). Chichester, England: John Wiley & Sons.

Rodríguez-Dagnino, R. M., & León-García, A. (1998). "An Explicit Estimator for the Shape Parameter of the Generalized Gaussian Distribution". *Proceedings of the XII National Forum of Statistics*, (pp. pp. 169-175). Monterrey, N. L., Mexico.

Rothenberg, T. J., Fisher, F. M., & Tilanus, C. B. (1964). "A Note on Estimation from a Cauchy Sample". *Journal of the American Statistical Association , Vol. 59* (Iss. 306), pp. 460-463.

Salomon, D. (2007). *Data Compression: The Complete Reference* (4th ed.). London, England: Springer-Verlag.

Schwarz, H., Marpe, D., & Wiegand, T. (2007). "Overview of the Scalable Video Coding Extension of the H.264/AVC Standard". *IEEE Transactions on Circuits and Systems for Video Technology , Vol. 17* (Iss. 9), pp. 1103-1120.

Shannon, C. E. (1948). "A mathematical theory of communication". *Bell System Technical Journal , Vol. 27*, pp. 379-423 and 623-656.

Sharifi, K. (1995). *"Subband Decomposition of Video and Practical Performance Bounds". Doctoral dissertation.* University of Toronto.

Sharifi, K., & León-García, A. (1995). "Estimation of shape parameter for generalized Gaussian distributions in subband decompositions of video". *IEEE Transactions on Circuits and Systems for Video Technology , Vol. 5* (Iss. 1), pp. 52-56.

Stacy, E. W. (1962). "A Generalization of the Gamma Distribution". *The Annals of Mathematical Statistics , Vol. 33* (Iss. 3), pp. 1187-1192.

Stockhammer, T., Hannuksela, M. M., & Wiegand, T. (2003). "H.264/AVC in wireless environments". *IEEE Transactions on Circuits and Systems for Video Technology , Vol. 13* (Iss. 7), pp. 657-673.

Sühring, K. (Ed.). (2007, December 22). *J.M. H.264/AVC Reference Software*. Retrieved January 27, 2008, from Fraunhofer Institut für Nachrichtentechnik, Heinrich Hertz Institute: http://iphome.hhi.de/suehring/tml/

Sullivan, G. J., & Wiegand, T. (2005). "Video Compression - from concepts to the H.264/AVC standard". *Proceedings of the IEEE, Vol. 93 (Iss. 1)*, pp. 18-31.

Sun, J., Gao, W., Zhao, D., & Huang, Q. (2005). "Statistical model, analysis and approximation of rate-distortion function in MPEG-4 FGS videos". *Proceedings of the SPIE - Visual Communications and Image Processing, Vol. 5960*, pp. 1921-1932.

Symes, P. D. (2004). *"Digital Video Compression"* (1st ed.). New York, United States of America: McGraw-Hill.

Syu, E. (2005). *Implementing Rate-Distortion Optimization on a Resource-Limited H.264 Encoder. Thesis.* Massachusetts Institute of Technology.

Tourapis, A. M., Leontaris, A., Sühring, K., & Sullivan, G. (2007). *"H.264/MPEG-4 AVC Reference Software Manua, Rev.9" in Joint Video Team (JVT) of ISO/IEC MPEG & ITU-T VCEG Meeting: Geneva, Switzerland; July, 2007.* Retrieved November 11, 2007, from JVT site: http://ftp3.itu.ch/av-arch/jvt-site/2007_06_Geneva/JVT-X072.zip

Varanasi, M. K., & Aazhang, B. (1989). "Parametric generalized Gaussian density estimation". *Journal of the Acoustical Society of America , Vol. 86* (Iss. 4), pp. 1404-1415.

Video Traces Research Group. (2007, January 24). *YUV Video Sequences*. Retrieved June 6, 2007, from Arizona State University: http://trace.eas.asu.edu/yuv/index.html

Wenger, S. (2003). "H.264/AVC over IP". *IEEE Transactions on Circuits and Systems for Video Technology , Vol. 13* (Iss. 7), pp. 645-656.

Wiegand, T., Sullivan, G. J., Bjøtegaard, G., & Luthra, A. (2003). "Overview of the H.264/AVC video coding standard". *IEEE Transactions on Circuits and Systems for Video Technology , Vol. 13* (Iss. 7), pp. 560-576.

Wien, M. (2003). "Variable block-size transforms for H.264/AVC". *IEEE Transactions on Circuits and Systems for Video Technology , Vol. 13* (Iss. 7), pp. 604-613.

Winkler, S. (2005). *Digital Video Quality: Vision Models and Metrics* (1st ed.). Chichester, England: John Wiley & Sons.

Xiph.org. (2004, November 2). *Derf's collection*. Retrieved June 6, 2007, from Xiph.org Test Media: http://media.xiph.org/video/derf/

Xu, Y., & Zhou, Y. (2004). "H.264 video communication based refined error concealment schemes". *IEEE Transactions on Consumer Electronics , Vol. 50* (Iss. 4), pp. 1135-1141.